Structure-Function Analysis of the Cell Polarity Determinants Bud8p and Bud9p in *Saccharomyces cerevisiae*

Dissertation

zur Erlangung des Doktorgrades

der Mathematisch-Naturwissenschaftlichen Fakultäten

der Georg-August-Universität

zu Göttingen

vorgelegt von

Anne-Brit Krappmann

(geb. Obermayer)

aus

Cuxhaven

Göttingen, 2006

Die vorliegende Arbeit wurde von April 2002 bis September 2004 in der Arbeitsgruppe von Dr. Hans-Ulrich Mösch in der Abteilung MOLEKULARE MIKROBIOLOGIE UND GENETIK von Prof. Dr. Gerhard H. Braus am INSTITUT FÜR MIKROBIOLOGIE & GENETIK der Georg-August-Universität Göttingen angefertigt; von Oktober 2004 bis November 2005 erfolgten die Arbeiten in der Abteilung GENETIK von Prof. Dr. H.-U. Mösch des FACHBEREICHS BIOLOGIE an der Philipps-Universität Marburg.

D7

Referent:. Prof. Dr. Hans-Ulrich Mösch

Korreferent: Prof. Dr. Gerhard H. Braus

Tag der mündlichen Prüfung: 17.1.2007

FÜR JONAH UND SVEN

Table of Contents

Summary

Polarity is a fundamental cellular property of living organisms and a prerequisite for orientation and survival in a multidimensional environment. In the eukaryotic model organism *Saccharomyces cerevisiae*, the brewer's or baker's yeast, polarity is evident during the cell cycle when budding has to happen at a distinct site of the mother cell to give rise to a daughter cell. Budding is genetically determined in this process to follow precise patterns: haploid **a**- and α-cells bud in an axial fashion, by which mother as well as daughter cells bud predominantly at the proximal cell pole; diploid **a**/α cells of the yeast cell form bud in a bipolar manner with the budding process initiating equally at the proximal and distal cell pole.

A variety of *S. cerevisiae* genes and their products are required for the establishment of such budding patterns. According to a current model, components of a polarity-mediating signal transduction cascade are directed by specific marker proteins to the budding pole to result in reorganisation of cytoskeletal components and to initiate bud formation. Previous studies had characterised the gene products Bud8p and Bud9p as spatial markers and polarity determinants, however without gaining further insights related to their function and role in polarity establishment in yeast. The results of this thesis describe, besides co-localisation studies, a detailed structure-function analysis based on mutant Bud8 and Bud9 proteins; as a result, regions in each primary structure could be identified that are necessary for function, i. e. mediating the correct budding pattern, for localisation, or for interaction with specific components of a signal transduction module called the 'polarisome'. Distinct regions presumably mediate interaction with Bud5p, which is an element of a GTPase signalling module, and with Rax1p, a protein involved in expressing the bipolar budding pattern; other parts of both proteins appear to be important for their delivery to the cells' surface and poles. Moreover, it was found that transport of Bud8p and Bud9p to the cell poles *via* the secretory pathway is likely to occur independently of secretion pathway component Sec18p.

The achieved mass of data may explain the fact that the bipolar budding pattern is established after some cell division cycles. Furthermore, they allow an appropriate refinement of the model on polarity establishment in *S. cerevisiae*.

Zusammenfassung

Polarität stellt eine fundamentale zelluläre Eigenschaft von Lebewesen dar und ist eine Grundvoraussetzung für Orientierung und Überleben innerhalb einer mehrdimensionalen Umgebung. In dem eukaryotischen Modellorganismus *Saccharomyces cerevisiae*, der Bier- bzw. Bäckerhefe, wird Polarität im Rahmen der Zellteilung dann offensichtlich, wenn die Sprossung an einer bestimmten Stelle der Mutterzelle zur Abschnürung der Tochterzelle erfolgen soll. Dabei folgt die Sprossung in verschiedenen Zellformen nach genetisch determinierten Mustern: haploide **a**- bzw. α- Zellen sprossen nach einem axialen Sprossmuster, bei dem sowohl die Mutter- als auch die Tochterzelle die Sprossung vorwiegend am proximalen Zellpol beginnen; diploide **a**/α-Zellen der Hefeform sprossen nach einem bipolaren Muster, bei dem die Sprossung mit gleicher Wahrscheinlichkeit am proximalen oder distalen Zellpol beginnt.

Eine Vielzahl von Genen bzw. deren Produkte sind zur Ausbildung derartiger Sprossmuster in *S. cerevisiae* notwendig. Einem aktuellen Modell zufolge dirigieren spezifische Markerproteine das Modul einer Polaritäts-Signaltransduktionskaskade zum Sprosspol, mit dem Ergebnis, dass Komponenten des Zytoskeletts dorthin ausgerichtet werden, um die Ausbildung des Tochtersprosses zu veranlassen. Vorangegangene Arbeiten hatten die Genprodukte Bud8p und Bud9p als räumliche Marker und Polaritätsdeterminanten charakterisiert, ohne jedoch genauere Erkenntnisse bzgl. deren Funktion und Rolle innerhalb der Polaritätsetablierung in Hefe zu liefern. Die in dieser Arbeit präsentierten Ergebnisse beschreiben neben Co-Lokalisierungsstudien eine detaillierte Struktur-Funktionsanalyse von mutanten Bud8- bzw. Bud9-Proteinen; im Ergebnis wurden hierbei distinkte Bereiche der jeweiligen Primärstruktur identifiziert, die zur Funktion, d. h. der Vermittlung des korrekten Sprossmusters, zur Lokalisierung oder für die Interaktion mit bestimmten Komponenten des als 'Polarisom' bezeichneten Signaltransduktionsmoduls notwendig sind. Bestimmte Regionen spielen vermutlich eine Funktion bei der Interaktion mit Bud5p, einer Komponenten des GTPase-Signalmoduls, und mit Rax1p, einem Protein, das an der Ausbildung des bipolaren Sprossmusters beteiligt ist; andere Bereiche beider Proteine scheinen für die Freisetzung an der Zelloberfläche und an den Zellpolen wichtig zu sein. Darüber hinaus konnte festgestellt werden, dass der Transport von Bud8p und Bud9p durch den sekretorischen Weg zu den Zellpolen unabhängig von der Sec18p-Komponente des Sekretionsappararates zu sein scheint.

Die erzielten Ergebnisse könnten eine Erklärung bieten, warum das bipolare Sprossmuster erst nach einigen Zyklen der Zellteilung etabliert ist. Sie erlauben außerdem die Verfeinerung des Modells zur Polaritätsvermittlung in *S. cerevisiae*.

1. Introduction

1.1 Definition and Importance of Cell Polarity

The polarization of a cell structure along a defined axis at a specific time point is an important event in the lives of many cell types (Chant and Pringle, 1991). In general, cell polarity is most simply defined as an asymmetric distribution of specific proteins, nucleic acids, macromolecular assemblies, and organelles near a defined spatial site, thereby allowing the expansion of the surface in an asymmetrical or polar fashion. This process is fundamentally important for differentiation, proliferation, morphogenesis, and function of unicellular and multicellular organisms.

Prokaryotic as well as eukaryotic cells respond to extracellular and intracellular signals to direct asymmetric cell growth and cell division (Madden and Snyder, 1998). Polarized cell growth involves asymmetric growth from a distinct region of a cell to form specific cell structures and shapes. These structures play a key role for the function of different cell types and often mediate diverse cellular interactions during development. Examples of cellular processes that rely on the formation of polarized cell structures are nutrient absorption by the microvilli of epithelial cells (Mooseker, 1985), plant fertilization (Bedinger *et al*., 1994), or the interaction of helper T cells with antigen-presenting B cells (Kupfer *et al*., 1986, Madden and Snyder, 1998).

Directional cell division is a process in which cells divide along specific cleavage planes. It occurs during the life cycle of many organisms, for instance during early embryogenesis in the nematode *Caenorhabditis elegans* (Hyman and White, 1987), neurogenesis in the fruit fly *Drosophila melanogaster* (Kraut *et al*., 1996), spore development in *Bacillus subtilis* (Shapiro, 1993), or development of the snail body plan (Freeman and Lundelius, 1982). In the yeasts *Saccharomyces cerevisiae* and *Schizosaccharomyces pombe*, cell polarization plays an important role in cell division and the mating process (Bähler and Peter, 2000). However, the mechanisms for selecting sites of polarized growth and division as well as for directing growth toward these sites are only beginning to be understood (Madden and Snyder, 1998).

As one of the best-characterized eukaryotic organisms, the budding yeast *S. cerevisiae* has become an excellent model system that is appropriate to study the establishment and maintenance of cell polarity. Basic biological research in this organism has contributed to get

a first insight into the framework of genes and their products that control cell polarity, among them many regulatory and cytoskeletal components. However, a number of proteins linked to cell polarity have been identified whose mechanism of action is not well understood and that have to be investigated in forthcoming works. The aim of this introductory chapter is to summarize recent advances on the molecular machinery that controls establishment and maintenance of cell polarity in *S. cerevisiae*.

1.2 Polarization in Yeast

The baker's yeast *S. cerevisiae* undergoes polarized growth during several stages of its life cycle, and growth occurs at defined positions on the cell surface (Madden and Snyder, 1998). Cells become highly polarized during three different phases (Figure 1): In the presence of ample nutrients, yeast grows by budding and exhibit polarized cell growth during this phase. The position where the bud forms ultimately determines the plane of cell division, and this location of the bud site depends on the mating type and pedigree of the cell (Freifelder, 1960; Chant and Pringle, 1995). During the late G1 stage, a bud emerges from a mother cell and continues to grow, first at the bud tip and then throughout the bud, until late nuclear division and cytokinesis occur (Lew and Reed, 1993). A second form of polarized growth in yeast occurs when the access to nitrogen is limited. Under these conditions diploid yeast cells switch from their yeast form (YF) to so-called pseudohyphal (PH) growth and cell morphology is altered from ellipsoidal-shaped yeast-form cells to long, thin pseudohyphal cells. Furthermore, pseudohyphae exhibit invasive growth behavior resulting in direct substrate invasion. Moreover, cell separation switches from complete to incomplete scission leading to multicellular growth where cells remain attached to each other (Gimeno *et al*., 1992; Kron *et al*., 1994). A related response occurs in haploids, termed haploid invasive growth, in which daughter cells bud to form chains of cells that penetrate an agar medium (Roberts and Fink, 1994). It is known that specific mechanisms exist to ensure that defined sites for growth are used during budding and the pseudohyphal response (Madden and Snyder, 1998). A third form of polarized growth occurs in yeast during the mating response. Haploid yeasts are of two kinds of cell types, either *MAT***a** or *MAT*α. After exposure to pheromone from cells of the opposite mating type, cells arrest in late G1 and form an elongated mating projection (Cross *et al*., 1988; Sprague and Thorner, 1992). Growth usually occurs at a cell surface location that is nearest to the mating partner (Madden and Snyder,

1992). Thus, in contrast to bud site selection, in which defined sites for growth are used, external factors influence the selection of sites for polarized growth during mating.
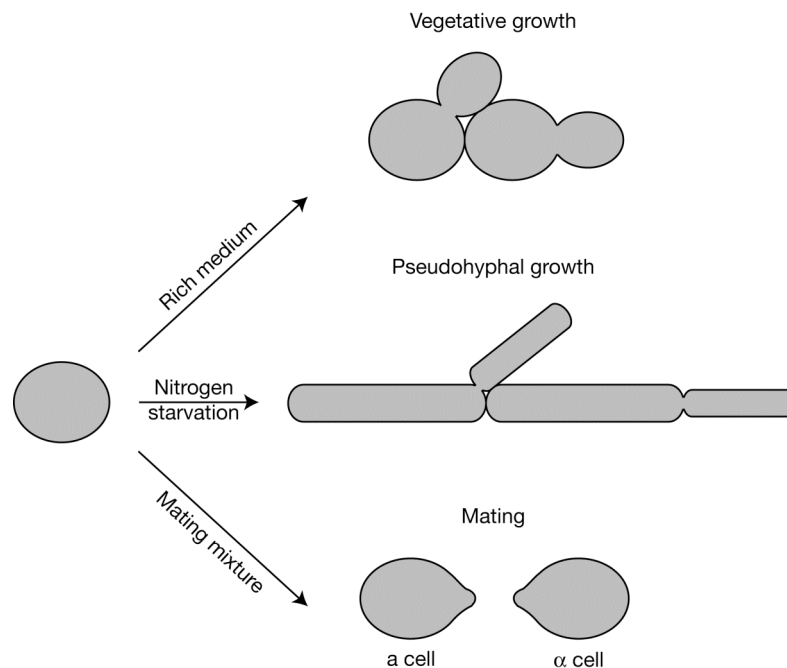
Figure 1: Polarization in yeast. Three phases of the *Saccharomyces cerevisiae* life cycle exhibit polarized cell growth. Cells grown in a rich medium are round or oval and have defined budding patterns that depend on the mating type. Under nitrogen starvation conditions cells elongate and bud from the distal end to form pseudohyphae. Haploid cells exposed to pheromone from cells of the opposite mating type arrest in G1 and extend a projection towards their mating partner.

Although vegetative growth, pseudohyphal growth, and mating response are distinct cellular processes, in each instance the cellular organization is very similar (Madden *et al.*, 1992). Virtually all aspects of cell polarization derive from polarization of the actin cytoskeleton, which is organized primarily into cortical patches and actin cables (Chant, 1999; Pruyne and Bretscher, 2000a). Actin directs secretion to the bud tip (in YF or PH cells) or a mating projection to enable the cell to grow selectively at this region. During both processes, budding and mating, actin patches cluster at the tip of the yeast cell. In case of budding, these patches accumulate around regions of cell surface growth and may serve as docking site for vesicles or, in case of mating, as endocytosis sites for membrane retrieval. Strikingly, the actin patches display a rapid movement (Doyle and Botstein, 1996; Waddle *et al.*, 1996), presumably powered by myosin molecules that are associated with the patches (Belmont and Drubin, 1998). Probably, actin cables that emanate from the bud site or mating projection tip serve as tracks for myosin-directed movement of vesicles and organelles to the growth site. At the end of each budding or mating process, cortical cables and actin patches redistribute

randomly in the mother and daughter cell or diploid zygote, respectively, until repolarization occurs during the next budding or mating event.

The establishment of polarity can be divided into three different steps, which are independent of the cell type and the budding pattern (Fig. 2). The formation of a polarized axis is unfold in temporal sequence and can be distinguished genetically. In a first step, the cell integrates relevant information to choose a direction for polarization. Budding yeast cells use spatial landmark proteins to produce precise patterns of polarization, from which bud formation and cell division follows. Mating cells polarize in the direction of their mating partner, which is defined by gradients of secreted peptide mating pheromones. In a second step, an axis is build in that the pursued direction is recognized by a series of further proteins that are collectively called polarity establishment proteins or actin-organizing complex. In a last step, the polarity establishment proteins recruit the machinery required to organize and polymerize the actin cytoskeleton.
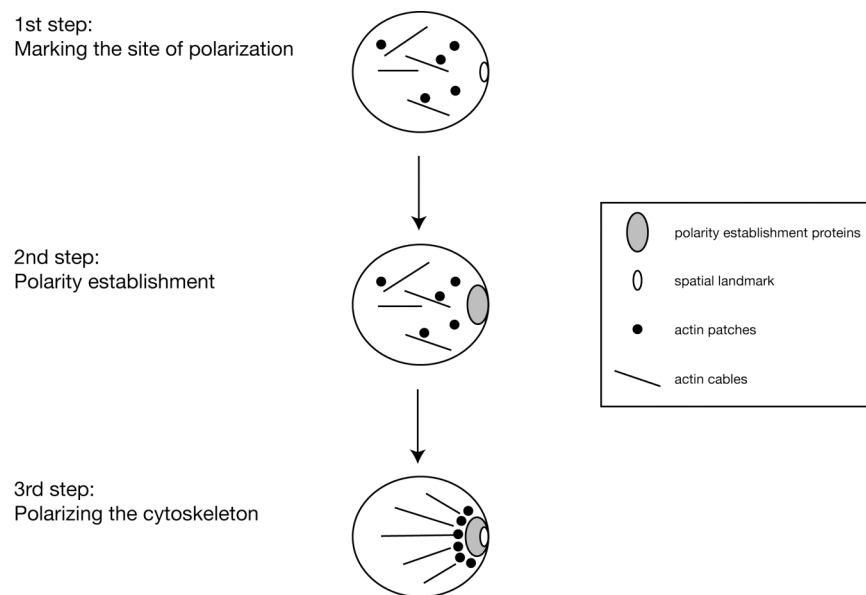
Fig. 2: Basic steps of polarity establishment in yeast. The establishment of polarity can be divided into three different steps. (1) Establishment of cell polarity requires a spatial site (landmark) on the cell cortex towards cells will polarize; the position of this site can be defined genetically or in response to internal and external signals. (2) Once a site of polarization has been chosen, this landmark recruits a number of proteins, collectively termed polarity establishment proteins or actin-organizing components. (3) The polarity establishment proteins eventually recruit the machinery required to organize and polymerize actin patches and actin cables.

1.3 Genetic Control of Bud Site Selection in **Saccharomyces cerevisiae**

1.3.1 Budding in cell-type-specific patterns

Although *S. cerevisiae* is a unicellular organism, it can grow in form of different specialized cell types, which play distinctive and important roles in its life cycle. Two of the specialized cell types are haploid **a** and α cells, which mate with nearly 100% efficiency with each other when placed adjacent to each other (Herskowitz, 1988). The result of this mating process, in which cells and nuclei fuse, is a diploid cell. This zygote has a distinctive shape and is able to produce diploid daughter cells of the usual shape by budding. The diploid **a**/α cell formed by mating is the third kind of specialized cell: this cell type is unable to mate with **a** or α cells, but it is capable of undergoing meiosis under conditions of nutritional starvation. A result from a single meiosis is the formation of four haploid spores that are wrapped up together in the ascus (Herskowitz, 1988). When diploid cells are limited for nitrogen, they are also able to switch to a multicellular growth form where *S. cerevisiae* grows as linear filaments of pseudohyphal cells (Kron *et al.*, 1994).

      The precise selection of budding sites appears to be of great importance for free-living yeasts, because yeast cells have maintained highly regulated control mechanisms of budding patterns that depend on the cell type and environmental conditions (Fig. 3). They divide in precise spatial patterns (Freifelder *et al.*, 1960; Hicks *et al.*, 1977; Chant and Pringle, 1995; Chant, 1999): Haploid **a** or α cells divide in an axial pattern, in which the mother and daughter cell are constrained to form their buds immediately adjacent to the previous site of cell separation; diploid **a**/α YF cells divide in a bipolar pattern, where buds form either at the proximal pole (that corresponds to the birth site) or at the site opposite to it, called the distal pole; upon nitrogen starvation, diploid cells that have switched to growth as pseudohyphal filaments preferentially bud in a unipolar distal pattern, where most of the buds emerge at the distal cell pole (Gimeno *et al.* 1992; Kron *et al.*, 1994).
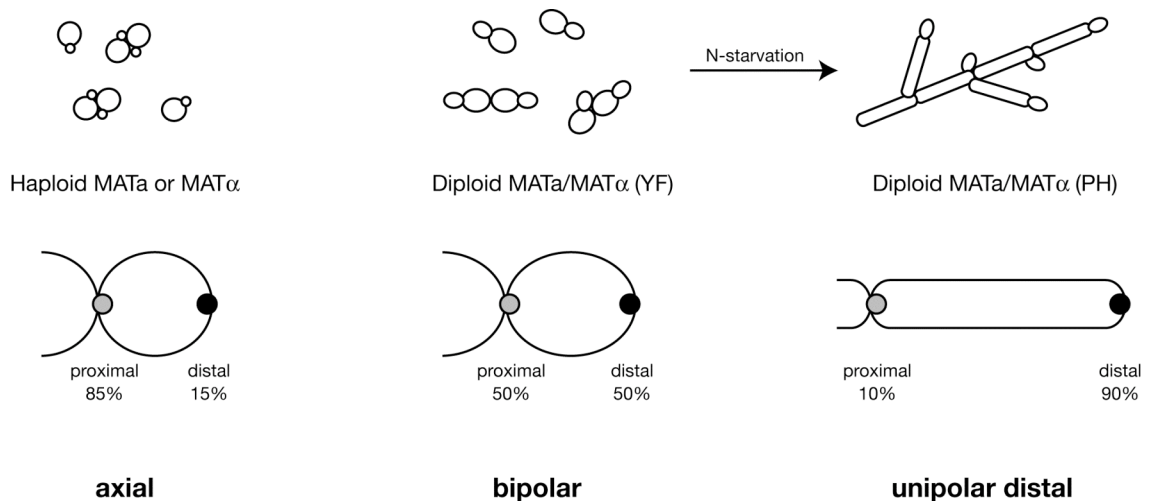
Fig. 3: Bud site selection patterns of different yeast cell types. Haploid **a** and α cells preferentially form buds in an axial pattern at the proximal pole, which corresponds to the birth site. Diploid **a**/α yeast form (YF) cells bud in a bipolar pattern, where buds are formed either at the proximal pole (that corresponds to the birth site) or at the site opposite to it, called the distal pole. Upon nitrogen starvation, diploid pseudohyphal (PH) cells bud in a unipolar distal pattern, where most buds emerge at the distal cell pole.

1.3.2 Choosing a direction for polarization: orienting axes for budding

Genetic analyses have revealed that selection of cell division sites is regulated by at least three different classes of genes and corresponding proteins (Madden and Snyder, 1998; Chant, 1999). The first class of genes is required for axial, bipolar and unipolar distal budding. This class includes *RSR1/BUD1*, *BUD2*, and *BUD5* (Bender and Pringle, 1989; Chant and Herskowitz, 1991; Chant *et al.*, 1991), and mutations in any of these genes cause random budding patterns in haploid and diploid cells. The corresponding gene products (Rsr1p/Bud1p, Bud2p, and Bud5p) constitute a GTPase signaling module that is assumed to assist in directing bud formation components to the selected site of growth. A second class is specifically required for the axial pattern of haploid cells without affecting the bipolar pattern of diploids. This class comprises the genes *AXL1*, *AXL2/BUD10*, *BUD3*, and *BUD4* (Chant and Herskowitz, 1991; Fujita *et al.*, 1994; Roemer *et al.*, 1996; Halme *et al.,* 1996). The products of these genes are involved in marking the mother-bud neck during one cell cycle as a site for budding in the next cell cycle. A third class is required for the bipolar budding pattern of diploid cells but not for haploid axial budding. Genetic screens have identified many genes corresponding to this class, including *AIP3/BUD6*, *BUD7*, *BUD8*, *BUD9*, *BNI1*, *PEA2*, and *SPA2* (Snyder, 1989; Valtz and Herskowitz, 1996; Zahner *et al.*, 1996). Mutations in most of these genes cause random budding specifically in diploid cells without affecting axial budding in haploids. Only two genes of this class, *BUD8* and *BUD9*, have been

6

described to shift the budding pattern from a bipolar pattern to a unipolar pattern and therefore appear to exhibit the most specific effects on bipolar budding. Mutations in *BUD8* cause a unipolar proximal budding pattern in diploids, whereas *bud9* mutants bud with a high frequency from the distal cell pole (Zahner *et al.*, 1996). Therefore, Bud8p and Bud9p have been proposed to act as bipolar landmarks that might recruit components of the common budding factors, e.g. Bud2p, Bud5p, or Rsr1p/Bud1p, to either one of the cell poles (Chant, 1999).

1.3.3 General polarity genes

As outlined above, *RSR1/BUD1*, *BUD2,* and *BUD5* belong to a class of genes that are important for axial budding, bipolar budding as well as for unipolar distal budding. The corresponding proteins Rsr1p/Bud1p, Bud2p, and Bud5p constitute a GTPase signaling module, which is thought to help direct bud formation components to the selected site of growth. Mutations in one of these genes lead to randomization of the budding patterns in haploid and diploid cells but no other obvious morphological phenotypes (Bender and Pringle, 1989; Chant *et al*., 1991; Chant and Herskowitz, 1991; Park *et al*., 1993). *RSR1/BUD1* encodes a Ras-related GTPase, whereas preceding experiments indicate that *BUD2* and *BUD5* encode a GTPase-activating protein (GAP) (Bender, 1993; Park *et al*., 1993) and a guanine-nucleotide exchange factor (GEF) (Chant *et al*., 1991; Powers *et al*., 1991; Zheng *et al*., 1995) for the Rsr1p/Bud1p GTPase, respectively. It is predicted that the activity of either Bud2p or Bud5p at the future bud site might regulate Rsr1p/Bud1p and hence mediate proper bud site selection (Madden and Snyder 1998).

Presumably, the Rsr1p/Bud1p GTPase signaling module directs bud formation components to cortical landmark proteins at future bud sites (Chant *et al*., 1991; Chant and Herskowitz, 1991; Herskowitz *et al*., 1995; Michelitch and Chant, 1996; Park *et al*., 1993). This hypothesis is consistent with the results of a previous study, which stated that Bud5p plays a key role in linking a spatial signal to polarity establishment (Kang *et al*., 2001). It was shown that Bud5p physically interacts with the axial landmark protein Axl2p/Bud10p. Recently, also a direct physical link between Bud5p and Bud8p could be established (Kang *et al*., 2004a).

Further genetic analyses suggest an interaction between the Rsr1p/Bud1p GTPase module and the polarity-establishment components Cdc42p, Cdc24p, and Bem1p. Cdc42p is a

Rac/Rho-type GTPase (Johnson and Pringle, 1990), whose activity is regulated by the GEF Cdc24p (Zheng *et al.*, 1995). Bem1p is an SH3-domain protein and functions as a scaffold protein that binds Cdc24p and Cdc42p (Leeuw *et al.*, 1995). All these proteins are involved in the establishment of yeast cell polarity, but up to the present, the mechanism by which the GTPase module and the polarity establishment components interact with the cortical tags is not known.

1.3.4 Genes required for the axial budding pattern
Cells exhibiting an axial budding pattern utilize a cytokinesis tag in which a component at the cytokinesis site persists into the next cell cycle and directs formation of a new bud at an adjacent site (Madden and Snyder, 1998). Presumably, this tag functions as template for directing assembly of bud formation components at the selected site growth (Chant and Herskowitz, 1991; Madden *et al.*, 1992; Snyder *et al.*, 1991). Different yeast septin proteins such as Cdc3p, Cdc10p, Cdc11, and Cdc12p (Chant *et al.*, 1995 Flescher *et al.*, 1993) as well as Bud3p (Chant and Herskowitz, 1991; Chant *et al.*, 1995), Bud4p (Chant and Herskowitz, 1991; Sanders and Herskowitz, 1996), and Axl2p/Bud10p (Halme *et al.*, 1996; Roemer *et al.*, 1996) may be components of this tag.

Genetic studies led to identification of four proteins specifically required for axial budding: Bud3p, Bud4p, Axl1p, and Axl2p/Bud10p. Loss of any of these four proteins results in a bipolar budding pattern (Adames *et al.*, 1995; Fujita *et al.*, 1994; Sanders and Herskowitz, 1996). Bud3p and Bud4p were identified in a screen for mutants that are characterized to be defective in bud site selection (Chant and Herskowitz, 1991). The predicted Bud3p sequence is somewhat uninformative (Chant, 1999), whereas Bud4p contains a potential GTP-binding motif near its carboxy terminus. Both proteins could be localized as double rings encircling the mother-bud neck during mitosis, a pattern that is similar to that of the septins. Previous studies also exhibited that localization of Bud3p and Bud4p is dependent on the neck filament-associated proteins Cdc3p, Cdc4p, Cdc11p, and Cdc12p (Chant *et al.*, 1995; Sanders and Herskowitz, 1996). Conversely, there is no evidence for septin localization requiring Bud3p and Bud4p. These observations indicate that Bud3p and Bud4p assemble at the septin complex and that they help select cortical sites for axial budding (Madden and Snyder, 1998).

AXL2/BUD10 encodes a single-spanning integral membrane glycoprotein, which is required for axial budding in haploid cells (Halme *et al.*, 1996; Roemer *et al.*, 1996). The protein consists of a 300 amino acid (aa) intracellular domain and a 500 aa extracellular domain (Halme *et al.*, 1996; Roemer *et al.*, 1996), which is highly *O*-glycosylated by the mannosyltransferase Pmt4p (Sanders *et al.*, 1999). The localization pattern of Axl2p/Bud10p resembles that of many proteins involved in polarized growth as it localizes as a patch at the incipient bud site and at the bud periphery of small-budded cells (Roemer *et al.*, 1996). Moreover, Axl2p/Bud10p is also present in form of a ring at the bud neck in medium- and large-budded cells (Halme *et al.*, 1996, Roemer *et al.*, 1996), which is similar to the localization pattern of the putative neck filament proteins, Bud3p and Bud4p. The exact mechanism by which Axl2p/Bud10p participates in choosing the bud site is not yet known. Currently, it is assumed that there are two possibilities how Axl2p/Bud10p might function in axial bud site selection (Halme *et al.*, 1996, Roemer *et al.*, 1996). One possibility is that Axl2p/Bud10p functions together with the septin proteins Bud3p and/or Bud4p as part of the cytokinesis tag, which marks the site of cell division and recruits other proteins required for the establishment of polarized growth (Halme *et al.*, 1996, Roemer *et al.*, 1996); another possibility is that Axl2p/Bud10p is involved in tag recognition (Roemer *et al.*, 1996). Coincident with the hypothesis that Axl2p/Bud10p plays a role in tag recognition are observations that it localizes to the incipient bud site and that the *axl2Δ*/*bud10Δ* mutant strains contain 'droopy' buds, a phenotype suggestive of a role in the early steps of the bud formation (Roemer *et al.*, 1996; Madden and Snyder, 1998). A further convincing reason for the involvement of the protein in tag recognition is the fact that Axl2p/Bud10p physically interacts with Bud5p, which is part of the GTPase signaling module (Kang *et al.*, 2001).

A fourth gene that plays a role in axial bud site selection is *AXL1* (Adames *et al.*, 1995; Fujita *et al.*, 1994). This gene encodes a haploid-specific endoprotease, which performs one of two NH_2-terminal cleavages during maturation of the **a**-factor mating pheromone. However, the protease activity is not required for axial bud site selection (Adames *et al.*, 1995; Chen *et al.*, 1997; Fujita *et al.*, 1994; Lord *et al.*, 2002). *AXL1* is particularly interesting, because its expression is specific to haploid cells (Adames *et al.*, 1995; Fujita *et al.*, 1994). Furthermore, artificial high-level expression of *AXL1* in diploid cells promotes axial budding (Fujita *et al.*, 1994). However, this result must be interpreted cautiously, because *AXL1* was highly overexpressed and only a modest, twofold increase in budding at

the proximal pole was observed. Nevertheless, Axl1p is a candidate for a haploid-specific gene product that specifies axial budding in haploid cells (Madden and Snyder, 1998).

At least two further genes, *KRE9* and *HKR1*, are important for axial bud site selection. The gene product of *KRE9* encodes a glycoprotein that is involved in cell wall $(1 \rightarrow 6)$ β-glucan assembly, whereas Hkr1p is a serine/threonine-rich cell surface protein that plays a role in the regulation of cell wall $(1 \rightarrow 3)$ β-glucan biosynthesis (Brown and Bussey, 1993; Yabe *et al.*, 1996). Deletion of either *KRE9* or *HKR1* leads to an increase of budding events at random sites. There are two possibilities how the proteins might participate in the axial bud site selection: On the one hand, the mutations might affect either the localization or the function of a cortical tag like Axl2p/Bud10p, which has an extracellular domain, or, on the other hand, the mutations might disturb underlying cytoskeletal components to disrupt bud site selection. Thus, a combination of different proteins – intracellular cortical proteins, transmembrane proteins, and extracellular proteins – appears to be crucial for axial bud site selection in yeast (Madden and Snyder, 1998).

1.3.5 Genes required for the bipolar budding pattern

The bipolar budding pattern is more complex than axial budding in haploid cells. Generally, daughter cells bud at the distal pole, whereas mother cells choose either the proximal or the distal pole. A lot of genes have been identified in previous studies that are important for the establishment and maintenance of the bipolar budding pattern in diploid cells. However, much less is known about the molecular mechanisms by which proximal and distal sites are selected. A model according to Madden and Snyder (1998) is "that 'growth and polarity' components deposited at the cell surface during early bud formation and growth can serve as cortical tags for selecting distal sites in daughters." Another group of proteins localized at the neck region during cytokinesis might be involved in selecting proximal sites (Chant and Herskowitz, 1991; Chant *et al.*, 1995; Snyder *et al.*, 1991; Zahner *et al.*, 1996). As for the axial budding process in haploids, recognition of these components is thought to require the Rsr1p GTPase module.

1.3.5.1 The actin cytoskeleton and actin-binding proteins

The actin cytoskeleton and actin-binding proteins play an important role in the bipolar budding process. The yeast actin cytoskeleton consists of two filament-based structures: the

actin cortical patches and the actin cables (Adams and Pringle, 1984; Kilmartin and Adams, 1984), which are both assembled from monomers encoded by the *ACT1* gene. The actin cytoskeleton is essential for different processes, and, therefore, it is not astonishing that the actin cortical patches show a polarized distribution that changes during the cell cycle. First, actin localizes at the incipient bud, suggesting a role in bud emergence. Soon thereafter it is also found within the growing bud, indicating a role in bud growth. Late in the cell cycle the actin cortical patches reorganize into two rings in the neck, where they are believed to be involved in septation and cytokinesis.

A number of mutations in the *ACT1* gene that affect the bipolar budding in diploid cells have been identified (Drubin *et al.*, 1993; Yang *et al.*, 1997). Strikingly, these mutations only affect the budding pattern of diploid mother cells, which bud more and more randomly with each cell division. Interestingly, *ACT1* mutations do not influence the budding pattern of daughter cells and additionally have little or no effect on axial budding in haploid cells (Madden and Snyder, 1998). In further experiments, a distinct region on the actin protein was found that is thought to recognize bipolar-specific proteins or cues (Kabsch *et al.*, 1990; Wertman *et al.*, 1992; Yang *et al.*, 1997).

It should be noted that mutations in several genes would shift the bipolar pattern to a random pattern without affecting the axial pattern. One such group includes several genes encoding actin-associated proteins (e.g. Sac6p, Srv2p, Sla2p, Rvs167p), another contains genes whose gene products disrupt actin organization (e.g. Sla1p, Rvs161p). All mutations cause defects that are similar to those of *act1* mutations (Adams *et al.*, 1991; Amberg *et al.*, 1995; Bauer *et al.*, 1993; Crouzet *et al.*, 1991; Drubin, 1990; Drubin *et al.*, 1988; Freeman *et al.*, 1996; Holtzman *et al.*, 1993; McCann and Craig, 1997; Sivadon *et al.*, 1997; Vojtek *et al.*, 1991; Zhao *et al.*, 1995). It seems unlikely that all these gene products have a direct mechanistic role in bipolar budding, so most, if not all, of these genes are expected to affect the actin cytoskeleton or the secretory pathway (Chant, 1999).

Although most actin-associated proteins are apparently not important for distal budding of diploid cells, there is one exception: Bni1p. This protein belongs to the highly conserved formin protein family that can be found in *S. cerevisiae* (Evangelista *et al.*, 1997), *S. pombe* (Chang *et al.*, 1997, Petersen *et al.*, 1995), mouse (Mass *et al.*, 1990), and *Drosophila* (Castrillon and Wasserman, 1994; Emmons *et al.*, 1995). It could be demonstrated that Bni1p interacts with regulators of the actin cytoskeleton such as Cdc42p or profilin

(Evangelista *et al.*, 1997). Mutations in the *BNI1* gene become obvious only in diploid strains, which are characterized by a randomized budding pattern in the first and in subsequent divisions, whereas haploid *bni1Δ* strains exhibit a quite normal budding (Zahner *et al.*, 1996). Therefore, it is assumed that Bni1p might also be involved in the establishment of the distal tag in diploid daughter cells beside its function in bipolar budding of mother cells (Madden and Snyder, 1998).

1.3.5.2 Additional proteins participating in diploid bud site selection

Beside actin and actin-associated proteins, a variety of further components have been identified that also play a role in bipolar budding. It is evident that some of these proteins may also regulate the actin cytoskeleton. Spa2p, Pea2p, and Aip3p/Bud6p belong to a class of proteins, which are important for bipolar bud site selection (Amberg *et al.*, 1997; Snyder, 1989; Valtz and Herskowitz, 1996; Zahner *et al.*, 1996). Effects of mutations in *SPA2*, *PEA2*, and *AIP3/BUD6* are similar to *act1* mutations: selection of distal bud sites in diploid daughter cells is not affected, but the number of cells which choose random sites during budding increases with the number of successive cell divisions. A current model is that Spa2p, Pea2p, Aip3p/Bud6p, and Bni1p form a multiprotein complex - the 12S polarisome - that helps to concentrate the actin cytoskeleton and/or exocytic vesicles at growth sites (Sheu *et al.*, 1998). This idea is consistent with several observations: First, Spa2p, Pea2p, Aip3p/Bud6p, and Bni1p are able to interact with one another (Fujiwara *et al.*, 1998; Sheu *et al.*, 1998); second, Spa2p, Pea2p, Aip3p/Bud6p, and Bni1p co-localize at the tips of buds and mating projections (Amberg *et al.*, 1997; Evangelista *et al.*, 1997; Gehrung and Snyder, 1990; Snyder, 1989; Snyder *et al.*, 1991; Valtz and Herskowitz, 1996); and third, the examination of distribution of the polarized secretion marker Sec4p demonstrates that *spa2Δ, pea2Δ, aip3Δ/bud6Δ*, or *bni1Δ* mutant strains fail to concentrate Sec4p at the bud tip during apical growth and at the division site during repolarization just prior to cytokinesis (Sheu *et al.*, 1998). Therefore, it is likely that the 12S polarisome comprising Spa2p, Pea2p, Aip3p/Bud6p, and Bni1p concentrates components of the actin cytoskeleton and secretory vesicles at growth sites during growth and separation (Sheu *et al.*, 1998).

Two further proteins that appear to be implicated in the bipolar budding are Rax1p and Rax2p (Kang *et al.*, 2004b). The gene product that is encoded by *RAX2* is suggested to be an integral membrane protein with type I orientation. Rax1p also appears to be an integral

membrane protein but a detailed characterization of this protein requires considerable further investigations. Both genes, *RAX1* and *RAX2,* were originally identified in a mutant screen in which an *axl1* strain, which buds in the bipolar budding pattern, was mutagenized and examined for isolates defective for the bipolar budding pattern (Chen *et al.*, 2000; Fujita *et al.*, 1994). However, it became clear that this phenotype reflects the involvement of Rax1p and Rax2p in bipolar rather than in axial budding. Further examinations of the mutant phenotypes then revealed that *rax1* and *rax2* mutations do not influence the axial budding of haploid cells but that they disrupt bipolar budding of diploids (Chen *et al.*, 2000; Kang *et al.*, 2004b; Ni and Snyder, 2001). It could be shown that both proteins play a role in selecting bud sites at both the distal and the proximal poles of daughter cells as well as near previously used division sites on mother cells (Kang *et al.*, 2004b). Careful analysis suggests that Rax1p and Rax2p function together in helping to mark the sites that are thought to possess landmarks used in bipolar budding (Chant and Pringle, 1995). Several additional observations are consistent with this model (Kang *et al.*, 2004b). First, Rax1p and Rax2p localize interdependently at the tips of buds and the distal poles of daughter cells as well as at the division site on both mother and daughter cell. Localization to the division site was persistent through multiple cell cycles. Second, in co-purification experiments it was shown that Rax1p interacts with both Bud8p at the bud tip and the distal pole and with Bud9p at the proximal pole. Because of the existing association between Rax1p and Rax2p an interaction between Rax1p and the potential marker proteins Bud8p and Bud9p can be assumed. In additional experiments, it was also found that the localization of Rax1p and Rax2p to the bud tip and the distal pole depends on the presence of Bud8p, whereas a normal localization of Bud8p is only partially dependent on Rax1p and Rax2p. Although localization of Rax1p and Rax2p to the division site did not appear to depend on Bud9p, normal localization of the proximal pole marker appeared largely or entirely dependent on Rax1p and Rax2p (Kang *et al.*, 2004b). Taken together, these data indicate that Rax1p and Rax2p interact closely with each other and with the landmark proteins Bud8p and Bud9p in the establishment and/or maintenance of the cortical landmarks for bipolar budding.

The genes *SUR4*, *FEN1*, and *BUD7* encode additional proteins required for the bipolar budding. *SUR4* and *FEN1* code for homologous and functionally redundant proteins (Revardel *et al.*, 1995). Unfortunately, less is known about these proteins. To date, it is known that mutations in *SUR4* and *FEN1* cause randomization of the bipolar budding pattern. This

defect has not been analyzed in detail but suggests the involvement of the proteins in the bipolar budding process (Durrens *et al.*, 1995; Revardel *et al.*, 1995). A mutation in *BUD7* causes heterogeneous defects in bipolar budding: in contrast to a normal budding, the **a**/α cells produce chains of bud sites starting at the distal pole or the equatorial region, as well as the proximal pole (Zahner *et al.*, 1996); a null allele of *BUD7* has not been reported. Further studies with respect to *SUR4, FEN1*, and *BUD7* may provide additional insights into mechanisms for recognition of sites during bipolar budding of diploid yeast cells (Madden and Snyder, 1998).

1.3.5.3 The role of Ste20p and the diploid-specific landmark proteins Bud8p and Bud9p

Beside the proteins described above, three further components - Bud8p, Bud9p, and Ste20p - play essential roles in the bipolar budding process. Deletions of the corresponding genes cause a unipolar budding pattern in diploid cells (Sheu *et al.*, 2000; Taheri *et al.*, 2000; Zahner *et al.*, 1996).

STE20 encodes a signal transducting kinase of the PAK (p21-activated kinase) family. It could be demonstrated by Sheu *et al.* (2000) that Ste20p is involved in both apical growth and bipolar bud site selection. Disruption of the gene results in cell elongation defects and shortens the apical growth phase. Furthermore, mutations in *STE20* result in a unipolar budding pattern with bud scars clustered adjacent to the birth scar, at the proximal pole (Sheu *et al.*, 2000). This budding pattern is identical to that of diploid *bud8Δ* mutants and *ste20Δ bud8Δ* double mutants. The observation of this phenotype indicates that Ste20p and Bud8p, which is proposed as cortical tag at the distal cell pole, function in the same pathway to promote budding at the distal pole. In addition, it has been shown that Ste20p and Bud8p interact in the yeast two-hybrid system (Drees *et al.*, 2001). However, the exact function of Ste20p could not be clarified in detail. It is supposed that Ste20p might be involved in phosphorylating the potential distal tag Bud8p in addition to its role in apical growth. Another hypothesis according to Sheu *et al.* (2000) is that Bud8p may function in apical growth like Ste20p. More information about Ste20p is given below (see chapter 1.3.7).

The bipolar budding pattern of diploid cells appears to depend on persistent spatial markers in the cortex at the two poles of the cell. Previous analysis of mutants that affect the bipolar budding pattern of diploid cells but not the axial pattern of haploids identified two interesting candidates, *BUD8* and *BUD9*. Corresponding gene products potentially represent

components of markers at the poles distal and proximal to the birth scar, respectively, a hypothesis that is supported by further studies. Mutations in *BUD8* and *BUD9* have been described to shift the bipolar to a unipolar budding pattern with bias to either the distal or the proximal pole. Thus, *BUD8* and *BUD9* appear to have the most specific effects on bipolar budding (Mösch and Fink, 1997; Taheri *et al.*, 2000; Zahner *et al.*, 1996). Diploid *bud8Δ/bud8Δ* mutant strains bud predominantly at the proximal pole, whereas *bud9Δ/bud9Δ* mutants choose the distal pole for budding (Chant, 1999; Harkins *et al.*, 2001; Taheri *et al.*, 2000). Strains lacking both genes exhibit a randomization of their budding pattern with bud scars being scattered all over the cell surface. This phenotype suggests that the bipolar budding pathway has been totally disabled. Furthermore, it could be shown that the expression of these genes at high levels can cause either an increased bias for budding at the distal (*BUD8*) or the proximal (*BUD9*) pole or a randomization of the bud position, depending on the level of expression (Harkins *et al.*, 2001).

The biochemical properties and localizations of Bud8p and Bud9p are consistent with their postulated roles as cortical landmark proteins. Both proteins appear to be integral membrane proteins of the plasma membrane. The overall structures of Bud8p and Bud9p are similar in that both are predicted to consist of a large NH_2-terminal extracellular domain that is highly *N*- and *O*-glycosylated followed by a pair of putative membrane-spanning domains, surrounding a short loop which is presumably cytoplasmic, and a very short extracellular domain at the COOH-terminus (Chant, 1999; Harkins *et al.*, 2001; Taheri *et al.*, 2000). The putative transmembrane and cytoplasmic domains of the two proteins are very similar in sequence, suggesting that these parts of Bud8p and Bud9p might be important for the recruitment of the common budding factors, e.g. Rsr1p/Bud1p, Bud2p, and Bud5p, which are necessary to transmit the positional information from (the axial and bipolar) cortical markers to the proteins responsible for cell polarization (Chant, 1999; Harkins *et al.*, 2001; Pringle *et al.*, 1995; Taheri *et al.*, 2000).

When Bud8p and Bud9p are localized by fluorescence microscopy, each protein can be found at the expected location: Bud8p appears to localize primarily to the presumptive bud site, the distal pole of the bud, and the distal pole of daughter cells (Harkins *et al.*, 2001; Taheri *et al.*, 2000). Bud9p localizes at the presumptive bud site, the bud tip of growing daughter cells, as well as the mother-daughter neck region, apparently the proximal pole of the daughter cell (Harkins *et al.*, 2001). Because Bud9p is also found at the distal pole and

physically interacts with Bud8p, it might fulfil an additional function at the this pole where it seems to act as a nutritionally controlled inhibitor of distal budding (Fig. 4; Taheri *et al.*, 2000). Further examinations concerning the localization of both proteins exhibited that the delivery of Bud8p is dependent on actin, whereas the delivery of Bud9p is dependent on actin and septin (Harkins *et al.*, 2001; Schenkman *et al.*, 2002).
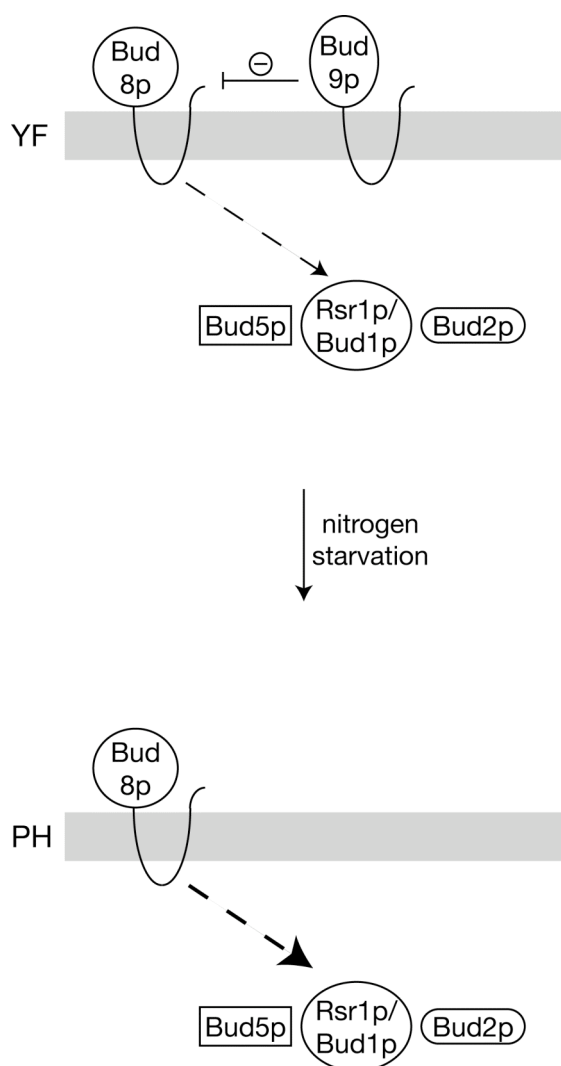
Fig. 4: Model for regulation of bud site selection at the distal cell pole of *S. cerevisiae.* In yeast form (YF) cells, Bud9p is localized at the distal cell pole and interferes with Bud8p-mediated bud site selection *via* the Rsr1p/Bud1p-Bud5p-Bud2p GTPase module. In pseudohyphal (PH) cells, nutritional starvation for nitrogen prevents distal localization of Bud9p, allowing efficient Bud8p-mediated distal budding.

Previous data indicate that the transcription of *BUD8* and *BUD9* is cell cycle-regulated. Examinations of Bud8p by fluorescence microscopy suggests that the protein is delivered to the nascent bud site shortly before or coincident with bud emergence, whereas Bud9p appears to be delivered to the neck very late in the cell cycle just before cytokinesis

16

(Schenkman *et al.*, 2002). In general agreement with the assumption that the delivery of Bud8p and Bud9p appears to be under different cell cycle control, further experiments exhibited that the *BUD8* mRNA peaks in G2/M, whereas *BUD9* mRNA peaks in late G1. These results were surprising in that each mRNA peaked long before the corresponding protein appears to be delivered to the cell surface (Schenkman *et al.*, 2002). The timing of gene expression seems to be the primary determinant of Bud8p and Bud9p localization and function: when Bud8p is expressed from the *BUD9* promoter, it localizes if it were Bud9p and appears fully competent to provide Bud9p (but not Bud8p) function. Moreover, when Bud9p is expressed from the *BUD8* promoter, it localizes as if it was Bud8p and is unable to provide Bud9p function; however, the protein at the distal pole is only partially effective in providing Bud8p function. Thus, features of the Bud8p polypeptide itself are likely to be important for its efficient delivery, stability, and/or function at the distal cell pole (Schenkman *et al.*, 2002).

Although genetic and cell biological analyses have led to the identification of a large number of components that constitute the bud site selection pathway in diploid yeast cells, the molecular functions of both Bud8p and Bud9p are poorly understood. For instance, distinct domains that are important for a correct function and polar localization of these potential landmark proteins are not known.

1.3.6 Genes required for the unipolar distal budding

In response to nitrogen starvation, diploid yeast cells are able to switch their bipolar budding pattern to a unipolar distal one, where most of the buds emerge at the distal cell pole. This unipolar distal budding program is required for the establishment of filamentous structures and therefore can be viewed as a process that is regulated by nutritional signals to guide the direction of the growing pseudohyphal filaments (Mösch, 2002). Therefore, pseudohyphal development is an optimal model to study factors that determine oriented cell division in response to external signals. However, the molecular mechanisms that control this change in cell polarity are only little understood, because most studies have addressed the function of genes controlling bud site selection under nutrient-rich conditions where *S. cerevisiae* will grow and divide as single yeast form cells. Only a few studies have aimed at identification of genes required for the unipolar distal pattern of the pseudohyphal growth form.

To date, no class of genes has been identified that is specifically required for the unipolar distal of PH cells without affecting the bipolar budding of YF cells. An initial study

has identified Rsr1p/Bud1p to be required for the pseudohyphal development, because expression in the dominant negative form of *RSR1/BUD1*, *RSR1^{Asn16}*, suppresses filament formation in response to nitrogen starvation (Gimeno *et al.*, 1992). This suggestion is confirmed by data from another study that showed that strains lacking *RSR1/BUD1* are not able to undergo filamentous growth (Taheri *et al.*, 2000).

A genetic screen directed at the identification of genes specifically required for pseudohyphal development has revealed several genes that are actually known to be important for bipolar bud site selection, e.g. *BUD8*, *BNI1*, *PEA2*, and *SPA2* (Mösch and Fink, 1997). These findings suggest that the pseudohyphal polarity switch might be achieved by alteration of components that control the bipolar budding process (Mösch, 2002).

1.3.7 The role of polarity establishment components

A set of proteins that are critical for bud formation in yeast are the polarity establishment proteins. These include Cdc42p, a GTPase most closely related to members of the Rho family, and its GEF, Cdc24p (Adams *et al.*, 1990; Sloat *et al.*, 1981; Zheng *et al.*, 1994). Cells containing temperature-sensitive mutations in either of these genes fail to form buds and form large, round, unbudded cells with multiple nuclei (Adams *et al.*, 1990; Field and Schekman, 1980; Sloat and Pringle, 1978; Sloat *et al.*, 1981). At restrictive temperature, these strains fail to localize many polarized components important for yeast budding properly, including Spa2p, actin patches, and septins (Adams and Pringle, 1984; Adams *et al.*, 1990; Johnson and Pringle, 1990; Snyder *et al.*, 1991; Ziman *et al.*, 1991).

In localization studies Cdc42p was detected at polarized sites of growth, whereas Cdc24p, its GEF, localizes over the entire cell periphery (Pringle *et al.*, 1995). Therefore, either Cdc24p functions only at polarized growth sites where Cdc42p accumulates or it has additional targets besides Cdc42p (Madden and Snyder, 1998). Published data from Zheng *et al.* (1993) suggest that Cdc24p regulates the activity of Cdc42p.

In mammalian cells, Cdc42p interacts with the PAK protein kinase to help mediating cell polarization (Manser *et al.*, 1994; Martin *et al.*, 1995). Yeast cells contain three PAK kinase homologs, Ste20p (see chapter 1.3.5.3), Cla4p, and Skm1p (Cvrcková *et al.*, 1995; Martin *et al.*, 1997). Strains containing either *ste20Δ* or *cla4Δ* or *skm1Δ* are viable and do not exhibit any apparent defects (Cvrcková *et al.*, 1995; Martin *et al.*, 1997). Interestingly, *ste20Δ cla4Δ* double mutant strains are not viable indicating that the functions between these two

kinases overlap (Cvrcková *et al.*, 1995). Combinations between the *skm1Δ* mutation with either *ste20Δ* or *cla4Δ* produced no detectable phenotype indicating that Skm1p is not redundant with Ste20p or Cla4p (Martin *et al.*, 1997), but the exact function of Skm1p is not known. Further studies revealed that Ste20p and Cla4p interact physically with Cdc42p and that this association is important for the function(s) of these proteins (Cvrcková *et al.*, 1995, Leberer *et al.*, 1997; Peter *et al.*, 1996; Simon *et al.*, 1995).

Another protein that helps to establish and maintain polarity in yeast is Bni1p. Bni1p is a member of the highly conserved formin protein family found in *S. cerevisiae* (Evangelista *et al.*, 1997), *S. pombe* (Chang *et al.*, 1997; Petersen *et al.*, 1995), mouse (Torres *et al.*, 1991), and *Drosophila* (Castrillon and Wasserman, 1994; Emmons *et al.*, 1995). Bni1p associated with actin in two-hybrid assays and with regulators of the actin cytoskeleton (Cdc42p) and its effectors (Ste20p and Cla4p) in co-immunoprecipitation or *in vitro* binding experiments (Evangelista *et al.*, 1997). Diploid *bni1Δ* mutant strains bud randomly both in the first division and in subsequent division (Zahner *et al.*, 1996), but *bni1Δ* haploid cells bud normally. Thus, Bni1p might play an important role in the establishment of the distal tag in diploid daughter cells.

Other components that genetically interact with Cdc42p and Cdc24p have been identified. These include Bem3p, a Rho-GAP homolog that serves as a GTPase activating protein for Cdc42p *in vitro* (Stevenson *et al.*, 1995; Zheng *et al.*, 1993; Zheng *et al.*, 1994). Rga1p and Rga2p, two Rho-GAP homologs, serve as GAPs for Cdc42p *in vivo* (Stevenson *et al.*, 1995). Moreover, both proteins are involved in control of septin organization, pheromone response, and haploid invasive growth (Smith *et al.*, 2002). Zds1p and Zds2p appear to down-regulate Cdc42p *in vivo* (Bi and Pringle, 1996). Mutations in another polarity establishment protein, *BEM1*, are co-lethal with *MSB1*, a high-copy suppressor of both *cdc24* and *cdc42* (Bender and Pringle, 1991). Bem1p is an SH3-domain protein that physically interacts with Cdc24p, Ste5p, and Ste20p (Leeuw *et al.*, 1995). It could be shown that this protein strongly facilitates bud emergence, possibly as a scaffold to assist the clustering of Cdc24p-Cdc42p (Pruyne and Bretscher, 2000a). Finally, two potential targets of Cdc42p, Gic1p and Gic2p, have been described recently; Gic1p and Gic2p interact genetically with Cdc42p and contain a CRIB domain, which is characteristic of many Cdc42p-interacting proteins (Brown *et al.*, 1997; Chen *et al.*, 1997). Bem1p, Gic1p, Gic2p, Zds1p, and Zds2p are all important for cell polarity in yeast, and each of these proteins except Zds2p is localized to sites of polarized cell

growth, similar to Cdc42p (Bi and Pringle, 1996; Brown *et al.*, 1997; Chen *et al.*, 1997; Pringle *et al.*, 1995).

1.3.8 A model for choosing bud sites in the axial and bipolar pattern

Both haploid and diploid yeast cells use spatial cues for producing the axial or bipolar budding pattern. In case of haploid cells, Bud10p is assumed to function as marker protein for the axial budding process (Fig. 5). The extracellular domain of Bud10p is highly glycosylated and may serve to anchor the protein in the cell wall. Besides Bud10p, septins, Bud3p, and Bud4p are also part of the so-called cytokinesis tag, and the tight clustering between these proteins presumably helps to generate a potent signal (Roemer *et al.*, 1996; Halme *et al.*, 1996). Kang *et al.* (2001) could show that Bud10p directly interacts with Bud5p, which is a component of the Bud1p GTPase signaling module. Local activation of the Bud1p GTPase in turn activates the Cdc42p GTPase, which leads to recruitment of other proteins required for establishment of polarized growth.

Diploid yeast cells use spatial cues for producing the bipolar pattern that are entirely distinct from those used in the axial pattern (Chant, 1999). In diploids, Bud8p and Bud9p were proposed to function as bipolar landmarks at the distal and proximal pole, respectively (Fig. 5). As described before, sequence analyses on Bud8p and Bud9p predict related transmembrane proteins that are highly glycosylated (Harkins *et al.*, 2000). A physical interaction between Bud8p and Bud5p was shown by Kang *et al.* (2004a), an association between Bud9p and Bud5p is demonstrated in this work. It is supposed that the same components needed for polarity establishment in haploids are involved in further signal transduction that finally leads to recruitment of components essential for polarized growth.
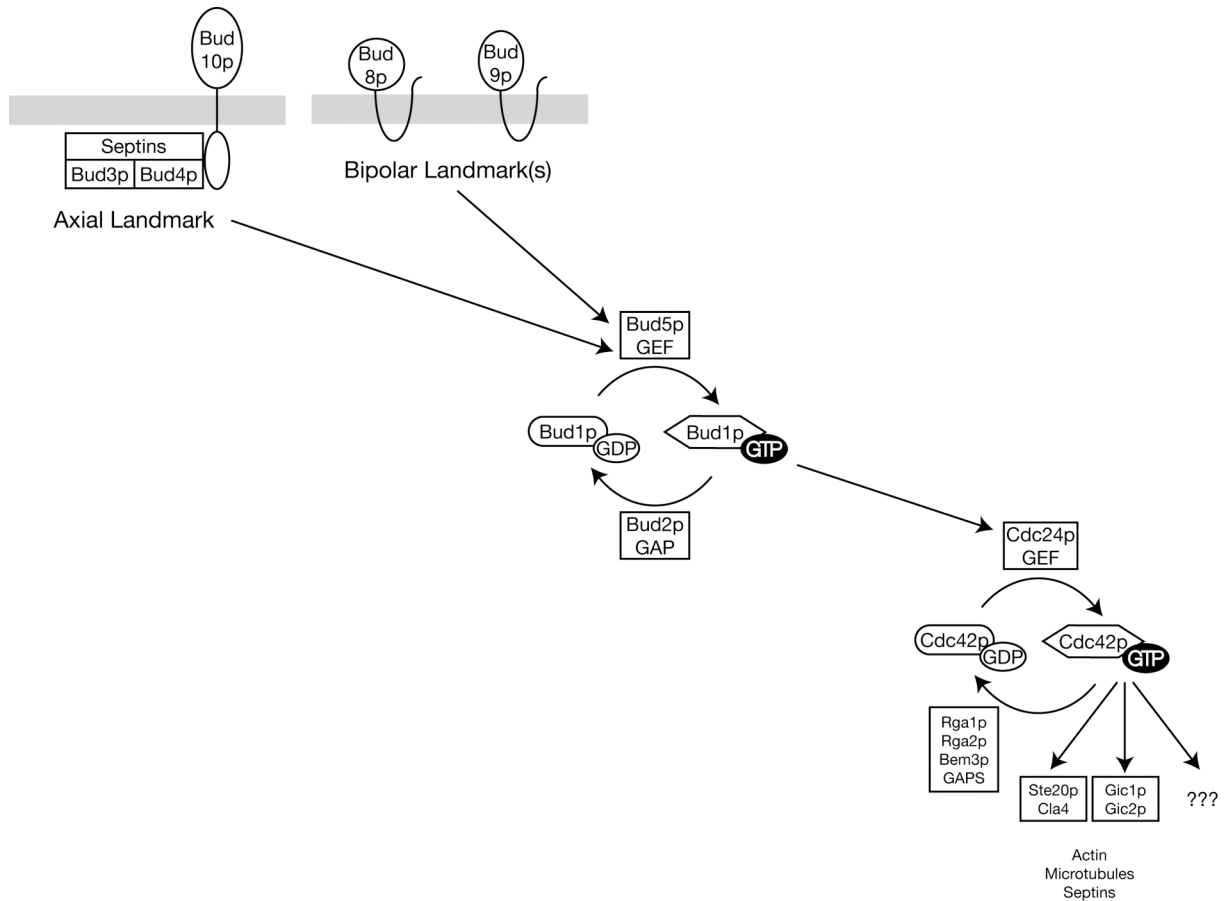
Fig. 5: Molecular machinery guiding the axes of polarization during budding. Both haploid and diploid yeast cells use spatial cues for producing the axial and bipolar budding pattern, respectively. In haploid yeast cells, Bud10p functions as spatial landmark protein for axial budding. In diploids, Bud8p and Bud9p fulfill a function as distal and proximal pole marker, respectively. These markers interact with Bud5p, a component of the Bud1p GTPase signaling module. Local activation of the Bud1p GTPase in turn activates the Cdc42p GTPase, which leads to recruitment of other proteins required for establishment of polarized growth.

1.4 Aim of this Work

Although genetic and cell biological analysis has led to the identification of a large number of components that constitute the bud site selection pathway in diploid yeast cells, the molecular function of the involved factors is poorly understood in many cases. Within the scope of this work, it was intended to better characterize individual components that play a role in the process of bud site selection in yeast.

The potential landmark proteins Bud8p and Bud9p are objects of peculiar interest. It is known that both Bud8p and Bud9p localize to the distal and the proximal pole, respectively, to fulfill their function as landmarks in the bipolar budding process of diploid cells. In former studies concerning the localization of Bud8p and Bud9p, the proteins were each investigated separately. To get a better insight in appearance of the landmark proteins, one purpose of this study should be the realization of co-localization experiments enabling the detection of both Bud8p and Bud9p within the same cell.

As described in above, the overall structure of Bud8p and Bud9p is similar in that both proteins are predicted to consist of a large NH_2-terminal extracellular domain, followed by a membrane-spanning domain (TM1), a short cytoplasmic loop, a second membrane-spanning domain (TM2), and a very short extracellular domain at the COOH-terminus. The NH_2-terminal portion of both proteins contains several *N*- and *O*-glycosylation sites that appear to be functional. However, characterization of distinct domains of the landmark proteins that are required for, e.g., correct function of the proteins, transport of the proteins to the cell poles, or that confer interaction with other proteins or downstream components of the budding machinery are not known. To answer this these questions, a systemic analysis of Bud8p and Bud9p should be carried out to better understand the structure and the function of the bipolar landmark proteins. Furthermore, deletion sets resulting from systemic analysis of Bud8p and Bud9p should be used to investigate the existing association between Bud8p and Bud9p and their interaction partners Bud5p and Rax1p *via* co-immunoprecipitation experiments.

In a last approach, investigations should be carried out to get more information on the intracellular transport of Bud8p and Bud9p to the yeast cell poles. Therefore, tagged versions of both proteins should be investigated by 'pulse-chase' experiments, which should allow predictions about secretion of the proteins *via* the secretory pathway and their half-life periods within the cell.

2. Materials and Methods

2.1 Materials

2.1.1 Chemicals, enzymes, and antibodies

Chemicals used for the production of solutions, buffers and culture media were sourced from MERCK (Darmstadt, D), ROCHE GMBH (Mannheim, D), CARL ROTH GMBH & CO KG (Karlsruhe, D), INVITROGEN GMBH (Karlsruhe, D), FLUKA (Neu-Ulm, D) and SIGMA-ALDRICH CHEMIE GMBH (Steinheim, D).

Restriction enzymes, DNA modifying enzymes as well as *Taq* and *Pfu* polymerase were provided by NEW ENGLAND BIOLABS (Ipswich, MA, USA), MBI FERMENTAS (Vilnius, Lit) and PROMEGA (Madison, WI, USA). KOD HIFI DNA polymerase is fabricated by NOVAGEN (Darmstadt, D). As DNA size standards 'GENE RULER 1 kb DNA ladder Plus' from MBI FERMENTAS (Vilnius, Lit) and '1 kb DNA ladder' from NEW ENGLAND BIOLABS (Ipswich, MA, USA) were used. Agarose for preparation of gels was provided from CARL ROTH GMBH & CO KG. Preparation of plasmid DNA from *Escherichia coli* and extraction of DNA from gels was carried out using kits from QIAGEN (Hilden, D).

DNA sequencing chemicals were provided by APPLIED BIOSYSTEMS GMBH (Weiterstadt, D). Synthetic oligonucleotides were purchased from INVITROGEN. Bradford solution for the determination of protein contents was provided by BIORAD INDUSTRIES GMBH (München, D).

'See Blue Pre-Stained' (Novex, San Diego CA, USA), 'Prestained Protein Molecular Weight Marker' (MBI FERMENTAS) as well as 'Rainbow marker RPN 756' from AMERSHAM LIFE SCIENCE (Uppsala, S) were used as marker for determination of protein weight. SDS protein gels were blotted on nitrocellulose membrane obtained from SCHLEICHER & SCHUELL (Dassel, D). Antibodies were produced by MOLECULAR PROBES (Eugene, OR, USA) and SANTA CRUZ BIOTECH INC. (Santa Cruz, CA, USA) and detected on Hyperfilm™-ECL™ (AMERSHAM PHARMACIA BIOTECH, Buckinghamshire, GB).

2.1.2 Yeast strains, plasmids, and oligonucleotides

The yeast strains used in this study are listed in Table 1. All strains are congenic to the Σ1278b genetic background. The construction of corresponding strains containing mutant alleles of *BUD8* and *BUD9*, respectively, and/or tagged genes is described below. Standard

methods for transformation and genetic crosses were used, and standard yeast culture YPD, YNB and SC media were prepared essentially as described (Guthrie and Fink, 1991). Plasmids used in this study are listed in Table 2, their construction is described below; sequences of oligonucleotides used in this study are listed in Table 3.

Table 1: *Saccaromyces cerevisiae* strains used in this study

Strain	Genotype	Source
RH2448	**a**/α *rsr1Δ::kanR/rsrΔ1::kanR ura3-52/ura3-52 leu2::hisG/LEU2 trp1::hisG/TRP1*	Taheri *et al.*, 2000
RH2449	**a**/α *bud8Δ::HIS3/bud8Δ::HIS3 ura3-52/ura3-52 his3::hisG/his3::hisG leu2::hisG/LEU2 trp1::hisG/TRP1*	Taheri *et al.*, 2000
RH2453	**a**/α *bud8Δ::HIS3/bud8Δ::HIS3 bud9Δ::HIS3/bud9Δ::HIS3 ura3-52/ura3-52 his3::hisG/his3::hisG leu2::hisG/LEU2 trp1::hisG/TRP1*	Taheri *et al.*, 2000
RH2495	**a**/α *ura3-52/ura3-52 leu2::hisG/leu2::hisG his3::hisG/HIS3 trp1::hisG/TRP1*	Taheri *et al.*, 2000
RH2905	**a** *myc⁹-BUD9-TRP1 bud9Δ::HIS3 ura3-52 his3::hisG leu2::hisG trp1::hisG*	this study
RH2906	**a** *myc⁹-BUD9^{Δ8-48}-TRP1 bud9Δ::HIS3 ura3-52 his3::hisG leu2::hisG trp1::hisG*	this study
RH2907	**a** *myc⁹-BUD9^{Δ8-130}-TRP1 bud9Δ::HIS3 ura3-52 his3::hisG leu2::hisG trp1::hisG*	this study
RH2908	**a** *myc⁹-BUD9^{Δ91-130}-TRP1 bud9Δ::HIS3 ura3-52 his3::hisG leu2::hisG trp1::hisG*	this study
RH2909	**a** *myc⁹-BUD9^{Δ91-218}-TRP1 bud9Δ::HIS3 ura3-52 his3::hisG leu2::hisG trp1::hisG*	this study
RH2910	**a** *myc⁹-BUD9^{Δ168-218}-TRP1 bud9Δ::HIS3 ura3-52 his3::hisG leu2::hisG trp1::hisG*	this study
RH2911	**a** *myc⁹-BUD9^{Δ168-283}-TRP1 bud9Δ::HIS3 ura3-52 his3::hisG leu2::hisG trp1::hisG*	this study
RH2912	**a** *myc⁹-BUD9^{Δ244-283}-TRP1 bud9Δ::HIS3 ura3-52 his3::hisG leu2::hisG trp1::hisG*	this study
RH2913	**a** *myc⁹-BUD9^{Δ244-369}-TRP1 bud9Δ::HIS3 ura3-52 his3::hisG leu2::hisG trp1::hisG*	this study
RH2914	**a** *myc⁹-BUD9^{Δ323-369}-TRP1 bud9Δ::HIS3 ura3-52 his3::hisG leu2::hisG trp1::hisG*	this study
RH2915	**a** *myc⁹-BUD9^{Δ323-450}-TRP1 bud9Δ::HIS3 ura3-52 his3::hisG leu2::hisG trp1::hisG*	this study
RH2916	**a** *myc⁹-BUD9^{Δ406-450}-TRP1 bud9Δ::HIS3 ura3-52 his3::hisG leu2::hisG trp1::hisG*	this study
RH2917	**a** *myc⁹-BUD9^{Δ406-544}-TRP1 bud9Δ::HIS3 ura3-52 his3::hisG leu2::hisG trp1::hisG*	this study

RH2918	**a** *myc⁹-BUD9^{Δ460-544}-TRP1 bud9Δ::HIS3 ura3-52 his3::hisG leu2::hisG trp1::hisG*	this study
RH2919	α *myc⁹-BUD9-LEU2 bud9Δ::HIS3 ura3-52 his3::hisG leu2::hisG trp1::hisG*	this study
RH2920	α *myc⁹-BUD9^{Δ8-48}-LEU2 bud9Δ::HIS3 ura3-52 his3::hisG leu2::hisG trp1::hisG*	this study
RH2921	α *myc⁹-BUD9^{Δ8-130}-LEU2 bud9Δ::HIS3 ura3-52 his3::hisG leu2::hisG trp1::hisG*	this study
RH2922	α *myc⁹-BUD9^{Δ91-130}-LEU2 bud9Δ::HIS3 ura3-52 his3::hisG leu2::hisG trp1::hisG*	this study
RH2923	α *myc⁹-BUD9^{Δ91-218}-LEU2 bud9Δ::HIS3 ura3-52 his3::hisG leu2::hisG trp1::hisG*	this study
RH2924	α *myc⁹-BUD9^{Δ168-218}-LEU2 bud9Δ::HIS3 ura3-52 his3::hisG leu2::hisG trp1::hisG*	this study
RH2925	α *myc⁹-BUD9^{Δ168-283}-LEU2 bud9Δ::HIS3 ura3-52 his3::hisG leu2::hisG trp1::hisG*	this study
RH2926	α *myc⁹-BUD9^{Δ244-283}-LEU2 bud9Δ::HIS3 ura3-52 his3::hisG leu2::hisG trp1::hisG*	this study
RH2927	α *myc⁹-BUD9^{Δ244-369}-LEU2 bud9Δ::HIS3 ura3-52 his3::hisG leu2::hisG trp1::hisG*	this study
RH2928	α *myc⁹-BUD9^{Δ323-369}-LEU2 bud9Δ::HIS3 ura3-52 his3::hisG leu2::hisG trp1::hisG*	this study
RH2929	α *myc⁹-BUD9^{Δ323-450}-LEU2 bud9Δ::HIS3 ura3-52 his3::hisG leu2::hisG trp1::hisG*	this study
RH2930	α *myc⁹-BUD9^{Δ406-450}-LEU2 bud9Δ::HIS3 ura3-52 his3::hisG leu2::hisG trp1::hisG*	this study
RH2931	α *myc⁹-BUD9^{Δ406-544}-LEU2 bud9Δ::HIS3 ura3-52 his3::hisG leu2::hisG trp1::hisG*	this study
RH2932	α *myc⁹-BUD9^{Δ460-544}-LEU2 bud9Δ::HIS3 ura3-52 his3::hisG leu2::hisG trp1::hisG*	this study
YHUM829	**a**/α *ura3-52/ura3-52 his3::hisG/his3::hisG leu2::hisG/leu2::hisG*	strain collection H.-U. Mösch
YHUM992	**a**/α *bud8Δ::HIS3/bud8Δ::HIS3 his3::hisG/his3::hisG leu2::hisG/LEU2 trp1::hisG/TRP1*	this study
YHUM993	**a**/α *bud9Δ::HIS3/bud9Δ::HIS3 his3::hisG/his3::hisG ura3-52/ura3-52 TRP1/trp1::hisG leu2::hisG/LEU2*	this study
YHUM904	**a** *bud8Δ::HIS3 ura3-52 his3::hisG trp1::hisG*	strain collection H.-U. Mösch
YHUM861	α *bud8Δ::HIS3 ura3-52 his3::hisG leu2::hisG*	strain collection H.-U. Mösch
YHUM994	**a** *bud9Δ::HIS3 ura3-52 his3::hisG leu2::hisG trp1::hisG*	this study
YHUM995	α *bud9Δ::HIS3 ura3-52 his3::hisG leu2::hisG trp1::hisG*	this study

25

YHUM842	**a**/α *myc^6-BUD8-URA3/myc^6-BUD8-URA3 bud8Δ::HIS3/bud8Δ::HIS3 his3::hisG/his3::hisG leu2::hisG/LEU2 trp1::hisG/TRP1*	this study
YHUM843	**a**/α *myc^6-BUD8$^{Δ7-53}$-URA3/myc^6-BUD8$^{Δ7-53}$-URA3 bud8Δ::HIS3/bud8Δ::HIS3 his3::hisG/his3::hisG leu2::hisG/LEU2 trp1::hisG/TRP1*	this study
YHUM844	**a**/α *myc^6-BUD8$^{Δ7-114}$-URA3/myc^6-BUD8$^{Δ7-114}$-URA3 bud8Δ::HIS3/bud8Δ::HIS3 his3::hisG/his3::hisG leu2::hisG/LEU2 trp1::hisG/TRP1*	this study
YHUM847	**a**/α *myc^6-BUD8$^{Δ74-114}$-URA3/myc^6-BUD8$^{Δ74-114}$-URA3 bud8Δ::HIS3/bud8Δ::HIS3 his3::hisG/his3::hisG leu2::hisG/LEU2 trp1::hisG/TRP1*	this study
YHUM848	**a**/α *myc^6-BUD8$^{Δ74-216}$-URA3/myc^6-BUD8$^{Δ74-216}$-URA3 bud8Δ::HIS3/bud8Δ::HIS3 his3::hisG/his3::hisG leu2::hisG/LEU2 trp1::hisG/TRP1*	this study
YHUM849	**a**/α *myc^6-BUD8$^{Δ173-216}$-URA3/myc^6-BUD8$^{Δ173-216}$-URA3 bud8Δ::HIS3/bud8Δ::HIS3 his3::hisG/his3::hisG leu2::hisG/LEU2 trp1::hisG/TRP1*	this study
YHUM850	**a**/α *myc^6-BUD8$^{Δ173-325}$-URA3/myc^6-BUD8$^{Δ173-325}$-URA3 bud8Δ::HIS3/bud8Δ::HIS3 his3::hisG/his3::hisG leu2::hisG/LEU2 trp1::hisG/TRP1*	this study
YHUM851	**a**/α *myc^6-BUD8$^{Δ268-325}$-URA3/myc^6-BUD8$^{Δ268-325}$-URA3 bud8Δ::HIS3/bud8Δ::HIS3 his3::hisG/his3::hisG leu2::hisG/LEU2 trp1::hisG/TRP1*	this study
YHUM852	**a**/α *myc^6-BUD8$^{Δ268-417}$-URA3/myc^6-BUD8$^{Δ268-417}$-URA3 bud8Δ::HIS3/bud8Δ::HIS3 his3::hisG/his3::hisG leu2::hisG/LEU2 trp1::hisG/TRP1*	this study
YHUM853	**a**/α *myc^6-BUD8$^{Δ375-417}$-URA3/myc^6-BUD8$^{Δ375-417}$-URA3 bud8Δ::HIS3/bud8Δ::HIS3 his3::hisG/his3::hisG leu2::hisG/LEU2 trp1::hisG/TRP1*	this study
YHUM854	**a**/α *myc^6-BUD8$^{Δ375-505}$-URA3/myc^6-BUD8$^{Δ375-505}$-URA3 bud8Δ::HIS3/bud8Δ::HIS3 his3::hisG/his3::hisG leu2::hisG/LEU2 trp1::hisG/TRP1*	this study
YHUM855	**a**/α *myc^6-BUD8$^{Δ468-505}$-URA3/myc^6-BUD8$^{Δ468-505}$-URA3 bud8Δ::HIS3/bud8Δ::HIS3 his3::hisG/his3::hisG leu2::hisG/LEU2 trp1::hisG/TRP1*	this study
YHUM856	**a**/α *myc^6-BUD8$^{Δ513-600}$-URA3/myc^6-BUD8$^{Δ513-600}$-URA3 bud8Δ::HIS3/bud8Δ::HIS3 his3::hisG/his3::hisG leu2::hisG/LEU2 trp1::hisG/TRP1*	this study
YHUM865	**a** *myc^6-BUD8-URA3 bud8Δ::HIS3 ura3-52 his3::hisG trp1::hisG*	this study
YHUM866	**a** *myc^6-BUD8$^{Δ7-53}$-URA3 bud8Δ::HIS3 ura3-52 his3::hisG trp1::hisG*	this study
YHUM867	**a** *myc^6-BUD8$^{Δ7-114}$-URA3 bud8Δ::HIS3 ura3-52 his3::hisG trp1::hisG*	this study
YHUM870	**a** *myc^6-BUD8$^{Δ74-114}$-URA3 bud8Δ::HIS3 ura3-52 his3::hisG trp1::hisG*	this study
YHUM871	**a** *myc^6-BUD8$^{Δ74-216}$-URA3 bud8Δ::HIS3 ura3-52 his3::hisG trp1::hisG*	this study

26

YHUM872	**a** *myc^6-BUD8$^{\Delta173-216}$-URA3 bud8Δ::HIS3 ura3-52 his3::hisG trp1::hisG*	this study
YHUM873	**a** *myc^6-BUD8$^{\Delta173-325}$-URA3 bud8Δ::HIS3 ura3-52 his3::hisG trp1::hisG*	this study
YHUM874	**a** *myc^6-BUD8$^{\Delta268-325}$-URA3 bud8Δ::HIS3 ura3-52 his3::hisG trp1::hisG*	this study
YHUM875	**a** *myc^6-BUD8$^{\Delta268-417}$-URA3 bud8Δ::HIS3 ura3-52 his3::hisG trp1::hisG*	this study
YHUM876	**a** *myc^6-BUD8$^{\Delta375-417}$-URA3 bud8Δ::HIS3 ura3-52 his3::hisG trp1::hisG*	this study
YHUM877	**a** *myc^6-BUD8$^{\Delta375-505}$-URA3 bud8Δ::HIS3 ura3-52 his3::hisG trp1::hisG*	this study
YHUM878	**a** *myc^6-BUD8$^{\Delta468-505}$-URA3 bud8Δ::HIS3 ura3-52 his3::hisG trp1::hisG*	this study
YHUM879	**a** *myc^6-BUD8$^{\Delta513-600}$-URA3 bud8Δ::HIS3 ura3-52 his3::hisG trp1::hisG*	this study
YHUM882	α *myc^6-BUD8-URA3 bud8Δ::HIS3 ura3-52 his3::hisG leu2::hisG*	this study
YHUM883	α *myc^6-BUD8$^{\Delta7-53}$-URA3 bud8Δ::HIS3 ura3-52 his3::hisG leu2::hisG*	this study
YHUM884	α *myc^6-BUD8$^{\Delta7-114}$-URA3 bud8Δ::HIS3 ura3-52 his3::hisG leu2::hisG*	this study
YHUM887	α *myc^6-BUD8$^{\Delta74-114}$-URA3 bud8Δ::HIS3 ura3-52 his3::hisG leu2::hisG*	this study
YHUM888	α *myc^6-BUD8$^{\Delta74-216}$-URA3 bud8Δ::HIS3 ura3-52 his3::hisG leu2::hisG*	this study
YHUM889	α *myc^6-BUD8$^{\Delta173-216}$-URA3 bud8Δ::HIS3 ura3-52 his3::hisG leu2::hisG*	this study
YHUM890	α *myc^6-BUD8$^{\Delta173-325}$-URA3 bud8Δ::HIS3 ura3-52 his3::hisG leu2::hisG*	this study
YHUM891	α *myc^6-BUD8$^{\Delta268-325}$-URA3 bud8Δ::HIS3 ura3-52 his3::hisG leu2::hisG*	this study
YHUM892	α *myc^6-BUD8$^{\Delta268-417}$-URA3 bud8Δ::HIS3 ura3-52 his3::hisG leu2::hisG*	this study
YHUM893	α *myc^6-BUD8$^{\Delta375-417}$-URA3 bud8Δ::HIS3 ura3-52 his3::hisG leu2::hisG*	this study
YHUM894	α *myc^6-BUD8$^{\Delta375-505}$-URA3 bud8Δ::HIS3 ura3-52 his3::hisG leu2::hisG*	this study
YHUM895	α *myc^6-BUD8$^{\Delta468-505}$-URA3 bud8Δ::HIS3 ura3-52 his3::hisG leu2::hisG*	this study
YHUM896	α *myc^6-BUD8$^{\Delta513-600}$-URA3 bud8Δ::HIS3 ura3-52 his3::hisG leu2::hisG*	this study
YHUM1007	**a** *bud8Δ::HIS3 ura3-52 his3::hisG leu2::hisG trp1::hisG*	strain collection H.-U. Mösch
YHUM1008	α *bud8Δ::HIS3 ura3-52 his3::hisG leu2::hisG trp1::hisG*	strain collection H.-U. Mösch
YHUM1009	**a**/α *myc^9-BUD9-TRP1/trp1::hisG leu2::hisG/myc^9-BUD9-LEU2 bud9Δ::HIS3/bud9Δ::HIS3 ura3-52/ura3-52 his3::hisG/his3::hisG*	this study
YHUM1010	**a**/α *myc^9-BUD9$^{\Delta8-47}$-TRP1/trp1::hisG leu2::hisG/myc^9-BUD9$^{\Delta8-47}$-LEU2 bud9Δ::HIS3/bud9Δ::HIS3 ura3-52/ura3-52 his3::hisG/his3::hisG*	this study
YHUM1011	**a**/α *myc^9-BUD9$^{\Delta8-130}$-TRP1/trp1::hisG leu2::hisG/myc^9-BUD9$^{\Delta8-130}$-LEU2 bud9Δ::HIS3/bud9Δ::HIS3 ura3-52/ura3-52 his3::hisG/his3::hisG*	this study
YHUM1012	**a**/α *myc^9-BUD9$^{\Delta91-130}$-TRP1/trp1::hisG leu2::hisG/myc^9-BUD9$^{\Delta91-130}$-LEU2 bud9Δ::HIS3/bud9Δ::HIS3 ura3-52/ura3-52 his3::hisG/his3::hisG*	this study
YHUM1013	**a**/α *myc^9-BUD9$^{\Delta91-218}$-TRP1/trp1::hisG leu2::hisG/myc^9-BUD9$^{\Delta91-218}$-LEU2 bud9Δ::HIS3/bud9Δ::HIS3 ura3-52/ura3-52 his3::hisG/his3::hisG*	this study
YHUM1014	**a**/α *myc^9-BUD9$^{\Delta168-218}$-TRP1/trp1::hisG leu2::hisG/myc^9-BUD9$^{\Delta168-218}$-LEU2 bud9Δ::HIS3/bud9Δ::HIS3 ura3-52/ura3-52 his3::hisG/his3::hisG*	this study
YHUM1015	**a**/α *myc^9-BUD9$^{\Delta168-283}$-TRP1/trp1::hisG leu2::hisG/myc^9-BUD9$^{\Delta168-283}$-LEU2 bud9Δ::HIS3/bud9Δ::HIS3 ura3-52/ura3-52 his3::hisG/his3::hisG*	this study
YHUM1016	**a**/α *myc^9-BUD9$^{\Delta244-283}$-TRP1/trp1::hisG leu2::hisG/myc^9-BUD9$^{\Delta244-283}$-LEU2 bud9Δ::HIS3/bud9Δ::HIS3 ura3-52/ura3-52 his3::hisG/his3::hisG*	this study

27

YHUM1017	**a**/α *myc^9-BUD9$^{\Delta244-369}$-TRP1/trp1::hisG leu2::hisG/myc^9-BUD9$^{\Delta244-369}$-LEU2 bud9Δ::HIS3/bud9Δ::HIS3 ura3-52/ura3-52 his3::hisG/his3::hisG*	this study
YHUM1018	**a**/α *myc^9-BUD9$^{\Delta323-369}$-TRP1/trp1::hisG leu2::hisG/myc^9-BUD9$^{\Delta323-369}$-LEU2 bud9Δ::HIS3/bud9Δ::HIS3 ura3-52/ura3-52 his3::hisG/his3::hisG*	this study
YHUM1019	**a**/α *myc^9-BUD9$^{\Delta323-450}$-TRP1/trp1::hisG leu2::hisG/myc^9-BUD9$^{\Delta323-450}$-LEU2 bud9Δ::HIS3/bud9Δ::HIS3 ura3-52/ura3-52 his3::hisG/his3::hisG*	this study
YHUM1020	**a**/α *myc^9-BUD9$^{\Delta406-450}$-TRP1/trp1::hisG leu2::hisG/myc^9-BUD9$^{\Delta406-450}$-LEU2 bud9Δ::HIS3/bud9Δ::HIS3 ura3-52/ura3-52 his3::hisG/his3::hisG*	this study
YHUM1021	**a**/α *myc^9-BUD9$^{\Delta406-544}$-TRP1/trp1::hisG leu2::hisG/myc^9-BUD9$^{\Delta406-544}$-LEU2 bud9Δ::HIS3/bud9Δ::HIS3 ura3-52/ura3-52 his3::hisG/his3::hisG*	this study
YHUM1022	**a**/α *myc^9-BUD9$^{\Delta460-544}$-TRP1/trp1::hisG leu2::hisG/myc^9-BUD9$^{\Delta460-544}$-LEU2 bud9Δ::HIS3/bud9Δ::HIS3 ura3-52/ura3-52 his3::hisG/his3::hisG*	this study
YHUM1023	**a**/α *bud8Δ::HIS3/BUD8 myc^6-BUD8-URA3/ura3-52 his3::hisG/his3::hisG leu2::hisG/LEU2 trp1::hisG/TRP1*	this study
YHUM1024	**a**/α *bud8Δ::HIS3/BUD8 URA3/ura3-52 his3::hisG/his3::hisG leu2::hisG/LEU2 trp1::hisG/TRP1*	this study
YHUM1025	**a**/α *bud8Δ::HIS3/BUD8 myc^6-BUD8$^{\Delta173-216}$-URA3/ura3-52 his3::hisG/his3::hisG leu2::hisG/LEU2 trp1::hisG/TRP1*	this study
YHUM1026	**a**/α *bud8Δ::HIS3/BUD8 myc^6-BUD8$^{\Delta173-325}$-URA3/ura3-52 his3::hisG/his3::hisG leu2::hisG/LEU2 trp1::hisG/TRP1*	this study
YHUM1027	**a**/α *bud8Δ::HIS3/BUD8 myc^6-BUD8$^{\Delta268-325}$-URA3/ura3-52 his3::hisG/his3::hisG leu2::hisG/LEU2 trp1::hisG/TRP1*	this study
YHUM1028	**a**/α *bud8Δ::HIS3/BUD8 myc^6-BUD8$^{\Delta268-417}$-URA3/ura3-52 his3::hisG/his3::hisG leu2::hisG/LEU2 trp1::hisG/TRP1*	this study
YHUM1029	**a**/α *bud9Δ::HIS3/BUD9 myc^9-BUD9-TRP1/trp1::hisG ura3-52/ura3-52 his3::hisG/his3::hisG leu2::hisG/LEU2*	this study
YHUM1030	**a**/α *bud9Δ::HIS3/BUD9 ura3-52/ura3-52 his3::hisG/his3::hisG leu2::hisG/LEU2 TRP1/trp1::hisG*	this study
YHUM1031	**a**/α *myc^9-BUD9$^{\Delta244-369}$-TRP1/trp1::hisG bud9Δ::HIS3/BUD9 ura3-52/ura3-52 his3::hisG/his3::hisG leu2::hisG/LEU2*	this study
YHUM1032	**a**/α *myc^9-BUD9$^{\Delta323-369}$-TRP1/trp1::hisG bud9Δ::HIS3/BUD9 ura3-52/ura3-52 his3::hisG/his3::hisG leu2::hisG/LEU2*	this study
YHUM1049	**a**/α *bud9Δ::HIS3/bud9Δ::HIS3 ura3-52/ura3-52 his3::hisG/his3::hisG LEU2/leu2::hisG trp1::hisG/TRP1*	this study
YHUM1050	α *bud8Δ::HIS3 bud9Δ::HIS3 ura3-52 his3::hisG leu2::hisG*	this study
YHUM1051	**a** *bud8Δ::HIS3 bud9Δ::HIS3 ura3-52 his3::hisG leu2::hisG*	this study
BY4742	α *his3Δ1 leu2Δ0 lys2Δ0 ura3Δ0*	Brachmann *et al.*, 1998
Cl3-ABYS-86	α *ura3-Δ5 leu2-3,112 his-pra1-1 prb1-1 prc1-1 cps1-3 can^R*	W. Heinemann, Stuttgart
S18H3	α *sec18-1 his3Δ1 leu2Δ0 lysΔ0 uraΔ0*	H.-D. Schmitt, pers. comm.

Table 2: Plasmids used in this study

Plasmid	Description	Reference
pRS304	*TRP1*-marked integrative vector	Sikorski and Hieter (1989)
pRS305	*LEU2*-marked integrative vector	Sikorski and Hieter (1989)
pRS306	*URA3*-marked integrative vector	Sikorski and Hieter (1989)
pRS316	*URA3*-marked low-copy vector	Sikorski and Hieter (1989)
pRS425	*LEU2*-marked *2μm* vector	Sikorski and Hieter (1989)
pRS426	*URA3*-marked *2μm* vector	Sikorski and Hieter (1989)
BHUM393	*CFP*-carrying plasmid	plasmid coll. H.-U. Mösch
BHUM394	*YFP*-carrying plasmid	plasmid coll. H.-U. Mösch
BHUM426	*TAP* tag-carrying plasmid	plasmid coll. H.-U. Mösch
BHUM498	*BUD8prom-myc^6-BUD8* fusion in pRS426	this study
BHUM532	*BUD8prom-myc^6-BUD8* in pRS425	plasmid coll. H.-U. Mösch
BHUM706	*BUD8prom-myc^6-BUD8$^{\Delta513-600}$* in pRS425	plasmid coll. H.-U. Mösch
BHUM782	*BUD8prom-myc^6-BUD8* fusion in pRS306	this study
BHUM783	*BUD8prom-myc^6-BUD8$^{\Delta7-53}$* fusion in pRS306	this study
BHUM784	*BUD8prom-myc^6-BUD8$^{\Delta7-114}$* fusion in pRS306	this study
BHUM785	*BUD8prom-myc^6-BUD8$^{\Delta74-114}$* fusion in pRS306	this study
BHUM786	*BUD8prom-myc^6-BUD8$^{\Delta74-216}$* fusion in pRS306	this study
BHUM787	*BUD8prom-myc^6-BUD8$^{\Delta173-216}$* fusion in pRS306	this study
BHUM788	*BUD8prom-myc^6-BUD8$^{\Delta173-325}$* fusion in pRS306	this study
BHUM789	*BUD8prom-myc^6-BUD8$^{\Delta268-325}$* fusion in pRS306	this study
BHUM790	*BUD8prom-myc^6-BUD8$^{\Delta268-417}$* fusion in pRS306	this study
BHUM791	*BUD8prom-myc^6-BUD8$^{\Delta375-417}$* fusion in pRS306	this study
BHUM792	*BUD8prom-myc^6-BUD8$^{\Delta375-505}$* fusion in pRS306	this study
BHUM793	*BUD8prom-myc^6-BUD8$^{\Delta468-505}$* fusion in pRS306	this study
BHUM794	*BUD8prom-myc^6-BUD8$^{\Delta513-600}$* fusion in pRS306	this study
BHUM795	*BUD9prom-myc^3-BUD9* fusion in pRS426	plasmid coll. H.-U. Mösch
BHUM796	*BUD9prom-myc^9-BUD9* fusion in pRS304	this study
BHUM797	*BUD9prom-myc^9-BUD9$^{\Delta8-48}$* fusion in pRS304	this study
BHUM798	*BUD9prom-myc^9-BUD9$^{\Delta8-130}$* fusion in pRS304	this study
BHUM799	*BUD9prom-myc^9-BUD9$^{\Delta91-130}$* fusion in pRS304	this study
BHUM800	*BUD9prom-myc^9-BUD9$^{\Delta91-218}$* fusion in pRS304	this study
BHUM801	*BUD9prom-myc^9-BUD9$^{\Delta168-218}$* fusion in pRS304	this study
BHUM802	*BUD9prom-myc^9-BUD9$^{\Delta168-283}$* fusion in pRS304	this study
BHUM803	*BUD9prom-myc^9-BUD9$^{\Delta244-283}$* fusion in pRS304	this study
BHUM804	*BUD9prom-myc^9-BUD9$^{\Delta244-369}$* fusion in pRS304	this study
BHUM805	*BUD9prom-myc^9-BUD9$^{\Delta323-369}$* fusion in pRS304	this study
BHUM806	*BUD9prom-myc^9-BUD9$^{\Delta323-450}$* fusion in pRS304	this study

BHUM807	*BUD9prom-myc⁹-BUD9$^{\Delta406-450}$* fusion in pRS304	this study
BHUM808	*BUD9prom-myc⁹-BUD9$^{\Delta406-544}$* fusion in pRS304	this study
BHUM809	*BUD9prom-myc⁹-BUD9$^{\Delta460-544}$* fusion in pRS304	this study
BHUM810	*BUD9prom-myc⁹-BUD9* fusion in pRS305	this study
BHUM811	*BUD9prom-myc⁹-BUD9$^{\Delta8-48}$* fusion in pRS305	this study
BHUM812	*BUD9prom-myc⁹-BUD9$^{\Delta8-130}$* fusion in pRS305	this study
BHUM813	*BUD9prom-myc⁹-BUD9$^{\Delta91-130}$* fusion in pRS305	this study
BHUM814	*BUD9prom-myc⁹-BUD9$^{\Delta91-130}$* fusion in pRS305	this study
BHUM815	*BUD9prom-myc⁹-BUD9$^{\Delta168-218}$* fusion in pRS305	this study
BHUM816	*BUD9prom-myc⁹-BUD9$^{\Delta168-283}$* fusion in pRS305	this study
BHUM817	*BUD9prom-myc⁹-BUD9$^{\Delta244-283}$* fusion in pRS305	this study
BHUM818	*BUD9prom-myc⁹-BUD9$^{\Delta244-369}$* fusion in pRS305	this study
BHUM819	*BUD9prom-myc⁹-BUD9$^{\Delta323-369}$* fusion in pRS305	this study
BHUM820	*BUD9prom-myc⁹-BUD9$^{\Delta323-450}$* fusion in pRS305	this study
BHUM821	*BUD9prom-myc⁹-BUD9$^{\Delta406-450}$* fusion in pRS305	this study
BHUM822	*BUD9prom-myc⁹-BUD9$^{\Delta406-544}$* fusion in pRS305	this study
BHUM823	*BUD9prom-myc⁹-BUD9$^{\Delta460-544}$* fusion in pRS305	this study
BHUM824	*BUD8prom-GFP$_{UV}$-BUD8* fusion in pRS3426	this study
BHUM825	*BUD8prom-GFP$_{UV}$-BUD8$^{\Delta7-53}$* fusion in pRS3426	this study
BHUM826	*BUD8prom-GFP$_{UV}$-BUD8$^{\Delta7-114}$* fusion in pRS426	this study
BHUM827	*BUD8prom-GFP$_{UV}$-BUD8$^{\Delta74-114}$* fusion in pRS426	this study
BHUM828	*BUD8prom-GFP$_{UV}$-BUD8$^{\Delta74-216}$* fusion in pRS426	this study
BHUM829	*BUD8prom-GFP$_{UV}$-BUD8$^{\Delta173-216}$* fusion in pRS426	this study
BHUM830	*BUD8prom-GFP$_{UV}$-BUD8$^{\Delta173-325}$* fusion in pRS426	this study
BHUM831	*BUD8prom-GFP$_{UV}$-BUD8$^{\Delta268-325}$* fusion in pRS426	this study
BHUM832	*BUD8prom-GFP$_{UV}$-BUD8$^{\Delta268-417}$* fusion in pRS426	this study
BHUM833	*BUD8prom-GFP$_{UV}$-BUD8$^{\Delta375-417}$* fusion in pRS426	this study
BHUM834	*BUD8prom-GFP$_{UV}$-BUD8$^{\Delta375-505}$* fusion in pRS426	this study
BHUM835	*BUD8prom-GFP$_{UV}$-BUD8$^{\Delta468-505}$* fusion in pRS426	this study
BHUM836	*BUD8prom-GFP$_{UV}$-BUD8$^{\Delta513-600}$* fusion in pRS426	this study
BHUM837	*BUD9prom-YFP-BUD9* fusion in pRS426	this study
BHUM838	*BUD9prom-YFP-BUD9$^{\Delta8-48}$* fusion in pRS426	this study
BHUM839	*BUD9prom-YFP-BUD9$^{\Delta8-130}$* fusion in pRS426	this study
BHUM840	*BUD9prom-YFP-BUD9$^{\Delta91-130}$* fusion in pRS426	this study
BHUM841	*BUD9prom-YFP-BUD9$^{\Delta91-218}$* fusion in pRS426	this study
BHUM842	*BUD9prom-YFP-BUD9$^{\Delta168-218}$* fusion in pRS426	this study
BHUM843	*BUD9prom-YFP-BUD9$^{\Delta168-283}$* fusion in pRS426	this study
BHUM844	*BUD9prom-YFP-BUD9$^{\Delta244-283}$* fusion in pRS426	this study
BHUM845	*BUD9prom-YFP-BUD9$^{\Delta244-369}$* fusion in pRS426	this study

BHUM846	*BUD9prom-YFP-BUD9*$^{\Delta 323-369}$ fusion in pRS426	this study
BHUM847	*BUD9prom-YFP-BUD9*$^{\Delta 323-450}$ fusion in pRS426	this study
BHUM848	*BUD9prom-YFP-BUD9*$^{\Delta 406-450}$ fusion in pRS426	this study
BHUM849	*BUD9prom-YFP-BUD9*$^{\Delta 406-544}$ fusion in pRS426	this study
BHUM850	*BUD9prom-YFP-BUD9*$^{\Delta 460-544}$ fusion in pRS426	this study
BHUM867-879	*BUD8* mutant alleles as specified for BHUM782-BHUM794 in pRS426 backbone	this study
BHUM880-893	*BUD9* mutant alleles as specified for BHUM796-BHUM809 in pRS426 backbone	this study
BHUM894	*myc*^{9} as *Bgl*II fragment in pRS316 with inserted *Bgl*II restriction site	this study
BHUM895	*BUD9prom-YFP-BUD9* fusion in pRS304	this study
BHUM933	*BUD8prom-TAP-BUD8* in pRS316	this study
BHUM934	*BUD8prom-TAP-BUD8* in pRS426	this study
BHUM935	*BUD9prom-TAP-BUD9* in pRS316	this study
BHUM936	*BUD9prom-TAP-BUD9* in pRS426	this study
BHUM939	*BUD8prom-CFP-BUD8* in pRS316	this study
BHUM941	*BUD8prom-CFP-BUD8* in pRS425	this study
BHUM942	*BUD8prom-YFP-BUD8* in pRS425	this study
BHUM943	*BUD8prom-CFP-BUD8* in pRS426	this study
BHUM944	*BUD8prom-YFP-BUD8* in pRS426	this study
BHUM949	*BUD9prom-CFP-BUD9* in pRS316	this study
BHUM951	*BUD9prom-CFP-BUD9* in pRS426	this study
BHUM952	*BUD9prom-YFP-BUD9* in pRS426	this study
BHUM990	*BUD8prom-myc*^{6}*-BUD8*$^{\Delta 7-53}$ in pRS426	this study
BHUM991	*BUD8prom-myc*^{6}*-BUD8*$^{\Delta 7-114}$ in pRS426	this study
BHUM992	*BUD8prom-myc*^{6}*-BUD8*$^{\Delta 74-114}$ in pRS426	this study
BHUM993	*BUD8prom-myc*^{6}*-BUD8*$^{\Delta 74-216}$ in pRS426	this study
BHUM994	*BUD8prom-myc*^{6}*-BUD8*$^{\Delta 173-216}$ in pRS426	this study
BHUM995	*BUD8prom-myc*^{6}*-BUD8*$^{\Delta 173-325}$ in pRS426	this study
BHUM996	*BUD8prom-myc*^{6}*-BUD8*$^{\Delta 268-325}$ in pRS426	this study
BHUM997	*BUD8prom-myc*^{6}*-BUD8*$^{\Delta 268-417}$ in pRS426	this study
BHUM998	*BUD8prom-myc*^{6}*-BUD8*$^{\Delta 375-417}$ in pRS426	this study
BHUM999	*BUD8prom-myc*^{6}*-BUD8*$^{\Delta 375-505}$ in pRS426	this study
BHUM1000	*BUD8prom-myc*^{6}*-BUD8*$^{\Delta 468-505}$ in pRS426	this study
BHUM1001	*BUD8prom-myc*^{6}*-BUD8*$^{\Delta 513-600}$ in pRS426	this study
BHUM1002	*BUD9prom-myc*^{9}*-BUD9* in pRS426	this study
BHUM1003	*BUD9prom-myc*^{9}*-BUD9*$^{\Delta 8-48}$ in pRS426	this study
BHUM1004	*BUD9prom-myc*^{9}*-BUD9*$^{\Delta 8-130}$ in pRS426	this study
BHUM1005	*BUD9prom-myc*^{9}*-BUD9*$^{\Delta 91-130}$ in pRS426	this study

BHUM1006	*BUD9prom-myc^9-BUD9$^{\Delta 91-218}$* in pRS426	this study
BHUM1007	*BUD9prom-myc^9-BUD9$^{\Delta 168-218}$* in pRS426	this study
BHUM1008	*BUD9prom-myc^9-BUD9$^{\Delta 168-283}$* in pRS426	this study
BHUM1009	*BUD9prom-myc^9-BUD9$^{\Delta 244-283}$* in pRS426	this study
BHUM1010	*BUD9prom-myc^9-BUD9$^{\Delta 244-369}$* in pRS426	this study
BHUM1011	*BUD9prom-myc^9-BUD9$^{\Delta 323-369}$* in pRS426	this study
BHUM1012	*BUD9prom-myc^9-BUD9$^{\Delta 323-450}$* in pRS426	this study
BHUM1013	*BUD9prom-myc^9-BUD9$^{\Delta 406-450}$* in pRS426	this study
BHUM1014	*BUD9prom-myc^9-BUD9$^{\Delta 406-544}$* in pRS426	this study
BHUM1015	*BUD9prom-myc^9-BUD9$^{\Delta 460-544}$* in pRS426	this study
BHUM1016	*BUD8prom-myc^6-BUD8$^{\Delta 7-53}$* in pRS425	this study
BHUM1017	*BUD8prom-myc^6-BUD8$^{\Delta 7-114}$* in pRS425	this study
BHUM1018	*BUD8prom-myc^6-BUD8$^{\Delta 74-114}$* in pRS425	this study
BHUM1019	*BUD8prom-myc^6-BUD8$^{\Delta 74-216}$* in pRS425	this study
BHUM1020	*BUD8prom-myc^6-BUD8$^{\Delta 173-216}$* in pRS425	this study
BHUM1021	*BUD8prom-myc^6-BUD8$^{\Delta 173-325}$* in pRS425	this study
BHUM1022	*BUD8prom-myc^6-BUD8$^{\Delta 268-325}$* in pRS425	this study
BHUM1023	*BUD8prom-myc^6-BUD8$^{\Delta 268-417}$* in pRS425	this study
BHUM1024	*BUD8prom-myc^6-BUD8$^{\Delta 375-417}$* in pRS425	this study
BHUM1025	*BUD8prom-myc^6-BUD8$^{\Delta 375-505}$* in pRS425	this study
BHUM1026	*BUD8prom-myc^6-BUD8$^{\Delta 468-505}$* in pRS425	this study
BHUM1027	*BUD9prom-myc^9-BUD9* in pRS425	this study
BHUM1028	*BUD9prom-myc^9-BUD9$^{\Delta 8-48}$* in pRS425	this study
BHUM1029	*BUD9prom-myc^9-BUD9$^{\Delta 8-130}$* in pRS425	this study
BHUM1030	*BUD9prom-myc^9-BUD9$^{\Delta 91-130}$* in pRS425	this study
BHUM1031	*BUD9prom-myc^9-BUD9$^{\Delta 91-218}$* in pRS425	this study
BHUM1032	*BUD9prom-myc^9-BUD9$^{\Delta 168-218}$* in pRS425	this study
BHUM1033	*BUD9prom-myc^9-BUD9$^{\Delta 168-283}$* in pRS425	this study
BHUM1034	*BUD9prom-myc^9-BUD9$^{\Delta 244-283}$* in pRS425	this study
BHUM1035	*BUD9prom-myc^9-BUD9$^{\Delta 244-369}$* in pRS425	this study
BHUM1036	*BUD9prom-myc^9-BUD9$^{\Delta 323-369}$* in pRS425	this study
BHUM1037	*BUD9prom-myc^9-BUD9$^{\Delta 323-450}$* in pRS425	this study
BHUM1038	*BUD9prom-myc^9-BUD9$^{\Delta 406-450}$* in pRS425	this study
BHUM1039	*BUD9prom-myc^9-BUD9$^{\Delta 406-544}$* in pRS425	this study
BHUM1040	*BUD9prom-myc^9-BUD9$^{\Delta 460-544}$* in pRS425	this study
pHP772	*pGST-BUD5-ΔN1-70* in pRS316-*GAL1-GST*	Kang *et al*., 2004a
pHP1301	*pGST-BUD5* in pRS316-*GAL1-GST*	Kang *et al*., 2004a
pHP1156	p*GALp-GST-HIS6-RAX1 in URA3*-marked *2µm* vector	Kang *et al*., 2004b
pME1771	*BUD8prom-GFP$_{UV}$-BUD8* fusion in pRS316	Taheri *et al.* (2000)

32

Table 3: Oligonucleotide primers used for cloning and sequencing

Primer	Sequence
BUD8DEL01	5'-GCG <u>AGA TCT</u> TTC GTC TGA TTG TAT AGA TCC GTT CAA G-3' [a]
BUD8DEL02	5'-GCG <u>AGA TCT</u> GTT GAT GTA TAC AGC AAA TCC TTG-3' [a]
BUD8DEL03	5'-GCG <u>AGA TCT</u> GCT TCC TTC AAC ATC TTC TCC CAT AAG-3' [a]
BUD8DEL04	5'-GCG <u>AGA TCT</u> GTA TTG ATC TAT GAC TTC ATC CTC GG-3' [a]
BUD8DEL05	5'-GCG <u>AGA TCT</u> GGG AAT TGA AGG TAG TCC AAT GGG-3' [a]
BUD8DEL06	5'-GCG <u>AGA TCT</u> TTT TTC TTG TTG CTT TCG TCG TAT GC-3' [a]
BUD8DEL07	5'-GCG <u>AGA TCT</u> GGA TTC AGG GAC GTT TAC AGC ATC G-3' [a]
BUD8DEL08	5'-GCG <u>AGA TCT</u> ATG AAC AAG AAG AAA AAT AAA ACG TTG-3' [a]
BUD8DEL09	5'-GCG <u>AGA TCT</u> TCA CAC AAT AGT GAC AGT AGT AAC G-3' [a]
BUD8DEL10	5'-GCG <u>AGA TCT</u> TCA TTT TTC TCA TAC CAT TAC GAT G-3' [a]
BUD8DEL11	5'-GCG <u>AGA TCT</u> CCA ACT TCA CTT CGA CGA GAC AAC G-3' [a]
BUD8DEL12	5'-GCG <u>AGA TCT</u> ATG GCT ACT GTT GCC TAT GAA ACC AC-3' [a]
BUD8DEL13	5'-CCG <u>CTC GAG</u> GGA CGG TAT CCA CTG TAA TTT GAC TC-3' [b]
BUD8X-6	5'-CCG <u>CTC GAG</u> ACT GGT AAA GAT TAC AAG GGT G-3' [b]
BUD9DEL01	5'-CCG <u>GAA TTC</u> ATC TCT GGT TAT TTT CGT GGA TC-3' [c]
BUD9DEL02	5'-CCG <u>GAA TTC</u> TTT ACC ATC AGT ACT ACT TG-3' [c]
BUD9DEL03	5'-CCG <u>GAA TTC</u> CAT ATT CAA CAG CAC CGA AG-3' [c]
BUD9DEL04	5'-CCG <u>GAA TTC</u> AAC AAG ATC TAC ACC ATA CCG-3' [c]
BUD9DEL05	5'-CCG <u>GAA TTC</u> AGA ACT TCG CTG GTC ATT AGC-3' [c]
BUD9DEL06	5'-CCG <u>GAA TTC</u> ATT GTC ACC TTT CCG ACC CC-3' [c]
BUD9DEL07	5'-CCG <u>GAA TTC</u> TGG AAT ACT ATA AAT CTC GG-3' [c]
BUD9DEL08	5'-CCG <u>GAA TTC</u> ATA AGA GAG TAA CTC CAT GC-3' [c]
BUD9DEL09	5'-CCG <u>GAA TTC</u> GGC TTC TCC GAG ATT TAT AG-3' [c]
BUD9DEL10	5'-CCG <u>GAA TTC</u> CTT GGT ATC GCA ATG GAC ACC-3' [c]
BUD9DEL11	5'-CCG <u>GAA TTC</u> AAC AGA ATA CCA GCG AAT AAG-3' [c]
BUD9DEL12	5'-CCG <u>GAA TTC</u> TCC GGA AAT AAG TCT ACA AGG-3' [c]
BUD9DEL13	5'-CCG <u>GAA TTC</u> CCA AAT TCA AAT GAG AGG AAC AG-3' [c]
BUD9DEL14	5'-CCG <u>GAA TTC</u> CTG TTC ATC GAA GGA TCT G-3' [c]
BUD9X-1	5'-CGG <u>ACT AGT</u> CCT ATA TTC AGC TTA GCA GTG-3' [d]
BUD9Y-1	5'-CCG <u>CTC GAG</u> AGT GTA TTG GCA TTC ATA CTC-3' [e]
AO-BUD8-1	5'-ACC CCA TAC TAA GAA CAG GCA ATT-3' [f]
AO-BUD8-2	5'-ATA CAG CAA ATC CTT GAC CTC TAC TTG TGG-3' [f]
AO-BUD9-1	5'-TTG CCA CAT ACG TAC ATT GAC ACG TAG-3' [g]
AO-BUD9-2	5'-ATT GTA TGA CTT CAC TTC TGA TGA TGG-3' [g]
AO-SEQ-FP	5'-TTG TAA CAG CTG CTG GGA TTA C-3' [h]
BUD8DEL01-P	5'-<u>GAT CT</u>T TCG TCT GAT TGT A-3' [i]
T3	5'-ATT AAC CCT CAC TAA AG-3' [k]

T7	5'-AAT ACG ACT CAC TAT AG-3' [k]
T3-I	5'-GAG CGG ATA ACA ATT TCA CAC AGG-3' [k]
T7-I	5'-GCC AGG GTT TTC CCA GTC ACG ACG-3' [k]
BUD8-SEQ-1	5'-AAT CGA AGC ATT TTT GAC AAT ACC-3' [k]
BUD8-SEQ-2	5'-TAC CAC TAT ATG AAG TTG ATG CTG-3' [k]
AO-FP-1-1	5'-CGC <u>GGA TCC</u> AAA GGA GAA GAA CTT TTC ACT GGA GTT G-3' [l]
AO-FP-1-2	5'-CGC <u>GGA TCC</u> GTA TAG TTC ATC CAT GCC ATG TGT AAT C-3' [l]
AO-FP-2-1	5'-GGA <u>AGA TCT</u> AAA GGA GAA GAA CTT TTC ACT GGA GTT G-3' [l]
AO-FP-2-2	5'-GGA <u>AGA TCT</u> GTA TAG TTC ATC CAT GCC ATG TGT AAT C-3' [l]

[a] Mutagenic primers used to introduce a *Bgl*II restriction site (underlined)

[b] Mutagenic primers used to introduce a *Xho*I restriction site (underlined) at the 3'-end of *BUD8* and *BUD8* mutant alleles

[c] Mutagenic primers used to introduce an *Eco*RI restriction site (underlined)

[d] Mutagenic primer used to introduce a *Spe*I restriction site (underlined) at the 5'-end of *BUD9* and *BUD9* mutant alleles

[e] Mutagenic primer used to introduce a *Xho*I restriction site (underlined) at the 3'-end of *BUD9* and *BUD9* mutant alleles

[f] Primers used to construct GFP_{UV}-*BUD8* fusion alleles carried by BHUM824 and BHUM827-836

[g] Primers used to construct *YFP*-*BUD9* fusion alleles carried by BHUM837 and BHUM840-850

[h] Primer used for sequencing of GFP_{UV}-*BUD8* and *YFP-BUD9* alleles

[i] 5'-phosphorylated primer used for construction of GFP_{UV}-*BUD8*$^{Δ7-53}$ and GFP_{UV}-*BUD8*$^{Δ7-114}$ carried by BHUM825 and BHUM826

[k] Primer used for sequencing of *BUD8* and *BUD9* mutant alleles

[l] Primers used to amplify GFP_{UV}, CFP or YFP coding sequences

2.1.2.1 Construction of CFP and YFP fusion proteins for co-localization studies

To construct full-length Bud8p versions fused to *CFP* and *YFP*, respectively, a PCR-based strategy was applied. *CFP* and *YFP* coding sequences (carried by BHUM393 and BHUM394) were amplified by polymerase chain reaction (PCR) as *Bgl*II-fragments using the oligonucleotides AO-FP-2-1 and AO-FP-2-2. In a following step, pME1771 (*BUD8prom-GFP$_{UV}$-BUD8* in pRS316) was digested with *Bgl*II to remove *GFP$_{UV}$*-coding sequence and replace it by a *CFP* or a *YFP* fragment. The obtained constructs were checked by restriction analysis. DNA sequencing using the ABI Prism Big Dye terminator sequencing kit and an ABI Prism 310 Genetic Analyzer (APPLIED BIOSYSTEMS, Weiterstadt, D) confirmed correct sequence and correct orientation of the CFP and YFP fragments.

Since co-localization experiments presuppose usage of a *2μm* vector containing a cassette encoding a *LEU2* selection marker, the obtained *CFP-BUD8* and *YFP-BUD8* coding sequences from the previous step were cloned in pRS425 (Christianson *et al.*, 1992) yielding the plasmids BHUM941 and BHUM942. BHUM943 (pRS426 (*2μm*, *URA3*), *CFP-BUD8*) and BHUM944 (pRS426 (*2μm*, *URA3*), *YFP-BUD8*), which were necessary for expression analysis, were constructed in a similar way as described for BHUM941 and BHUM942.

The generation of Bud9p variants fused to CFP and YFP was carried out analogously. CFP and YFP encoding sequences (carried by BHUM393 and BHUM394) were amplified by PCR as *Bam*HI fragments using the oligonucleotides AO-FP-1-1 and AO-FP-1-2. Restriction analysis followed DNA sequencing confirmed sequence and correct orientation of CFP and YFP. The obtained *CFP-* and *YFP-BUD9* constructs were each digested with proper enzymes and cloned into pRS426 yielding the plasmids BHUM951 and BHUM952.

2.1.2.2 Construction of *BUD8* and *BUD9* deletion sets

The set of *myc^6-BUD8* and *myc^9-BUD9* alleles carrying systematic deletions in their open reading frames was constructed by a PCR-based strategy involving several steps. To generate the strains YHUM842-YHUM855, fragments were amplified by polymerase chain reaction from a six-fold myc-tagged wild type version of *BUD8* (carried by BHUM498) as parts with differences in length. Six fragments were generated, comprising 924 bp of the upstream sequence and parts of the *BUD8* open reading frame (ORF), using the oligonucleotides T3 and BUD8DEL01-BUD8DEL06. All fragments of this group exhibit an inserted *Bgl*II restriction site at their 3'-end. Another six fragments, comprising parts of the *BUD8* ORF and

588 or 712 bp of the downstream sequence, were amplified using the primers BUD8DEL07-BUD8DEL12 as well as BUD8X-6 and BUD8DEL13, respectively. Fragments of this group display inserted *Bgl*II sites at their 5'-end. The fragments of both groups were first digested with *Not*I/*Bgl*II and *Bgl*II/*Xho*I, respectively, and then subcloned into pBlueskript KS (+/-). DNA sequencing using the ABI Prism Big Dye terminator sequencing kit (T3-I and T7-I were used as primers) and an ABI PRISM 310 Genetic Analyzer (APPLIED BIOSYSTEMS, Weiterstadt, Germany) confirmed that the fragments had been cloned. After verification selected fragments of both groups were joined together using the integrated *Bgl*II restriction site. The resulting *BUD8* deletions were cloned as *Not*I-*Xho*I fragments into the plasmid pRS306. The obtained plasmids BHUM782-BHUM793 as well as a myc-tagged full-length version of *BUD8* (BHUM498) were linearized within *URA3* by digestion with *Stu*I (*Eco*147I) and integrated in the haploid **a**- and α-strains YHUM904 and YHUM861. Successful integration of the constructs was confirmed by southern analysis. Haploid strains with corresponding constructs were combined to receive homozygous diploid strains for investigations. YHUM856 was constructed in a similar manner as described for the other *BUD8* constructs. For joining of the two amplified fragments, a *Xho*I restriction site was introduced instead of a *Bgl*II site. Confirmation of the obtained plasmid BHUM794 as well as transformation and crossing of corresponding yeast strains were carried out essentially as described above.

For construction of a *BUD9* deletion set a plasmid carrying a three-fold myc-tagged wild type version (BHUM795) was chosen as template. Seven fragments were generated that contain parts of the *BUD9* ORF plus 944 bp upstream sequence. For their amplification the oligonucleotides BUD9X-1 and BUD9DEL01-BUD9DEL07 were used, which introduce a *Spe*I restriction site at the 5'-end and an *Eco*RI site at the 3'-end of the PCR products. Additionally, the complete *BUD9* coding sequence plus 944 bp upstream sequence and 384 bp downstream sequence was amplified as *Spe*I-*Xho*I fragment with BUD9X-1 and BUD9Y-1. After subcloning of all fragments and the entire *BUD9* gene in pBlueskript KS (+/-) each myc^3-epitope was replaced with a myc^9-epitope that was cut out as *Bgl*II fragment from BHUM894. Another seven fragments comprising parts of the *BUD9* ORF and 384 bp of the downstream region were amplified as *Eco*RI-*Xho*I fragments using the oligonucleotides BUD9DEL08-BUD9DEL14 and BUD9Y-1 and then subcloned into pBlueskript KS (+/-) digested with *Eco*RI and *Xho*I. Sequencing confirmed the cloning of

each PCR product and the correct orientation of the myc^9-epitopes in the *Spe*I-*Eco*RI fragments and the full-length version of *BUD9*. Distinct fragments were combined using the inserted *Eco*RI restriction site and then cloned as *Spe*I-*Xho*I fragment into pRS304 and pRS305 yielding the plasmids BHUM796-BHUM823. The haploid MAT**a** *bud9* deletion strain BHUM994 was transformed with BHUM796-BHUM809 after digestion within the *TRP1* with *Bst*1107I. BHUM810-BHUM823 were linearized within the *LEU2* locus with *Bst*EII and then integrated in the haploid MATα deletion strain BHUM995. Successful integration of each construct at the *TRP1* and the *LEU2* locus, respectively, was confirmed by southern blot analysis. Appropriate transformants were mated to obtain the homozygous *bud9* deletion strains YHUM1009-YHUM1022.

2.1.2.3 Construction of Bud8p and Bud9p deletion constructs for Bud5p interaction studies

For co-immunoprecipitation of myc^6-tagged wild type versions of the landmark proteins Bud8p and Bud9p as well as selected deletion constructs of both proteins with a GST-fused version of the guanine nucleotide exchange factor Bud5p, sequences coding for *myc^6-BUD8* and *myc^9-BUD9* had to be cloned into a vector that allows selection and expression of a pair of plasmids within the cell. Furthermore the proteins should be produced at high levels to ensure expression of adequate protein amounts for co-purification experiments. Since *BUD5* encoding sequences are expressed from a vector containing a *URA3* cassette, corresponding *BUD8* and *BUD9* variants were cloned into pRS425, a vector carrying a *LEU2* selection marker.

In case of *BUD8*, the plasmids BHUM990 (*myc^6-BUD8$^{Δ7-53}$*), BHUM991 (*myc^6-BUD8$^{Δ7-114}$*), BHUM992 (*myc^6-BUD8$^{Δ74-114}$*), BHUM786 (*myc^6-BUD8$^{Δ74-216}$*), BHUM994 (*myc^6-BUD8$^{Δ173-216}$*), BHUM788 (*myc^6-BUD8$^{Δ173-325}$*), BHUM996 (*myc^6-BUD8$^{Δ268-325}$*), BHUM997 (*myc^6-BUD8$^{Δ268-417}$*), BHUM998 (*myc^6-BUD8$^{Δ375-417}$*), BHUM792 (*myc^6-BUD8$^{Δ375-505}$*), and BHUM1000 (*myc^6-BUD8$^{Δ468-505}$*) were digested with *Not*I and *Xho*I to isolate corresponding *BUD8* deletion constructs and insert them into pRS425 digested with the same restriction enzymes. The obtained plasmids were termed as BHUM1016 to BHUM1026. The *myc^6-BUD8* as well as the *myc^6-BUD8$^{Δ513-600}$* versions already existed as constructs cloned into a high-copy-number plasmid with *LEU2* selection marker (BHUM532 and BHUM706, respectively) and were directly used for the interaction studies.

The generation of suitable myc^9-Bud9p constructs was carried out analogously. Corresponding variants of *BUD9* were digested and isolated as *Spe*I/*Xho*I fragments from following plasmids: BHUM1002 (*myc^9-BUD9*), BHUM1003 (*myc^9-BUD9$^{\Delta 8-48}$*), BHUM1004 (*myc^9-BUD9$^{\Delta 8-130}$*), BHUM1005 (*myc^9-BUD9$^{\Delta 91-130}$*), BHUM800 (*myc^9-BUD9$^{\Delta 91-218}$*), BHUM1007 (*myc^9-BUD9$^{\Delta 168-218}$*), BHUM1008 (*myc^9-BUD9$^{\Delta 168-283}$*), BHUM1009 (*myc^9-BUD9$^{\Delta 244-283}$*), BHUM804 (*myc^9-BUD9$^{\Delta 244-369}$*), BHUM1011 (*myc^9-BUD9$^{\Delta 323-369}$*), BHUM1012 (*myc^9-BUD9$^{\Delta 323-450}$*), BHUM1013 (*myc^9-BUD9$^{\Delta 406-450}$*), BHUM808 (*myc^9-BUD9$^{\Delta 406-544}$*), and BHUM1015 (*myc^9-BUD9$^{\Delta 460-544}$*). The obtained fragments were cloned into pRS425 (*2μm, LEU2*) digested with SpeI and XhoI yielding the plasmids BHUM1027 to BHUM1040. Successful cloning was confirmed by restriction analyses of the obtained plasmids.

2.2 Methods

2.2.1 Cultivation of microorganisms

2.2.1.1 Cultivation of *Escherichia coli*

Cells were grown in Luria-Bertani (LB) medium (1% (w/v) Bacto-tryptone, 0.5% (w/v) yeast extract, 1% (w/v) NaCl) at 37°C. For selective media ampicillin in a concentration of 100μg/ml was added to the medium. Solid medium contained 1.5 to 2% (w/v) agar.

2.2.1.2 Cultivation of *Saccharomyces cerevisiae*

For cultivation of yeast cells YPD medium (1% (w/v) Bacto-tryptone, 1% (w/v) yeast extract, 2% glucose) or synthetic complete (SC) medium (0.15% (w/v) yeast nitrogen base, 0.5% (w/v) $(NH_4)_2SO_4$, 0.2 mM myo-inositol, 2% (w/v) glucose, 0.2% (w/v) amino acid mix-4 (2 g of each L-amino acid w/o histidine, leucine, tryptophan and uracil) lacking nutrients as needed to maintain various plasmids was used. Corresponding L-amino acids were supplemented as needed in following amounts: 0.3 mM histidine, 1.67 mM leucine, 0.4 mM tryptophan and 0.2 mM uracil, respectively. Investigation of pseudohyphal growth of diploid yeast cells was carried out using SLAD medium (1.5% (w/v) yeast nitrogen base, 2% (w/v) glucose, 5mM $(NH_4)_2SO_4$). Solid media contained 1.5 to 2% (w/v) agar. Cells were grown at 30°C.

2.2.2 Preparation and characterization of DNA

2.2.2.1 Quick boiling plasmid DNA preparation ('STET prep') from *E. coli* (Holmes *et al.*, 1981)

E. coli overnight cultures were harvested by centrifugation (13'000 rpm, 1 min) and resuspended in 400 μl STET buffer (8% (w/v) sucrose, 0.5% (v/v) Triton X-100, 50 mM EDTA (pH 8.0), 10 mM Tris-HCl (pH 8.0)). Lysis was triggered by addition of 25 μl lysozyme solution (12mg/ml) for 5 min and followed by 40 seconds incubation in a boiling water bath. Cell fragments were pelleted by centrifugation (13'000 rpm, 15 min) at 4°C. The sticky pellet was removed by a sterile toothpick. Plasmid DNA was precipitated by addition of 50 μl of 3 M and 500 μl isopropanol. After centrifugation (13'000 rpm, 15 min, 4°C), the DNA pellet was washed with 70% ethanol and air-dried. Finally, plasmid DNA was dissolved in 50 μl Tris-EDTA buffer (10 mM Tris-HCL (pH 8.0), 1 mM EDTA) and stored at -20°C.

2.2.2.2 QIAGEN plasmid DNA Mini preparation (QIAGEN, Hilden, D)

5 ml of an overnight culture of *E. coli* was harvested by centrifugation (13'000 rpm, 1 min). DNA preparation was carried out to supplier's specifications.

Optionally, the plasmid DNA was further purified. Therefore, 10 µl 3 M sodium acetate (pH 4.8) and 250 µl 96% EtOH p.a. were added to QIAGEN plasmid DNA Mini preparation. After centrifugation (13'000 rpm, 30 min), plasmid DNA was washed with 70% EtOH p.a. and air-dried. Finally, the purified plasmid DNA was dissolved in 50 µl water produced for HPLC and stored at -20°C.

2.2.2.3 QIAGEN plasmid DNA Midi preparation (QIAGEN, Hilden, D)

100 ml of an overnight culture of *E. coli* was harvested by centrifugation (4'500 rpm, 15 min, 4°C). DNA preparation was carried out to supplier's specifications.

2.2.2.4 Quick DNA preparation from yeast ('Smash & Grab'; Hoffmann and Winston, 1987)

A 10 ml overnight yeast culture was harvested by centrifugation (3'000 rpm, 3 min). After removal of the supernatant, cells were resuspended in 0.5 ml distilled water, removed in transferred to a 1.5 ml reaction tube and collected by centrifugation again (13'000 rpm, 1 min). The supernatant was discarded and the cells resuspended in the residual liquid. Then, 0.2 ml lysis buffer (2% (v/v) Triton X-100, 1% (w/v) SDS, 100 mM NaCl, 10 mM Tris, 1 mM EDTA (pH 8.0) together with 0.2 ml phenol/$MeCl_2$/Tris-EDTA and 200 µg glass beads were added and shaken for 10 min at 4°C. 0.2 ml TE buffer were added to the approach and spun again at maximum speed. After centrifugation aqueous layer was transferred to a fresh tube. To precipitate DNA, 1 ml 70% ethanol was added and the tube content was mixed by inversion. 30 min of centrifugation at maximum speed (13'000 rpm) pelleted the DNA, which was solved in 0.4 ml Tris-EDTA and 3 µl RNase (10mg/ml). After 10 min of incubation at 37°C again ethanol was added together with ammonium acetate (10µl of a 4 M solution). Mixing and following centrifugation (13'000 rpm, 2 min) resulted in a transparent pellet, which was finally solved in 50 µl Tris-EDTA. The DNA was stored at -20°C.

2.2.2.5 Determination of DNA concentration

The concentration of DNA was determined by measuring the optical density at 260 nm and calculated according to the following formula:

$$\mu g \text{ ds DNA/ml} = A_{260nm} \times 50 \times \text{dilution factor}$$

2.2.2.6 Polymerase chain reaction ('PCR', Saiki *et al*., 1985)

Polymerase chain reactions were carried out using the thermo-stable enzymes *Taq*-polymerase (FERMENTAS), *Pfu*-polymerase (PROMEGA) or KOD-Hifi-DNA polymerase (NOVAGEN). In general, 5-50 pmol of each primer and 10-100 ng DNA in a volume of 20-50 µl were used according to supplier's specifications. In case of colony-PCR, cells of an *E. coli* or an *S. cerevisiae* colony were directly used as template. The temperature profile was chosen in dependency of the DNA polymerase, the oligonucleotides and the template size.

2.2.2.7 DNA sequencing

For sequencing of dsDNA the ABI Prism® Big Dye terminator sequencing Kit (APPLIED BIOSYSTEMS GMBH, Weiterstadt, Germany) was used. About 500 ng dsDNA were mixed in reaction tubes with 5 pmol primer, 2 µl Premix (*Taq*-Polymerase, dNTPs, fluorescence-marked ddNTPs, reaction buffer) and 1 µl buffer filled up with HPLC-H_2O to 10 µl. 25 cycles of the following temperature profile were performed in a thermocycler: 10 s at 96°C, 5 s at primer-specific annealing temperature, 4 min at 60°C for elongation reaction. For elongation reaction the DNA was resuspended in 25 µl TSR buffer and renatured in a thermocycler. Fragments were separated automatically with an ABI Prism® 310 Genetic Analyzer (APPLIED BIOSYSTEMS GMBH, Weiterstadt, Germany).

2.2.3 Cloning techniques

2.2.3.1 DNA restriction

Analytical restrictions required 0.5 µg DNA routinely digested at 37°C for 2 h by 1-2 units of restriction enzymes in appropriate buffer (NEW ENGLAND BIOLABS (Ipswich, MA, USA), MBI FERMENTAS (Vilnius, Lit)). Preparative restrictions required, dependent on the strategy, more DNA.

2.2.3.2 Dephosphorylation of DNA

Linearized DNA fragments were dephosphorylated by incubating with 10 units shrimp alkaline phosphatase (ROCHE GMBH, Mannheim, D) in appropriate buffer for 30 min at 37°C. The reaction was stopped by heating at 65°C for 10 min.

2.2.3.3 Phosphorylation of DNA

Linearized DNA fragments were phosphorylated by incubating with 10 units T4 polynucleotide kinase (FERMENTAS, Vilnius, Lit) with 50 µM ATP in appropriate buffer for 30 min at 37°C; the reaction was stopped by heating at 70°C for 10 min.

2.2.3.4 Ligation of DNA fragments

Linear DNA fragments were mixed in ligation buffer (20 mM Tris-HCl, 10mM $MgCl_2$, 10 mM DTT, 0.6 mM ATP, pH 7.6) with 5 units T4-DNA-ligase (MBI FERMENTAS, Vilnius, Lit) in a total reaction volume of 20 µl and incubated overnight at 16°C or for 2 h at RT. Molar proportions between vector and insert were chosen approximately at 1:5 to 1:10. DNA was used for transformation without further purification.

2.2.3.5 Agarose gel electrophoresis

DNA solutions were mixed with 0.1 volumes DNA sample buffer (25% (v/v) Ficoll 4000, 0.25% (v/v) bromphenolblue, 0.25% (v/v) xylene cyanol), 200 mM EDTA (pH 8.0)). DNA fragments were separated in a horizontal agarose gel containing 1% agarose in TAE buffer (40 mM Tris-acetate, 20 mM sodium acetate, 2 mM EDTA (pH 8.0)) in presence of 0.5 µg/ml ethidium bromide applying a voltage of 80 volts maximum. DNA bands were detected on a UV-transilluminator at a wavelength of $\lambda = 254$ nm. Determination of fragment size was done using 'GENE RULER 1 kb DNA ladder Plus' from MBI FERMENTAS (Vilnius, Lit) or '1 kb DNA ladder' from NEW ENGLAND BIOLABS (Ipswich, MA, USA).

2.2.3.6 Isolation of DNA fragments

The desired DNA band was excised from agarose gel. DNA fragments were extracted from gel using a QIAquick gel extraction kit (QIAGEN, Hilden, D). Isolation was carried out according to supplier's specifications. The purified DNA was solved in distilled water and stored at -20°C until it was used.

2.2.4 Transformation methods

2.2.4.1 Preparation of competent *E. coli* cells (Inoue *et al.*, 1990)

250 ml SOB medium (2% (w/v) tryptone, 0.5% (w/v) yeast extract, 10 mM NaCl, 2.5 mM KCl, 10 mM $MgCl_2$, 10 mM $MgSO_4$) were inoculated with *E. coli* DH5α, SURE or XL1-blue in 2 l Erlenmeyer flask and shaken at 18°C at 2000 rpm/min for at least 24 h until an OD_{600nm} of 0.6 was achieved. Cells were chilled on ice for 10 min and then harvested by centrifugation (5000 × g, 10 min, 4°C). Supernatant was discarded. The bacterial pellet was resuspended in 80 ml of ice-cold transformation buffer TB (10 mM PIPES or 10 mM HEPES, 15 mM $CaCl_2$, and 250 mM KCl, 55 mM $MnCl_2$, pH 6.7), incubated for 10 min on ice and centrifuged again (5000 × g, 10 min, 4°C). Then, the cells were carefully resuspended in 20 ml TB. DMSO (a.k.a. Dimethylsulfoxide) was added to a final concentration of 7%. Careful mixing was followed by another chilling step on ice before cells were frozen in aliquots of 1 ml in liquid nitrogen and stored at -80°C until they were used.

2.2.4.2 Transformation of *E. coli* (Mandel and Higa, 1970)

200 µl of frozen, competent *E. coli* cells were thawed and incubated for 10-30 min with 1 µl of DNA to be transformed. After a heat shock (45 s, 42°C), cells were kept on ice for 5 min. 800 µl SOC medium (SOB medium + 20 mM glucose) were added and the mixture was kept at 37°C for 1 h. Finally, cells were plated out on appropriate selective medium.

2.2.4.3 Transformation of *S. cerevisiae*

2.2.4.3.1 Transformation of *S. cerevisiae* by LiOAc method (modified from Ito *et al.*, 1983)

A small amount of cells was inoculated in 5 ml of an appropriate medium (YPD medium or SC-medium) and incubated overnight at 30°C on a culture wheel. Medium for the main culture was inoculated with the cell suspension of the starter culture in a dilution of 1:50 and incubated at 30°C until an OD_{600nm} of 0.6 was reached. Cells were harvested by centrifugation (3'000 rpm, 3 min). After removal of the supernatant, the cell pellet was washed in 10 ml ice-cold Li-acetate/Tris-EDTA (0.1 M LiOAc, 10 mM Tris-HCl (pH 8.0), 1 mM EDTA (pH 8.0)) and finally dissolved in 400 µl Li-acetate × TE.

For each transformation an aliquot of 200 µl competent yeast cells was transferred to a sterile reaction tube. 20 µl denaturated salmon sperm DNA (ssDNA (10 mg/ml)), an

appropriate amount of DNA for transformation, and 800 µl PEG 4000 in Li-acetate/Tris-EDTA (50% (w/v) PEG (poly-ethylene-glycol) 4000, 0.1 M LiOAc, 2.5 mM Tris-HCl (pH 8.0), 0.25 mM EDTA (pH 8.0)) were added. Each approach was mixed by inverting the tube two or three times, incubated for 30 min at 30°C and heat-shocked for 25 min at 42°C. Cells were harvested by centrifugation (4'000 rpm, 1 min) and supernatant was carefully removed. After one hour of incubation in 1 ml YPD medium, cells were spun down (3'000 rpm, 1 min) and supernatant was removed. Cells were dissolved in the remaining liquid and spread out on appropriate selective media.

2.2.4.3.2 One-step-transformation of *S. cerevisiae*

15 to 20 ml of an overnight culture in YPD medium were harvested by centrifugation (3'000rpm, 2 min) at an OD_{600nm} of 0.8 to 1. The pellet was resuspended in 1 ml 'One-Step-Buffer' (40% (w/v) PEG 4000, 0.2 M LiOAc, 100 mM DTT). To 100 µl of this mixture, 50 ng to 1 µg plasmid DNA was added together with 10 µl of salmon sperm DNA (10mg/ml), which served as carrier. The suspension was mixed and heat-shocked (25 min, 42°C) until 100 µl of medium were added to ease plating on appropriate solid media.

2.2.5 Hybridization techniques

2.2.5.1 Labeling of hybridizing DNA probes

The probe was generated by amplification of template DNA by PCR and labelling by incorporation of α-^{32}P-dATP. For labeling of DNA probes the 'HexaLabel™ Plus DNA Labeling Kit' (FERMENTAS, Vilnius, Lit) was used according to supplier's specifications.

2.2.5.2 Southern hybridization (Southern, 1975)

For each approach 10 µg chromosomal DNA were digested for 12 h with an appropriate restriction enzyme. DNA fragments were separated in a horizontal agarose gel containing 1% agarose in TAE. After electrophoretic separation, gels were washed twice for 15 min in 0.25 M HCl solution and rinsed with H_2O. For denaturation gels were shaked gently once for 30 min in 0.5 M NaOH/1 M NaCl and twice for 30 min in 1 M NH_4OAc/0.02 M NaOH. DNA was transferred on nylon membranes ('Biodyne B Transfer Membrane', PALL GMBH, Dreieich, D) by capillary blotting for at least 4 h. DNA was cross-linked by illumination with UV-light (λ = 254 nm) for 2 min and baking at 80°C for 30 min. Then, membrane was pre-

hybridized in Church buffer (7% (w/v) SDS, 1 % (w/v) BSA, 1 mM EDTA, 250 mM Na-Phosphate, pH 7.2) for 2 h at 65°C. After pre-hybridization fresh Church buffer and labeled DNA-probe were added and membrane was hybridized overnight at 65°C. The probe solution was removed and membrane was washed twice with 0.1 × SSC (15 mM NaCl, 1.5 mM Na-Citrate)/0.1% (w/v) SDS for 30 min at 65°C. Detection of signals was carried using a 'Phospho Imager' (Fuji Photo Film Co., Ltd., Nakanuma, Japan).

2.2.6 Protein methods

2.2.6.1 Preparation of crude extracts

Protein extracts were prepared from cultures grown to mid-log phase (OD_{600} ~1.0). Cultures were kept on ice since cells were harvested by centrifugation (3'000 rpm, 3 min, 4°C). Cells were transferred in a fresh reaction tube and washed in 1 ml ice-cold Tris-EDTA buffer (10 mM Tris-HCl (pH 8.0), 1 mM EDTA). Cells were broken by adding 200 µg of glass beads (∅ 0.25 mm) and 280 µl of freshly prepared, ice-cold R-buffer (50 mM Tris-HCl (pH 7.5), 1 mM EDTA (pH 7.5), 50 mM DTT, 1mM PMSF, 0.5 mM TPCK, 0.025 mM TLCK, 1 µg/ml Pepstatin A) followed by shaking for 10 min at 4°C. Triton X-100 and SDS were added to a final concentration of 2% to each sample that were shaken for one further minute. The obtained crude lysates were kept for 15 min at room temperature and then spun down (3'000 rpm, 2 min, 4°C) to remove glass beads and large cell debris. The supernatant was collected as total cell lysate. 2 µl of each extract were removed to determine total protein concentration using a protein assay kit (BIO-RAD, München, Germany). An appropriate amount of 3 × SDS loading buffer (0.25 M Tris-HCl (pH 6.8), 15% (v/v) β-mercaptoethanol, 30% (v/v) glycerol, 7% (w/v) SDS, 0.3% (w/v) bromphenolblue) was added to each protein sample, which were finally denatured for 10 min at 65°C and stored at -20°C for further use.

2.2.6.2 Determination of protein concentration (Bradford, 1976)

Standards containing 100-1000 µg bovine serum albumin (a.k.a. BSA) per ml were prepared to plot a standard curve. 1:5 diluted Bradford solution was used as blank. 2 µl of crude extracts were mixed in a cuvette with 1 ml of 1:5 diluted Bradford reagent (BIO-RAD, München, D) and incubated for 5 min at RT. Absorbance at 595 nm was measured in a UV/Vis spectrophotometer.

2.2.6.3 SDS polyacrylamide gel electrophoresis (SDS-PAGE, Laemmli, 1970)

Electrophoretic separation of protein mixtures was carried out in 10% vertical gels, which consists of two gel types: running gel (3.5 ml water, 2.5 ml 4 × Lower Tris (1.5 M Tris base, 8 mM EDTA, 0.4% (w/v) SDS, pH 8.8), 4 ml polyacrylamide (acrylamide/bisacrylamide (30:0.8)), 25 µl APS (a.k.a. ammonium peroxidosulfate), 15 µl TEMED (N',N',N',N'-Tetramethyl-ethylendiamin) and stacking gel (3.4 ml water, 1.4 ml 4 × Upper Tris (0.5 M Tris base, 8 mM EDTA, 0.4% (w/v) SDS, pH 6.8), 0.6 ml PA (30:0.8), 40 µl APS, 20 µl TEMED). The gel types were cast and polymerized successively on each other. Volumes of equivalent protein concentrations of the extract were loaded in the gel. Gel electrophoresis was carried out in electrophoresis buffer (25 mM Tris base, 250 mM glycine, 0.1% (w/v) SDS) applying a voltage of 110 V for 10 min and 200 V for further 20 to 30 min.

2.2.6.4 Immunochemical detection of proteins ('Western blotting', Towbin *et al.*, 1979)

Preparation of yeast cell extracts and SDS-PAGE were performed as described. Transfer of electrophoretically separated proteins to a nitrocellulose membrane ('Protan', SCHLEICHER & SCHUELL, Dassel, Germany) was carried out overnight at 30 V in a 'MiniProtean 3 electrophoresis system' (BIO-RAD, München, D) in transfer buffer (25 mM Tris-Base, 192 mM glycine, 0.02% (w/v) SDS, 20% methanol).

To check the protein transfer the nitrocellulose membrane was stained for 1 min in Ponceau S solution (0.2% (w/v) Ponceau S, 3% (v/v) Trichlor-acetic-acid). To remove dye, nitrocellulose membrane was washed for 10 min in PBS (140 mM NaCl, 10 mM Na-Phosphate (pH 7.5)) with 3% (w/v) milk powder. Free binding sites on the nitrocellulose membrane were blocked by incubating the membrane for 1 h in fresh PBS/milk powder solution. Then, the primary antibody diluted in PBS/milk powder solution was applied for 2 h. For removing residual antibody, membrane was washed once for 10 min in PBS/milk powder solution and twice in PBS for 10 min each. Then, the membrane was incubated for 1 h with the secondary peroxidase-coupled antibody solved in PBS/milk powder solution. Removing of the antibody was carried out analogously. Finally, the membrane was washed twice in 100 mM Tris-HCl buffer (pH 8.5) for 5 min each.

Detection of the proteins on membrane was carried out using the 'Enhanced Chemiluminescence System' (ECL (Tesfaigzi *et al.*, 1994)) involving two solutions (solution A: 2.5 mM luminol, 40 µl paracoumaric acid, 100 mM Tris-HCl (pH 8.5) and

solution B: 5.4 mM H_2O_2, 100 mM Tris-HCl (pH 8.5)), in which the nitrocellulose membrane was incubated for 1 min. To visualize any signals, a Hyperfilm™-ECL™ was illuminated for 1 to 15 min and developed.

2.2.7 Co-immunoprecipitation

Extracts of strains expressing GST fusion proteins together with myc-tagged versions of Bud8p and Bud9p were prepared from cultures grown for 4 h to the exponential growth phase in SC medium lacking nutrients as needed to maintain plasmids. Cells were harvested by centrifugation (5 min, 3'000 rpm), washed in 2% galactose solution, and transferred to SC medium containing 2% galactose. After incubation for 6 h at 30°C, cultures were chilled on ice. Briefly, cells were harvested by centrifugation at 4°C and washed once in B-buffer (50mM HEPES (pH 7.5), 50 mM KCl, 5 mM EDTA (pH 7.5)). After centrifugation cells were resuspended in 300 µl ice-cold B-buffer containing protease inhibitors (50 mM DTT, 1mM PMSF, 0.5 mM TPCK, 0.025 mM TLCK, 1 µg/ml Pepstatin A) and transferred to 2 ml-reaction tubes. Cells were then broken by vortexing with glass beads at 4°C. After 10 min, 300 µl B-buffer plus protease inhibitors as well as Triton X-100 to a concentration of 1% were added to each sample and shaken again by vortexing at 4°C for 1 min. This step was followed by centrifugation for 3 min at 2000 rpm to remove glass beads and large cell debris. 10 µl of the extracts were removed to determine total protein concentration. 80 µl of the supernatant were transferred to a 1.5 ml-reaction tube and denatured by addition of 3× Laemmli buffer to each sample and heating for 5 min at 65°C. 175 µl of the remaining total extract were mixed with 800 µl B-buffer plus protease inhibitors plus 1% Triton X-100 and 100 µl 50% Glutathion-Sepharose™ 4B and incubated overnight at 4°C. Beads were repeatedly washed in B-buffer plus 0.1% Triton X-100 and collected to purify GST fusions and any associated proteins. Samples were denatured by heating at 65°C for 5 min in Laemmli buffer. Equal amounts of each sample were analyzed by Western blot analysis using either polyclonal anti-GST antibodies or the monoclonal mouse anti-myc antibody (9E10).

2.2.8 Pulse-chase experiments

For investigation of Bud8p and Bud9p processing cells of adequate strains were shifted to 37°C for indicated times, pulse-labeled for 10 min with Tran³⁵S-label (ICN) and chased for 60 min. The labeled proteins were immunoprecipitated using specific antibodies and

separated by SDS-PAGE. After incubating the gel with 'Amplify' (AMERSHAM PHARMACIA BIOTECH, Buckinghamshire, GB) for 45 min the proteins were detected by exposing the gels to X-Omat AR (EASTMAN KODAK CO., Rochester, NY, USA) at -80°C.

2.2.9 Protein localization by GFP fluorescence microscopy

Strains harbouring plasmids encoding GFP-Bud8p or GFP-Bud9p variants were individually grown to the mid-log phase in liquid YNB medium as described for bud scar staining. Cells from 1 ml of the cultures were harvested by centrifugation and immediately viewed *in vivo* on a ZEISS AXIOVERT microscope by either differential interference microscopy (DIC) or fluorescence microscopy using a GFP filter set (AHF ANALYSENTECHNIK AG, Tübingen, Germany). Cells were photographed using a HAMAMATSU ORCA ER digital camera and the IMPROVISION OPENLAB software (IMPROVISION, Coventry, UK).

2.2.10 Pseudohyphal growth assays

Assays for pseudohyphal development were performed as described previously (Mösch and Fink, 1997). After three days of growth at solid SLAD medium, pseudohyphal colonies were viewed with a ZEISS AXIOLAB microscope and photographed using a digital camera DX30 and the Kappa Image Base Noah software (KAPPA OPTO-ELECTRONICS, Gleichen, Germany).

2.2.11 Bud scar staining and determination of budding patterns

For characterization of budding patterns, bud scars and birth scars were visualized by fluorescence microscopy. Bud scar staining was performed on YF cells grown in to the exponential phase. Cells in the exponential phase were prepared by growing strains in liquid YPD medium at 30°C to an OD_{600} of 0.6 and then collected by centrifugation in conical polystyrene tubes. To disperse clumps, cells of diploid strains were resuspended in 1 ml water and sonicated briefly. Cells of haploid strains had been sonicated more intensively. Suspensions were generally fixed at room temperature for 2 h in 3.7% formaldehyde. Samples were rinsed twice in water and resuspended in 100 µl of a fresh stock of 1 mg/ml calcofluor white (Fluorescent Brightener 28; SIGMA, St. Louis, MO). After 10 min incubation with calcofluor solution samples were washed thrice and were then resuspended in water. Birth scars and bud scars were visualized by fluorescence microscopy using a ZEISS AXIOVERT microscope and photographed using HAMAMATSU ORCA ER digital camera and the

IMPROVISION OPENLAB software (IMPROVISION, Coventry, UK). Bud scar distribution of diploid cells was determined qualitatively and quantitatively. For qualitative analysis, cells with between 5 and 12 bud scars were divided in four classes: unipolar proximal, cells with (nearly) all bud scars at the proximal cell pole immediately adjacent to one another; unipolar distal, cells with (nearly) all bud scars at the distal cell pole immediately adjacent to one another; bipolar, cells with at least three bud scars at the distal cell pole and at least one bud scar at the proximal pole; and random, cells with bud scar distribution other than bipolar or unipolar. For each experiment, the budding pattern was determined for 200 cells. For quantitative evaluation, the position of all bud scars was determined for 100 cells with one, two, three, and four bud scars. Positions of bud scars were scored as proximal cell pole (the third of the cell centred on the birth scar), equatorial (the middle third of the cell), or the distal pole (the third of the cell most distal to the birth scar).

Bud scar distribution of haploid cells was determined qualitatively. For each experiment, the budding pattern of 200 cells with more than 4 bud scars was determined and divided in three different classes: axial (cells with bud scars immediately adjacent to the previous site of cell separation), bipolar, and random.

3. Results

3.1 Co-localization of the cortical tag proteins Bud8p and Bud9p in Saccharomyces cerevisiae

In accordance with their function as cortical tag proteins, Bud8p and Bud9p are localized at the cell poles of *S. cerevisiae*. Previous studies showed that Bud8p is localized at the distal pole of mother and daughter cells (Taheri *et al*., 2000; Harkins *et al*., 2001; Schenkman *et al*., 2002). In contrast to this, Bud9p could be detected at the proximal pole (Harkins *et al*., 2001; Schenkman *et al*., 2002; Kang *et al*., 2004b) as well as the distal pole (Taheri *et al*., 2000). Former studies were carried out *in vivo* by using GFP fusion proteins and *in situ* by using myc-tagged versions of both proteins. Because in previous studies only one of each protein had been labelled, co-localization studies by labelling both proteins with different fluorescence markers were performed. For this purpose, Bud8p and Bud9p were fused to CFP (cyan fluorescent protein) and YFP (yellow fluorescent protein). The obtained CFP and YFP fusion proteins are well-suited for the intended localization studies, because the different excitation (CFP: 436 nm; YFP: 514 nm) and emission wavelengths (CFP: 476 nm; YFP: 527 nm) of the fluorescence proteins ensure that either CFP or YFP is excited and consequently detected.

3.1.1 Expression of CFP and YFP fusion proteins in S. cerevisiae strains

To investigate their localization, *BUD8* and *BUD9* were fused to *CFP* and *YFP*. In this way, four different constructs were obtained: BHUM941 (*CFP-BUD8* in pRS426), BHUM942 (*YFP-BUD8* in pRS426), BHUM951 (*CFP-BUD9* in pRS426), and BHUM952 (*YFP-BUD9* in pRS426). To study the expression of these constructs, BHUM943 and BHUM944 were transformed into the diploid *bud8Δ* strain RH2449. BHUM951 and BHUM952 were transformed into the diploid *bud9Δ* strain YHUM1049. Expression of *BUD8* and *BUD9* constructs was determined by preparing total protein extracts from the obtained yeast strains and analysis by Western blot hybridization. Thus, equivalent amounts of each sample were subjected to SDS-PAGE, transferred to nitrocellulose, and probed with a polyclonal anti-GFP antibody (α-GFP) as primary antibody and a peroxidase-coupled anti-mouse antibody as secondary antibody. Bud8p fused to CFP and YFP, respectively, appeared reproducibly as pattern of multiple signals (Fig. 6). The lowest molecular form appeared around 85 kDa, and several bands of higher molecular weight could be observed around 180 kDa. Separation of

CFP- and YFP-Bud9p by SDS polyacrylamide gel electrophoresis typically led to appearance of double bands, whereof one could be observed in the range of 90 kDa and the other at a size of approximately 120 kDa (Fig. 6). The calculated molecular weight of each analyzed protein was lower than the observed one. Presumably, the appearance at a higher size than the predicted mass had been shown to result in part from glycosylation (Harkins *et al*., 2001). Our findings suggest that the four fusion proteins consisting of *BUD8* and *BUD9* fused to either CFP or YFP were expressed in adequate amounts. Conclusively, neither the expression of *BUD8* nor *BUD9* was disturbed by fusion with *CFP* or *YFP*.
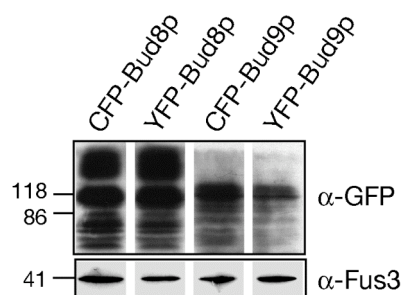

Fig. 6: Expression of Bud8p and Bud9p fusion proteins. Total protein extracts were prepared from a diploid *bud8Δ* strain expressing *CFP-BUD8* (BHUM943) or *YFP-BUD8* (BHUM944) and a diploid *bud9Δ* strain expressing *CFP-BUD9* (BHUM951) or *YFP-BUD9* (BHUM952). Extracts were analyzed for expression of Bud8p and Bud9p fused to CFP or YFP by Western blot analysis using a polyclonal anti-GFP antibody (α-GFP) (upper panel). As an internal control, the expression of Fus3p was measured using an anti-Fus3p antibody (lower panel). Molecular size standards (in kDa) are indicated on the left hand side.

3.1.2 Bud8p and Bud9p fusion proteins are partially functional

To study functionality of the Bud8p and Bud9p fusion proteins, their ability to confer bipolar budding in diploid yeast strains was investigated (Fig. 7). For this purpose, a diploid *bud8Δ* strain (RH2449) expressing either *CFP-BUD8* or *YFP-BUD8* and a diploid *bud9Δ* strain (YHUM993) carrying *CFP-BUD9* and *YFP-BUD9* were used. Furthermore, a diploid *bud8Δ bud9Δ* double mutant strain (RH2453) expressing *CFP-BUD8* in combination with *YFP-BUD9* or *vice versa* was examined. Also all strains, RH2449, BYHUM993, as well as RH2453, carrying no plasmids were used as reference strains. As additional controls, a diploid *bud1Δ* strain (RH2448) and a diploid wild type strain (RH2495) were inspected. Bud scars of cells growing in the yeast form (YF) to the exponential phase were stained with calcofluor, and budding patterns were determined by quantitative evaluation of the position of the first four bud scars as well as by determination of the final budding pattern of cells with four to twelve bud scars.
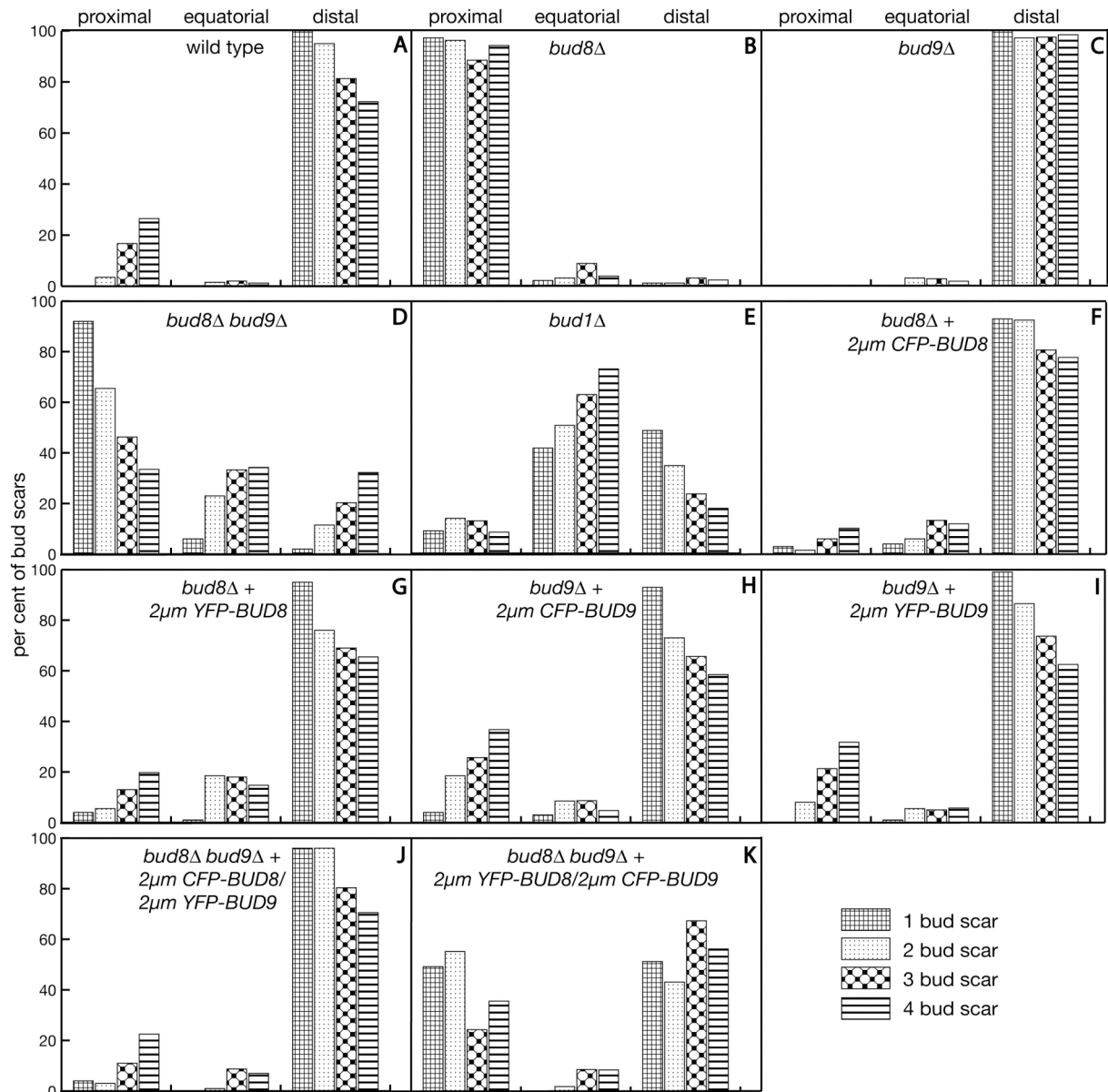
Fig. 7: Early budding patterns in yeast strains expressing CFP- and YFP-fusion proteins. Exponentially growing cultures from yeast strains expressing CFP- and YFP-fusion proteins were stained with calcofluor to evaluate the bud scar distribution by fluorescence imaging of cells. Following strains were investigated: (A) RH2495 (wild type), (B) RH2449 (*bud8Δ/bud8Δ*), (C) YHUM993 (*bud9Δ/bud9Δ*), (D) RH2453 (diploid *bud8Δ bud9Δ*), (E) RH2448 (*bud1Δ*), (F, G) RH2449 transformed with BHUM943 (*CFP-BUD8*) and BHUM944 (*YFP-BUD8*), respectively, (H, I) YHUM993 transformed with BHUM951 (*CFP-BUD9*) and BHUM952 (*YFP-BUD9*), respectively, and (J, K) RH2453 transformed with BHUM943/BHUM952 or BHUM944/BHUM951. For each strain, the positions of all bud scars were determined for 100 cells with one bud scar (representing in total 100 bud scars per bar), 100 cells with two bud scars (representing 200 bud scars per bar), 100 cells with three bud scars (representing 300 bud scars per bar), and 100 cells with four bud scars (representing 400 bud scars per bar). Bud scars were scored as proximal (the third comprising the birth end of the cell), equatorial (the middle third of the cell located between proximal and distal cell pole), or distal (the third that is at the opposite to the birth scar). Bars represent the percentage of cells at the proximal, the equatorial, and the distal region. For each strain the average value from two independent experiments is shown.

The analysis of the bud position of the first four bud scars showed that wild type yeast cells produce the first bud scar nearly always at the distal cell pole of the mother cell. The first bud scar at the proximal pole appeared soonest after formation of the third daughter cell. Mutant strains carrying a *BUD8* deletion bud almost exclusively from the proximal pole, whereas the absence of *BUD9* typically leads to a unipolar distal budding pattern (Zahner *et al*., 1996). Strains with null mutations in both genes, *BUD8* and *BUD9*, firstly also bud almost exclusively from the proximal pole (Zahner *et al*., 1996). In the course of further budding events, bud scars are scattered increasingly all over the cell surface. A *bud1Δ* strain displayed randomization of the budding pattern in combination with an increased frequency of budding events in the middle of the cell between the proximal and the distal cell pole. In case of the yeast strain carrying a *BUD8* deletion, the budding pattern defect could be rescued when such a strain was transformed with plasmids expressing *CFP-BUD8* and *YFP-BUD8*, respectively. In both cases, the transformants displayed bipolar budding.

The same was true for a diploid *bud9Δ* strain. Transformation of this strain with *CFP-* or *YFP-BUD9* led to nearly normal bipolar budding. Nevertheless, the amount of bud scars in the middle of the cell was slightly increased, which might be due to the fact that high copy number plasmids were used.

Re-establishment of bipolar budding in *bud8Δ bud9Δ* double mutants was successful when a corresponding strain (RH2453) was transformed with plasmids containing *CFP-BUD8* and *YFP-BUD9*, respectively. Similarly, expression of *YFP-BUD8* and *CFP-BUD9* in *bud8Δ bud9Δ* mutants principally re-established bipolar budding, although a higher percentage of cells were observed that select the proximal pole during the first or second division. Thus, the CFP-Bud8p, YFP-Bud8p, CFP-Bud9p, and YFP-Bud9p proteins appear to be functional, although with strongly reduced activity. The partial rescue of *bud8Δ bud9Δ* mutants by expression of both Bud8p and Bud9p fusion proteins might further be present due to overexpression of both proteins.

The results obtained with quantitative evaluation of the initial first four bud scars correlated with the further investigation of the final budding pattern (Fig. 8). This analysis showed that wild type cells typically bud in a bipolar budding pattern, where newborn daughter cells emerge from the proximal and the distal pole in a 1:1 distribution. As found in former studies, *bud8Δ* strains formed daughter cells with a high frequency at the proximal cell pole, and strains lacking *BUD9* exhibit a unipolar distal budding pattern. Strains, which are

not able to produce neither Bud8p nor Bud9p, are characterized by a randomization of bud site selection similar to *bud1Δ* strains. Expression of fluorescent variants of Bud8p and Bud9p led to re-establishment of the bipolar pattern, although a higher proportion of random budding was observed when compared to a control strain.
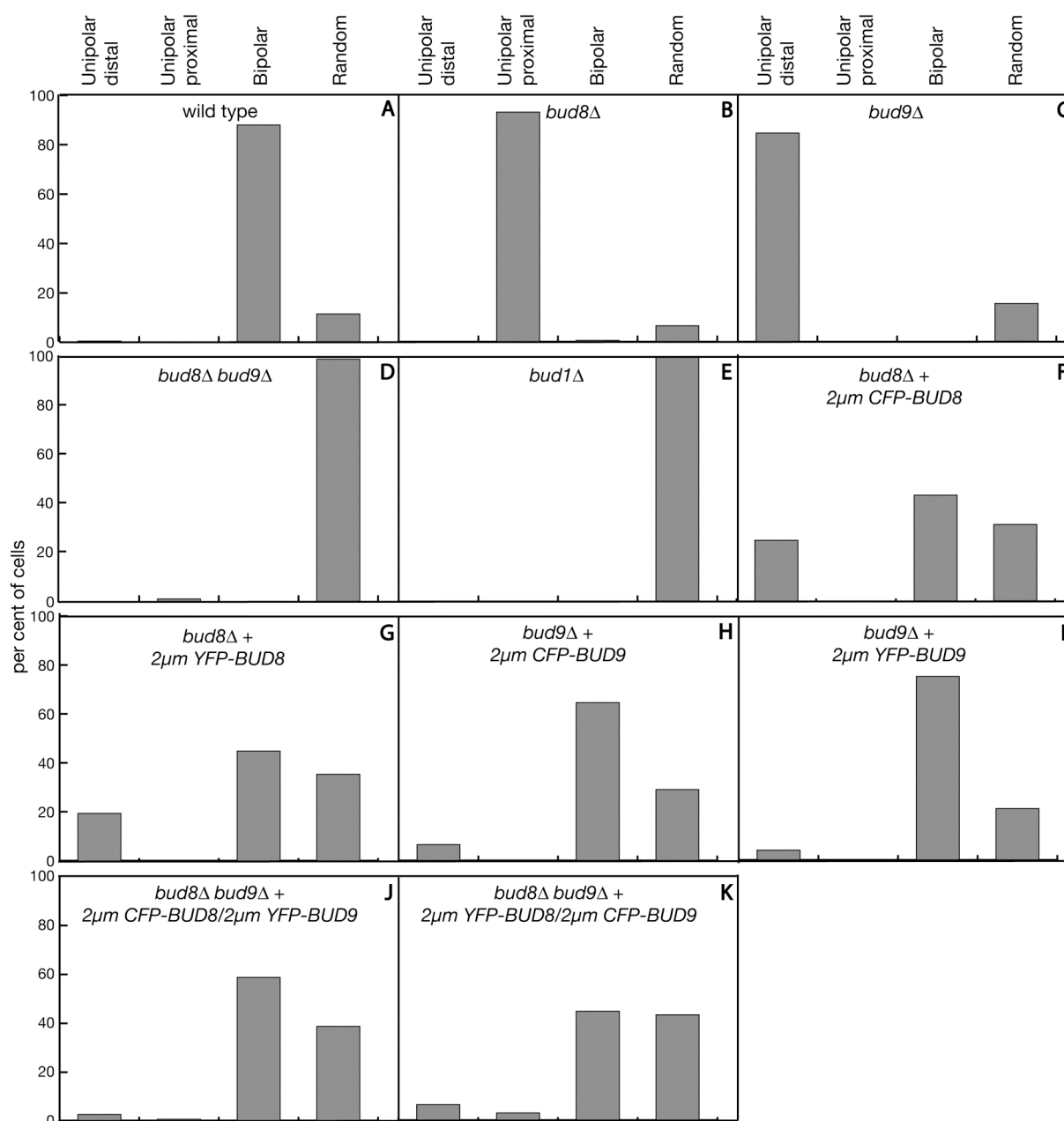

Fig. 8: Late budding pattern of yeast strains expressing CFP- and YFP-fusion proteins. Cells described in Fig. 7 were exponentially grown and stained with calcofluor. For qualitative evaluation of the budding pattern, cells with 5 to 12 bud scars were analyzed and divided in following classes: 'unipolar proximal' for cells with most bud scars at the proximal cell pole; 'unipolar distal' for cells with most bud scars at the distal cell pole immediately adjacent to one another; 'bipolar' for cells with at least three bud scars at the distal pole and at least one bud scar at the proximal pole; 'random' for cells with bud scar distribution other than unipolar or bipolar. For each strain and experiment at least 200 cells were analyzed.

Similar effects on the budding pattern were observed when *bud8Δ bud9Δ* double mutant strains expressed both fusion proteins (CFP-Bud8p together with YFP-Bud9p or YFP-Bud8p together with CFP-Bud9p) at high levels. Although bipolar budding was observed in 40-60% of the cells, more than 40% of the investigated cells displayed a random budding pattern. This effect is more pronounced in strains that express YFP-Bud8p in combination with CFP-Bud9p than in strains synthesizing CFP-Bud8p and YFP-Bud9p. Thus, although expression of fluorescent fusions of Bud8p and Bud9p does not completely rescue the budding defects of *bud8Δ bud9Δ* mutants, these proteins appear to be suitable for co-localization studies.

3.1.3 Co-localization of Bud8p and Bud9p using CFP- and YFP-fusion proteins

For co-localization studies *BUD8* and *BUD9* fused to *CFP* or *YFP* were each transformed into the haploid *bud8Δ bud9Δ* strains YHUM1050 (*MATα, bud8Δ::HIS3, bud9Δ::HIS3, ura3-52, his3::hisG, leu2::hisG*) and YHUM1051 (*MAT**a**, bud8Δ::HIS3, bud9Δ::HIS3, ura3-52, his3::hisG, leu2::hisG, trp1::hisG*), respectively. Four strains were obtained, which were crossed in a way that diploid strains were generated expressing either CFP-Bud8p in combination with YFP-Bud9p or YFP-Bud8p in combination with CFP-Bud9p. To localize fusion proteins, cultures of these diploid strains were grown in YNB medium to the exponential phase. Investigation of the proteins was done by microscopic visualization using a suited filter set for CFP and YFP, respectively.

The investigation of CFP- and YFP-Bud8p under the fluorescence microscope revealed that the proteins could be detected in unbudded cells as distinct signal at one of the both cell poles, presumably the distal pole (Fig. 9). In parallel, Bud9p fused to CFP or YFP could be detected as tiny spot at both poles (Fig. 9). Once cells begin to form a bud, Bud8p is localized asymmetrically at the site of the budding event. In rare cases (approximately 10% of all unbudded cells with a detectable signal), an additional signal could be observed at the site opposite of that, where the daughter cell emerged. We suggest that these signals might be unspecific aggregations because of the overexpression of the proteins within the cell. At this stage, Bud9p could be detected partly as a distinct signal at the bud tip. With increasing size of the daughter cell, localization patterns of Bud8p and Bud9p were maintained: Bud8p was still localized as an asymmetrical signal at the bud site of the mother cell and as crescent-like

structure at the emerging daughter cell, and Bud9p remained as tiny dot at the distal cell pole of the bud tip.
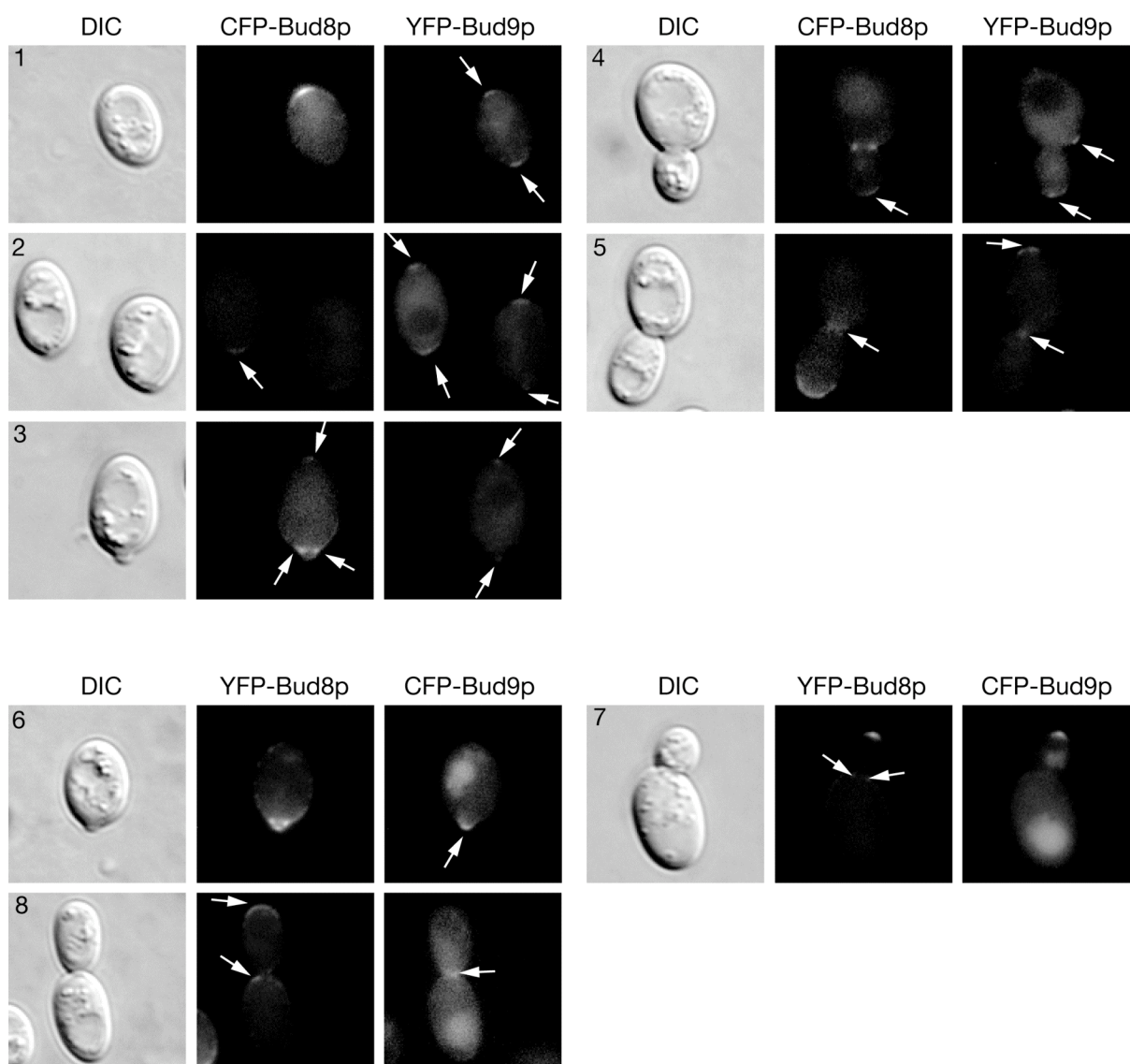

Fig. 9: Co-localization of CFP and YFP fusion proteins with Bud8p and Bud9p. Images show localization patters of CFP- and YFP-fused Bud8p and Bud9p proteins as visualized by CFP or YFP filter sets, respectively. Different stages of the cell cycle are shown: cells without a bud (1 & 2), with a small (3 & 4), middle-sized (5 & 6), or large (7 & 8) bud; cells were observed and photographed by Nomarski filter (DIC) or fluorescent microscopy (CFP/YFP). **(1-5)** *bud8Δ bud9Δ + CFP-BUD8/YFP-BUD9*; **(6-8)** *bud8Δ bud9Δ + YFP-BUD8/CFP-BUD9*.

In summary, these co-localization studies support that Bud8p and Bud9p function as marker at the distal and proximal cell pole, respectively. Bud8p is primarily detected at the distal pole, whereas Bud9p is found at both poles, substantiating the hypothesis that Bud9p does not only play a role as proximal pole marker but also as negative regulator of Bud8p at the distal pole.

3.2 Characterization of domains of landmark proteins Bud8p and Bud9p

3.2.1 Generation of Bud8p and Bud9p deletion sets

The exact mechanism, by which the potential landmark proteins Bud8p and Bud9p regulate site-specific initiation of cell division, is not known. The overall structures of Bud8p and Bud9p are similar in that both are predicted to consist of a large NH_2-terminal extracellular domain, followed by a membrane-spanning domain (TM1), a short cytoplasmic loop, a second membrane-spanning domain (TM2), and a very short extracellular domain at the COOH-terminus (Chant, 1999; Harkins *et al.*, 2001; Taheri *et al.*, 2000) (Fig. 10). The NH_2-terminal portion of both proteins contains several *N*- and *O*-glycosylation sites that appear to be functional (Harkins *et al.*, 2001).
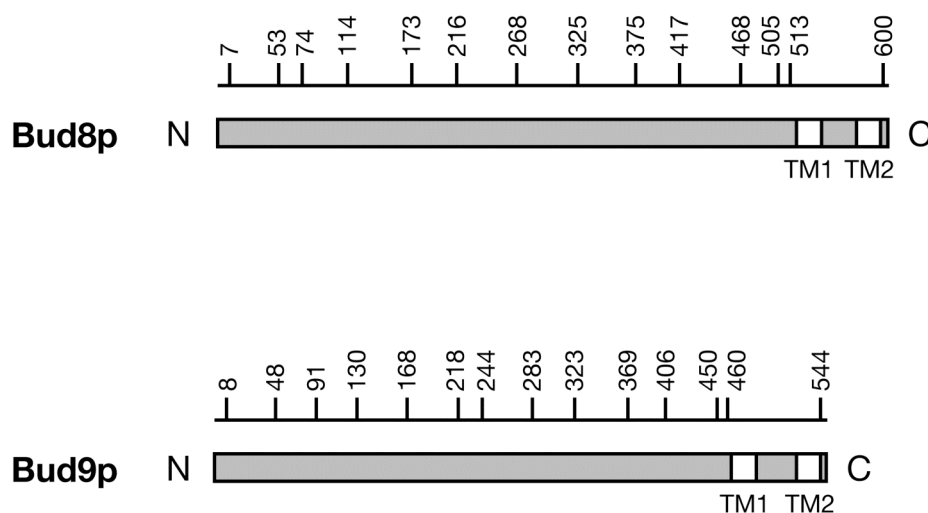

Fig. 10: Domain structures of Bud8p and Bud9p. Proteins are shown as bars from the NH_2- to the COOH-terminus with ruler on top numbering the position of amino acid residues. TM1 and TM2 indicate the positions of the two transmembrane domains.

To identify regions necessary for proper function and localization of Bud8p and Bud9p, deletion sets of both proteins were constructed. Generally, deletions were chosen in a way by which the deleted parts overlap. Furthermore, all proteins were tagged with myc-epitopes for detection by immunoblotting. In the case of *BUD8*, twelve deletion variants were generated. Constructs expressing deletion proteins were transformed into the haploid **a**-strain YHUM904 and the α-strain YHUM861. Strains with corresponding constructs were combined to receive diploid strains for investigations. In the case of *BUD9*, thirteen deletion constructs were established. These deletion constructs were transformed into the haploid **a**-strain YHUM994 and the α-strain YHUM995. Diploid strains were received by crossing of corresponding **a**- and α-strains.

To measure expression of the different Bud8p and Bud9p deletion variants, total protein extracts from corresponding diploid yeast strains were prepared and analyzed by Western blot analysis using monoclonal anti-myc antibodies. The expression of both proteins in endogenous amounts resulted in strong signals, which could be clearly visualized (Fig. 11 & Fig. 12). A wild-type strain expressing non-tagged full-length Bud8p and Bud9p proteins was used as control and does not display any signals. In case of Bud8p, all epitope-tagged mutant proteins produced specific and detectable signals when corresponding yeast strains were analyzed by Western blot analysis. The myc[6]-tagged full-length protein from *BUD8* (with a calculated mass of 75 kDa) reproducibly appeared as multiple signal-pattern when separated in a 10% SDS polyacrylamide gel electrophoresis (Fig. 11). The lowest molecular form appeared around 85 kDa, and several bands of a higher molecular weight could be observed between 130 kDa and 140 kDa. Appearance of Bud8p at a size higher than the calculated molecular weight was shown to result in part from glycosylation (Harkins *et al.*, 2001). Ten out of the twelve Bud8p mutant proteins also produced multiple bands, with one band appearing in the range of the calculated molecular weight and with further bands appearing at a higher size. In contrast, the two mutant proteins Bud8p$^{\Delta375-417}$ and Bud8p$^{\Delta375-505}$ produced only a single band, with Bud8p$^{\Delta375-417}$ appearing in the range of the calculated size and Bud8p$^{\Delta375-505}$ appearing at a size higher than the predicted. Essentially similar results were obtained in case of epitope-tagged myc[9]-Bud9p (Fig. 12). The calculated weight of this polypeptide is 75 kDa. Expression of myc[9]-Bud9p resulted in multiple signals where the lowest signal appeared around 80 kDa and further diverse bands around 110 and 130 kDa. The appearance of the Bud9p polypeptide at higher molecular levels than the predicted one reflects the glycosylation of the protein as found in case of Bud8p (Harkins *et al.*, 2001).
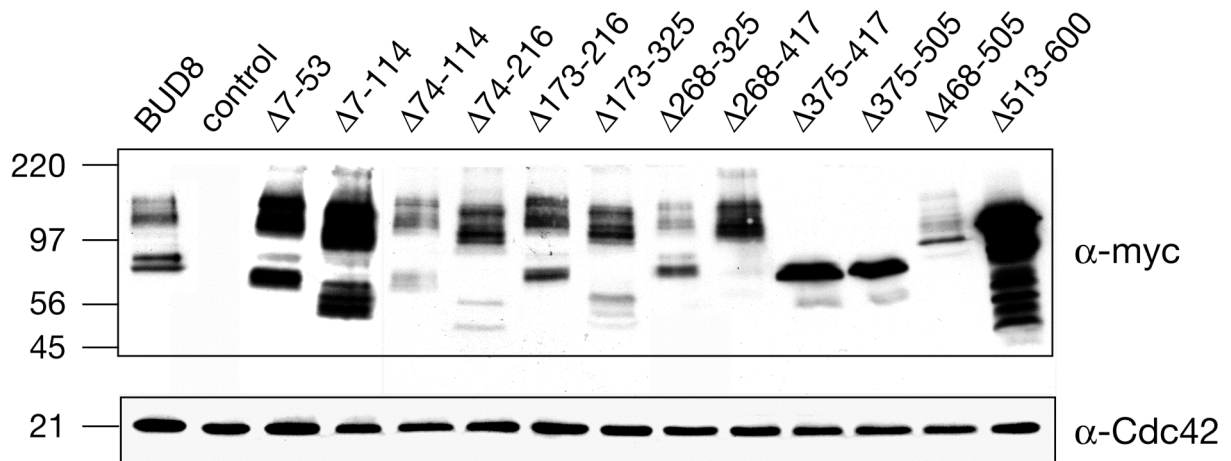
Fig. 11: Expression levels of Bud8p variants. Total protein extracts were prepared from strains expressing non-tagged *BUD8* (RH2495, control), *myc⁶-BUD8* (YHUM842, *BUD8*), and *myc⁶-BUD8* mutant alleles (YHUM843, *Δ7-53*; YHUM844, *Δ7-114*; YHUM847, *Δ74-114*; YHUM848, *Δ74-216*; YHUM849, *Δ173-216*; YHUM850, *Δ173-325*; YHUM851, *Δ268-325*; YHUM852, *Δ268-417*; YHUM853, *Δ375-417*; YHUM854, *Δ375-505*; YHUM855, *Δ468-505*; YHUM856, *Δ513-600*). Extracts were analyzed for expression of myc-epitope tagged proteins by Western blot analysis using a monoclonal anti-myc antibody (α-myc). As an internal control, the expression of Cdc42p was measured using an anti-Cdc42p antibody (lower panel). Molecular size standards (in kDa) are shown on the left hand side.
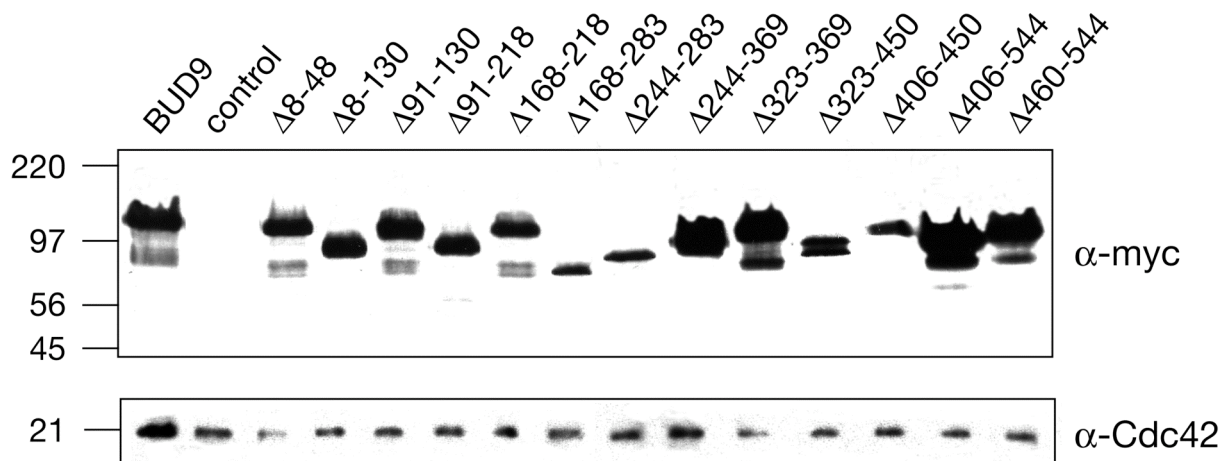

Fig. 12: Expression levels of Bud9p variants. Total protein extracts were prepared from a reference strain carrying the wild type allele of *BUD9* (RH2495), a strain carrying a *myc⁹-BUD9* allele (YHUM1009, *BUD9*) as well as strains expressing the epitope-tagged *BUD9* mutant alleles (YHUM1010, *Δ8-48*; YHUM1011, *Δ8-130*; YHUM1012, *Δ91-130*; YHUM1013, *Δ91-218*; YHUM1014, *Δ168-218*; YHUM1015, *Δ168-283*; YHUM1016, *Δ244-283*; YHUM1017, *Δ244-369*; YHUM1018, *Δ323-369*; YHUM1019, *Δ323-450*; YHUM1020, *Δ406-450*; YHUM1021, *Δ406-544*; YHUM1022, *460-544*). Equivalent amounts of each sample were subjected to SDS-PAGE, transferred to nitrocellulose and probed with a monoclonal anti-myc antibody (α-myc). As an internal control, protein levels of Cdc42p were measured in the same extracts using a polyclonal anti-Cdc42p antibody (α-Cdc42p); molecular size standards (in kDa) are shown on the left hand side.

3.2.2 Functionality and localization of Bud8p and Bud9p mutant proteins

3.2.2.1 Bipolar budding of diploid strains

To test the functionality of Bud8p and Bud9p deletion proteins, the budding patterns produced by corresponding mutant strains were determined by staining bud scars with calcofluor and early (first four) and late (cells with 5 to 12 bud scars) bud site selection patterns (Fig. 13 & Fig. 14; Table 4) were analyzed.

As previously shown, diploid *bud8Δ/bud8Δ* deletion strains elaborated a unipolar proximal budding pattern (Harkins *et al.*, 2001; Taheri *et al.*, 2000). A strain expressing the myc^6-tagged full-length version of *BUD8* was phenotypically indistinguishable from a strain expressing the non-tagged *BUD8* wild type gene in that both produced a bipolar budding pattern in YF cells (Fig. 13). The analysis of the *BUD8* mutants revealed three different phenotypic classes. A first class included four mutants (*BUD8$^{Δ7-53}$*, *BUD8$^{Δ7-114}$*, *BUD8$^{Δ74-114}$*, and *BUD8$^{Δ468-505}$*) establishing a bipolar budding pattern like a wild-type strain or a strain expressing a six fold myc-tagged wild-type version of *BUD8* (Fig. 13). Evaluation of the bud positions of the first four bud scars revealed that three strains expressing either *BUD8$^{Δ7-53}$*, *BUD8$^{Δ7-114}$* or *BUD8$^{Δ74-114}$*, formed their first and second bud scars almost exclusively at the distal cell pole (Fig. 14). This pattern is also characteristic for the wild-type strain. The fourth mutant of this class expresses the *BUD8$^{Δ468-505}$* allele, coding for one variant of Bud8p lacking a segment that is situated close to the first of two putative transmembrane domains at the C-terminus. However, the bipolar budding pattern of this strain is not identical to the wild type pattern, because the amount of cells with a random budding is slightly enhanced. Analysis of the early budding pattern revealed that the *BUD8$^{Δ468-505}$* mutant strain formed bud scars at both cell poles with almost equal frequency already during the first rounds of cell division of newborn cells, whereas the initial bud scars of a control strain emerged predominantly from the distal pole.

The second class included four mutants, which expressed the *BUD8$^{Δ74-216}$*, *BUD8$^{Δ375-417}$*, *BUD8$^{Δ375-505}$*, or *BUD8$^{Δ513-600}$* alleles. All of these strains selected the proximal pole for budding with a frequency that is similar to strains in which *BUD8* is completely deleted (Fig. 13 and Fig. 14). These mutants define two segments of Bud8p, one residing in the NH$_2$-terminal portion and the other being located at the COOH-terminal part, that appear to be indispensable for functionality of the protein.

A third class included the strains expressing $BUD8^{\Delta173-216}$, $BUD8^{\Delta173-325}$, $BUD8^{\Delta268-325}$, and $BUD8^{\Delta268-417}$. Surprisingly, these strains produced a random budding pattern with a very high frequency (Fig. 13; Table 4). The lowest amount of randomized cells in a population (around 56%) was determined in case of the mutant strain, which expressed the $BUD8^{\Delta173-216}$ allele. The remaining strains ($BUD8^{\Delta173-325}$, $BUD8^{\Delta268-325}$, and $BUD8^{\Delta268-417}$) established this phenotype with a significant higher frequency: 75-83% of the cells developed a random budding pattern. To date this budding phenotype has not been observed for *BUD8* mutants, except when *BUD8* is completely deleted together with *BUD9* resulting in more than 90% of randomly budding cells (Taheri *et al.*, 2000). In addition, random budding is typical for mutations in general budding genes, such as *RSR1/BUD1*, *BUD2* or *BUD5*, and for mutations affecting the actin cytoskeleton (Chant *et al.*, 1991; Chant and Herskowitz, 1991; Ni and Snyder, 2001).

However, the evaluation of the early budding pattern revealed that the random phenotypes of the *BUD8* variants differ somewhat from the *bud8Δ bud9Δ* double mutant (Fig. 15, Fig. 16) as well as the *rsr1Δ/bud1Δ* mutant strain (Fig. 13, Fig. 14). While strains with a *bud8Δ bud9Δ* or an *rsr1Δ/bud1Δ* deletion bud randomly already during the initial rounds of cell division of newborn daughter cells, the random budding pattern observed for $BUD8^{\Delta173-216}$, $BUD8^{\Delta173-325}$, $BUD8^{\Delta268-325}$, and $BUD8^{\Delta268-417}$ mutants required several rounds of cell division to be fully established. However, after 5 to 10 rounds of cell division, the final budding pattern of these mutant strains is very similar to strains lacking *BUD8* and *BUD9* (Table 4).
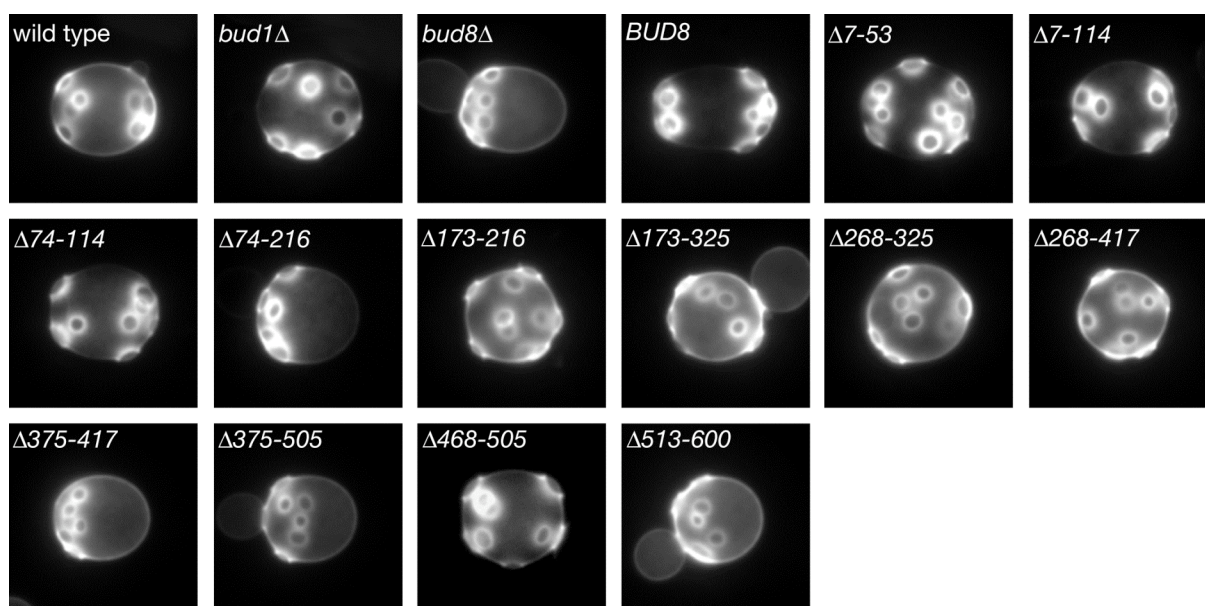
Fig. 13: Regulation of bud site selection by *BUD8* mutant alleles in diploid YF cells. Exponentially growing cells were stained with calcofluor to evaluate the budding pattern by fluorescence imaging of YF cells. Representative cells of the diploid strains are shown. RH2495 (wild-type), RH2449 (*bud8Δ/bud8Δ*), RH2448 (*bud1Δ/bud1Δ*), and YHUM996 (*BUD8*), a strain expressing a myc-epitope-tagged version of *BUD8*, were used as reference strains. The strains carrying truncated versions of *BUD8* fused to six myc-epitopes were termed as YHUM843 (*Δ7-53*), YHUM844 (*Δ7-114*), YHUM847 (*Δ74-114*), YHUM848 (*Δ74-216*), YHUM849 (*Δ173-216*), YHUM850 (*Δ173-325*), YHUM851 (*Δ268-325*), YHUM852 (*Δ268-417*); YHUM853 (*Δ375-417*), YHUM854 (*Δ375-505*), YHUM855 (*Δ468-505*), and YHUM856 (*Δ513-600*). For each strain, the budding pattern of 200 cells was determined from two independent experiments.

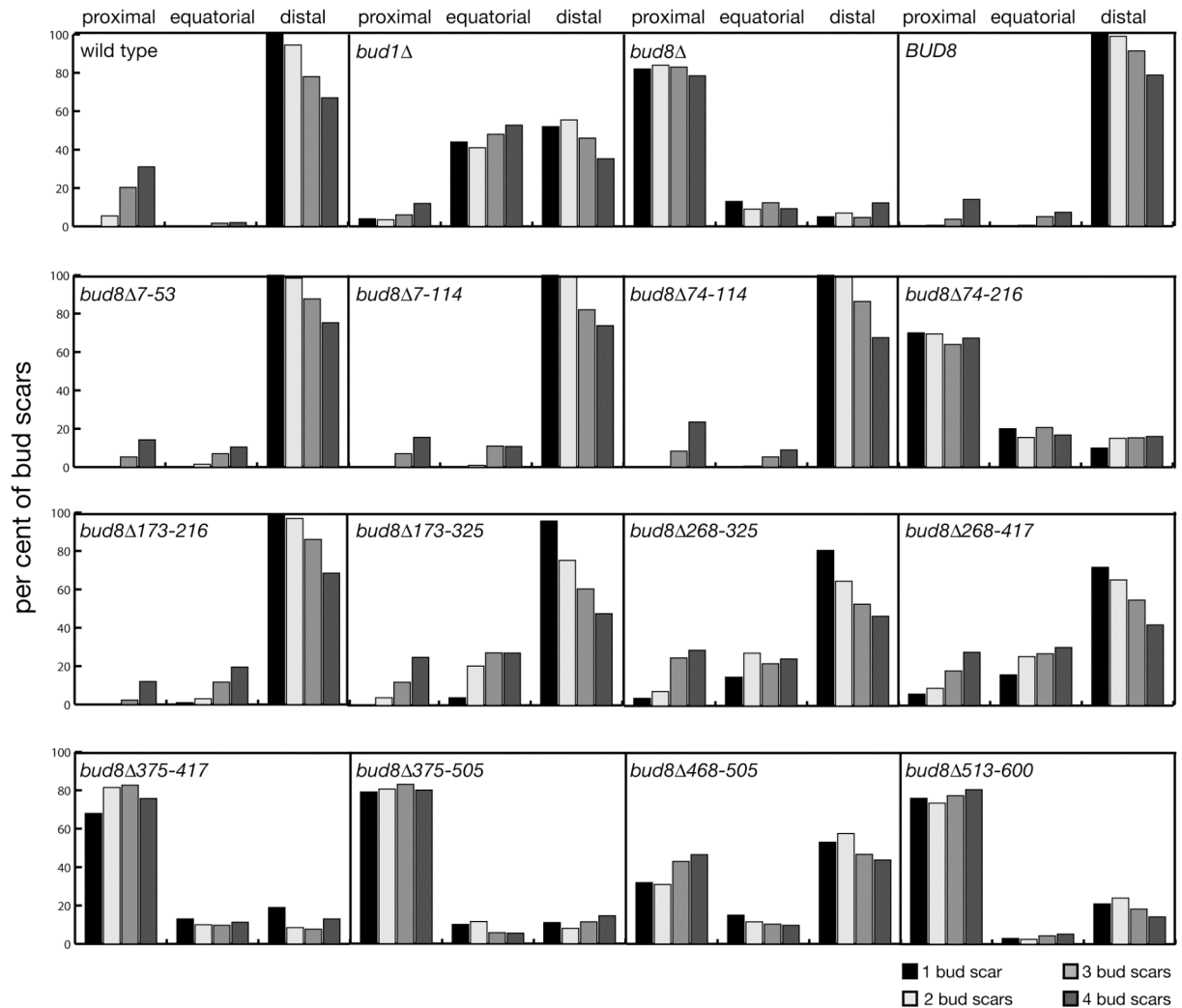**Fig. 14: Quantitative evaluation of the bud scar distribution in *BUD8* mutant strains.** The reference strains RH2495 (wild-type), RH2449 (*bud8Δ/bud8Δ*), RH2448 (*bud1Δ/bud1Δ*), and YHUM842 (*BUD8*) expressing the myc-tagged wild-type protein of *BUD8*, as well as the strains carrying integrated versions of different myc-epitope tagged *BUD8* alleles (*BUD8^{Δ7-53}*, *BUD8^{Δ7-114}*, *BUD8^{Δ74-114}*, *BUD8^{Δ74-216}*, *BUD8^{Δ173-216}*, *BUD8^{Δ173-325}*, *BUD8^{Δ268-325}*, *BUD8^{Δ268-417}*, *BUD8^{Δ375-417}*, *BUD8^{Δ375-505}*, *BUD8^{Δ468-505}*, and *BUD8^{Δ513-600}*) were grown in YPD medium to the logarithmic phase. Cells of the indicated strains were stained with calcofluor to visualize the bud scars. For each strain, the positions of all bud scars were determined for 100 cells with one bud scar (representing totally 100 bud scars per bar), 100 cells with two bud scars (representing totally 200 bud scars per bar), 100 cells with three bud scars (representing totally 300 bud scars per bar), and 100 cells with four bud scars (representing totally 400 bud scars per bar). Bud scars were scored as proximal (the third comprising the birth end of the cell), equatorial (the middle third of the cell located between proximal and distal cell pole), or distal (the third that is at the opposite to the birth scar). Bars represent the percentage of cells at the proximal, the equatorial and the distal region. For each strain, the average value from two independent experiments is shown.

Table 4: Regulation of bud site selection patterns in homo- and heterozygous *BUD8* and *BUD9* deletion strains

	Budding Pattern [%]							
	homozygous				heterozygous			
	bipolar	uni. prox.	uni. dist.	random	bipolar	uni. prox.	uni. dist.	random
wild type	82	<1	8	10				
bud8Δ	5	90	<1	6	78	9	2	14
bud9Δ	3	<1	89	9	69	<1	24	8
bud8Δ/bud9Δ	6	2	<1	92				
bud1Δ	2	<1	<1	98				
BUD8	70	<1	15	15	69	1	13	18
bud8Δ7-53	76	<1	10	14				
bud8Δ7-114	58	<1	22	21				
bud8Δ74-114	81	<1	12	8				
bud8Δ74-216	12	78	<1	11				
bud8Δ173-216	23	1	21	56	17	<1	36	48
bud8Δ173-325	17	1	6	76	17	<1	5	77
bud8Δ268-325	25	<1	3	73	34	<1	4	63
bud8Δ268-417	14	<1	4	83	32	<1	8	61
bud8Δ375-417	8	87	<1	6				
bud8Δ375-505	6	85	<1	9				
bud8Δ468-505	53	28	<1	19				
bud8Δ513-600	5	90	<1	6				
BUD9	76	<1	12	13	72	<1	19	10
bud9Δ8-48	80	<1	6	15				
bud9Δ8-130	75	<1	11	15				
bud9Δ91-130	80	<1	7	14				
bud9Δ91-218	5	<1	86	9				
bud9Δ168-218	9	1	83	8				
bud9Δ168-283	11	<1	79	11				
bud9Δ244-283	3	<1	94	4				
bud9Δ244-369	46	<1	6	49	54	2	7	38
bud9Δ323-369	45	2	8	46	58	<1	8	35
bud9Δ323-450	4	<1	86	11				
bud9Δ406-450	5	<1	83	13				
bud9Δ406-544	2	<1	86	13				
bud9Δ460-544	1	<1	91	9				

These novel variants of Bud8p were further tested with respect to their stability to induce random budding in presence of the full-length Bud8p protein, by crossing haploid strains carrying the random alleles with a haploid wild-type strain to obtain heterozygous diploid strains. Analysis of budding patterns revealed that the heterozygous *BUD8* mutant strains also exhibit a random budding pattern, although somewhat less pronounced as observed in the homozygous diploid mutants (Table 4). Nevertheless, the presence of the *BUD8* wild-type gene was not able to rescue the bipolar phenotype, indicating that all of the mutations are dominant. These data suggest that the segments deleted in the third class of *BUD8* mutant alleles might be required for site-specific interaction of Bud8p with the general bud site selection machinery, because these Bud8p variants are able to initiate budding at random sites even in the presence of functional Bud8p. If interaction with the bud site selection machinery was completely lost, the *BUD8* alleles would be expected to cause a unipolar proximal pattern as observed in the complete absence of Bud8p.

The investigation of the *BUD9* mutant alleles with respect to their functionality in bud site selection was performed as in case of the *BUD8* mutants and also revealed three different classes (Figure 15 & 16, Table 4). The first class comprises three mutant alleles, which code for Bud9p versions truncated at the NH_2-terminus ($BUD9^{\Delta 8-48}$, $BUD9^{\Delta 8-130}$, or $BUD9^{\Delta 91-130}$). Yeast strains expressing these variants established a bipolar budding pattern and did not differ significantly from a strain expressing the wild-type or a myc-tagged *BUD9* gene (Fig. 15). Thus, similar to Bud8p, the NH_2-terminal part of Bud9p (residues 8-130) is not required for establishment of the bipolar budding.

A second class included eight mutants, which carried the $BUD9^{\Delta 91-218}$, $BUD9^{\Delta 168-218}$, $BUD9^{\Delta 168-283}$, $BUD9^{\Delta 244-283}$, $BUD9^{\Delta 323-450}$, $BUD9^{\Delta 406-450}$, $BUD9^{\Delta 406-544}$, or $BUD9^{\Delta 460-544}$ allele. These mutants select the distal cell pole for budding with a very high frequency over many generations similar to a strain carrying a full deletion of *BUD9* (Fig. 15 & Fig. 16). Thus, the segments deleted in these Bud9p variants are likely to fulfil an essential function of the protein.

Two further strains expressing $BUD9^{\Delta 244-369}$ and $BUD9^{\Delta 323-369}$, respectively, presented a third class of mutants. Similar to randomly budding *BUD8* mutants, these *BUD9* mutant strains normally recognized the distal cell pole during early rounds of cell division, but had produced a random budding pattern after a larger number of budding events (Fig. 15 & Fig. 16; Table 4). However, random budding frequency was significantly lower than in *bud8Δ*

bud9Δ double mutants. When compared to the homozygous *BUD9* mutant strains, the corresponding heterozygous *BUD9* mutants of this class maintained a significant increase in randomly budding cells, albeit not as pronounced (Table 4). These results indicate that both alleles $BUD9^{\Delta244-369}$ and $BUD9^{\Delta323-369}$ are dominant and that corresponding Bud9p proteins might interfere with regular execution of the bipolar budding program.
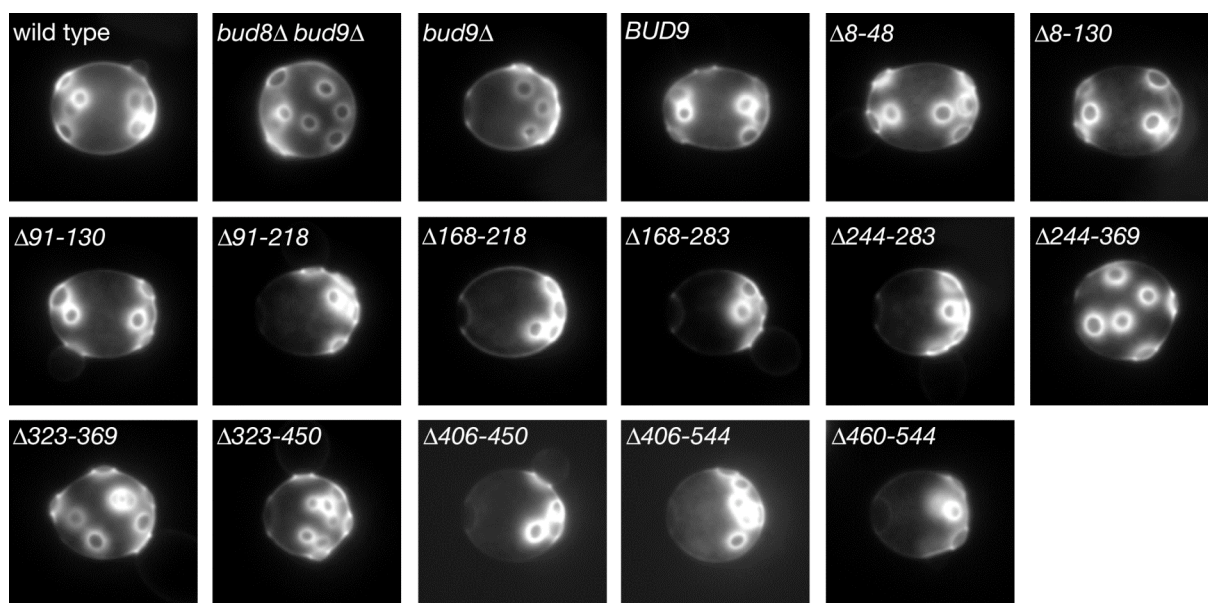

Fig. 15: Regulation of bud site selection by *BUD9* mutant alleles in diploid YF cells. Cells that were exponentially grown in YPD medium were stained with calcofluor to determine the budding pattern by fluorescence microscopy of YF cells. Representative cells of the diploid strains were shown. RH2495 (wild-type), YHUM993 (*bud9Δ/bud9Δ*), RH2453 (*bud8Δ/bud8Δ bud9Δ/bud9Δ*), and YHUM1009 (*BUD9*), a strain carrying a myc-tagged wild-type version of the protein, were used as controls. The strains expressing truncated versions of *BUD9* tagged with nine myc-epitopes were termed as YHUM1010 (Δ*8-48*), YHUM1011 (Δ*8-130*), YHUM1012 (Δ*91-130*), YHUM1013 (Δ*91-218*), YHUM1014 (Δ*168-218*), YHUM1015 (Δ*168-283*), YHUM1016 (Δ*244-283*), YHUM1017 (Δ*244-369*); YHUM1018 (Δ*323-369*), YHUM1019 (Δ*323-450*), YHUM1020 (Δ*406-450*), YHUM1021 (Δ*406-544*), and YHUM1022 (Δ*460-544*). For each strain, the budding pattern of 200 cells was determined. The average value from two independent experiments is displayed.
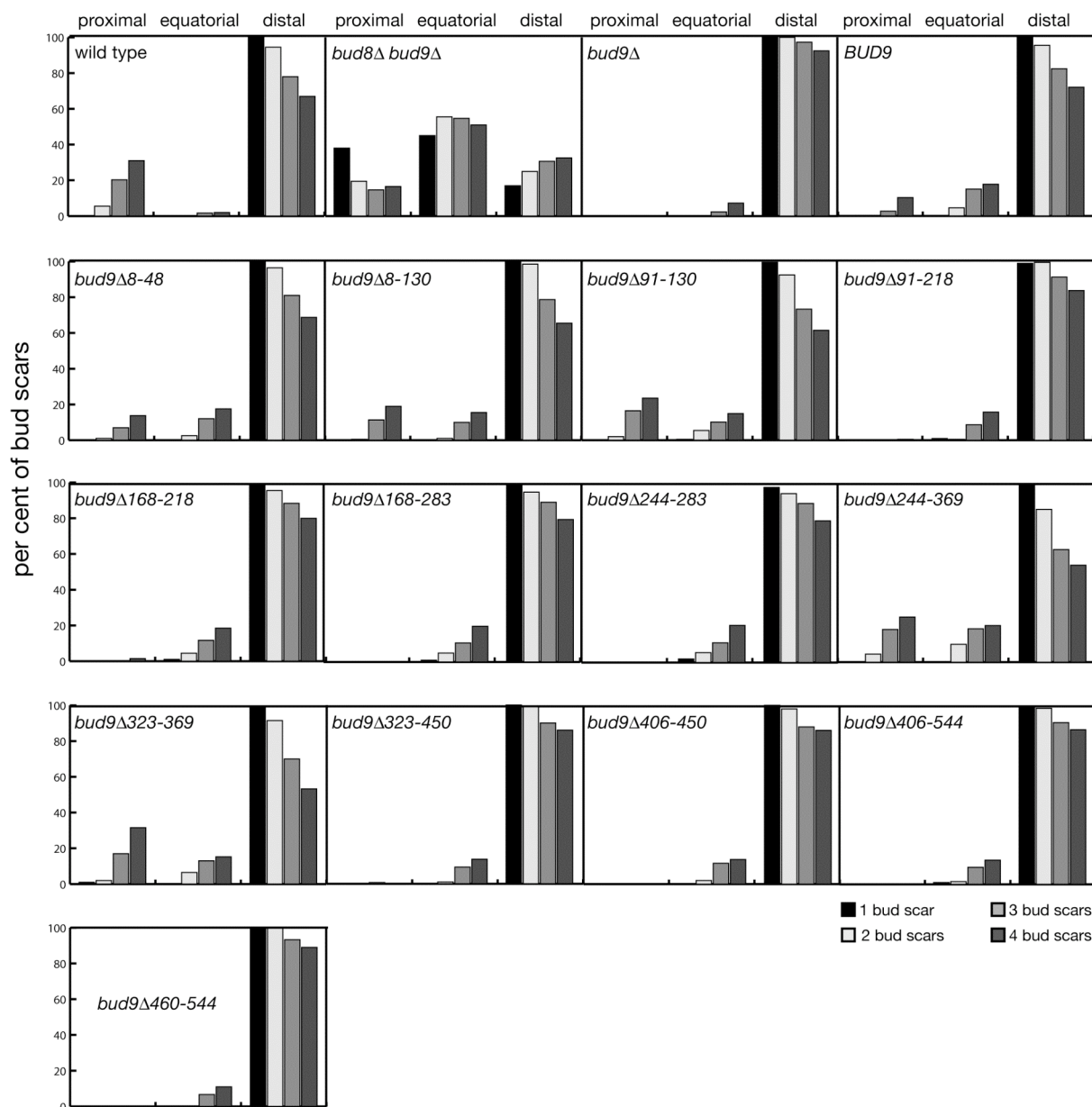
Fig. 16: Quantitative evaluation of the bud scar distribution in *BUD9* mutant strains. The distribution of bud scars of wild type and myc-epitope tagged *BUD9* mutant strains was determined by fluorescence imaging. Therefore, cells of the indicated strains were exponentially grown in YPD medium and then stained with calcofluor to visualize the bud scars. RH2495 (wild-type), YHUM993 (*bud9Δ/bud9Δ*), RH2453 (*bud8Δ/bud8Δ bud9Δ/bud9Δ*), and YHUM1009 (*BUD9*) expressing the myc-tagged wild-type protein were used as reference strains. Strains expressing truncated versions of *BUD9* fused to a myc[9] epitope were termed as YHUM1010 (Δ*8-48*), YHUM1011 (Δ*8-130*), YHUM1012 (Δ*91-130*), YHUM1013 (Δ*91-218*), YHUM1014 (Δ*168-218*), YHUM1015 (Δ*168-283*), YHUM1016 (Δ*244-283*), YHUM1017 (Δ*244-369*); YHUM1018 (Δ*323-369*), YHUM1019 (Δ*323-450*), YHUM1020 (Δ*406-450*), YHUM1021 (Δ*406-544*), and YHUM1022 (Δ*460-544*). For each experiment, the positions of all bud scars were determined for 100 cells with one bud scar, 100 cells with two bud scars, 100 cells with three bud scars, and 100 cells with four bud scars (representing in total 100, 200, 300 or 400 bud scars per bar). The positions of all bud scars were scored as proximal cell pole (the third comprising the birth end of the cell), equatorial (the middle third of the cell located between proximal and distal cell pole), or distal cell pole (the third that is at the opposite to the birth scar). Bars represent the percentage of cells at the proximal, the equatorial, or the distal third. For each strain, the average value from two independent experiments is shown.

67

3.2.2.2 Axial budding of haploid strains

Previous studies have shown that *BUD8* and *BUD9* are expressed also in haploid strains, although in this cell type the haploid-specific landmark protein Bud10p mainly functions as spatial landmark at the proximal pole. Thus, it is possible that altered variants of Bud8p and Bud9p could influence the budding pattern of haploid yeast cells. To test this possibility, the budding patterns of haploid **a**-strains expressing selected *BUD8* and *BUD9* mutant alleles were determined (Table 5). A strain expressing wild-type Bud8p and Bud9p produced the well-known axial budding pattern, in which the mother and daughter cells are constrained to form their buds immediately adjacent to the previous site of cell separation with a very high frequency (Table 5). In the case of Bud8p, the budding pattern of a haploid strain expressing a myc[6]-tagged full-length version of *BUD8* was phenotypically almost indistinguishable from the haploid wild-type strain, as more than 90% of cells of this strain developed an axial pattern. Similarly, development of an axial pattern could be observed for most of the strains expressing truncated *BUD8* versions including $BUD8^{\Delta7-53}$, $BUD8^{\Delta7-114}$, $BUD8^{\Delta74-216}$, $BUD8^{\Delta173-325}$, $BUD8^{\Delta268-325}$, $BUD8^{\Delta375-505}$, $BUD8^{\Delta468-505}$, and $BUD8^{\Delta513-600}$. However, in the case of a strain expressing the $Bud8p^{\Delta268-417}$ variant, every forth cell produced either a random or a bipolar pattern, and only 75% of the cells divided in an axial pattern. Thus, this variant of Bud8p might interfere with downstream components required for the bud site selection programs not only in diploids (see 3.2.2.1) but also in haploid cells.

The evaluation of the budding patterns of haploid strains expressing different *BUD9* variants revealed similar results as found for the haploid *BUD9* mutants. A haploid strain expressing the myc[9]-tagged full-length version of *BUD9* produced an axial pattern that does not distinguishable from the haploid reference strain. All of the examined strains producing the truncated versions $Bud9p^{\Delta8-48}$, $Bud9p^{\Delta8-130}$, $Bud9p^{\Delta91-218}$, $Bud9p^{\Delta168-218}$, $Bud9p^{\Delta168-283}$, $Bud9p^{\Delta244-369}$, $Bud9p^{\Delta323-450}$, $Bud9p^{\Delta406-450}$, $Bud9p^{\Delta406-544}$ or $Bud9p^{\Delta460-544}$ also produced an axial budding pattern with a very high frequency.

In summary, most of the Bud8p and Bud9p mutant proteins do not interfere with haploid budding process indicating that although Bud8p and Bud9p are expressed in this cell type, levels might be sufficient to affect the interaction of Bud10p with downstream acting general budding components.

Table 5: Budding pattern of haploid *S. cerevisiae* strains expressing *BUD8* or *BUD9* variants

	Budding Pattern [%]		
	<u>axial</u>	<u>bipolar</u>	<u>random</u>
wild type	98	<1	<1
BUD8	93	6	1
bud8Δ	99	<1	<1
bud8Δ7-53	96	2	2
bud8Δ7-114	92	8	1
bud8Δ74-114	n.d.	n.d.	n.d.
bud8Δ74-216	99	<1	<1
bud8Δ173-216	n.d.	n.d.	n.d.
bud8Δ173-325	88	9	3
bud8Δ268-325	91	5	4
bud8Δ268-417	75	20	5
bud8Δ375-417	n.d.	n.d.	n.d.
bud8Δ375-505	99	1	<1
bud8Δ468-505	87	12	1
bud8Δ513-600	99	<1	<1
BUD9	99	1	<1
bud9Δ	95	3	2
bud9Δ8-48	99	1	<1
bud9Δ8-130	98	2	<1
bud9Δ91-130	n.d.	n.d.	n.d.
bud9Δ91-218	98	1	<1
bud9Δ168-218	99	<1	1
bud9Δ168-283	98	2	<1
bud9Δ244-283	n.d.	n.d.	n.d.
bud9Δ244-369	99	<1	1
bud9Δ323-369	n.d.	n.d.	n.d.
bud9Δ323-450	99	1	<1
bud9Δ406-450	99	1	<1
bud9Δ406-544	99	1	<1
bud9Δ460-544	99	1	<1

3.2.3 Localization studies

In a next step, the different Bud8p and Bud9p deletion proteins should be used to identify regions of the proteins that are required for the correct localization of these landmark proteins. For this purpose, fusions to fluorescent proteins should be created. To ensure that signals were produced that are suitable for the measurements, different fluorescent marker proteins were fused to unaltered Bud8p and Bud9p by creation of gene fusions that were also expressed at different levels.

3.2.3.1 Investigation of different Bud8p and Bud9p fusion proteins for localization studies

First, fusion genes of GFP with *BUD8* and *BUD9* that are expressed from their own promoters had to be generated. When *GFP-BUD8* was expressed from low-copy plasmids, the signals produced were very weak, and only in exceptional cases GFP-Bud8p could be localized by GFP fluorescence microscopy. In the case of strains carrying a low-copy *GFP-BUD9* plasmid no fluorescent signal was detectable. Because of the difficulties *GFP-BUD8* and *GFP-BUD9* were expressed from high-copy-number plasmids.

In general, high-copy expression of *GFP-BUD8* led to a remarkable increase of cells with a detectable signal. Furthermore, the signals were brighter and more defined than signals obtained using low-copy-number plasmids, although the localization patterns were comparable. In contrast, strains carrying a high-copy *GFP-BUD9* plasmid, still only little or no signals were detectable. Therefore, the GFP portion was replaced with YFP, and *YFP-BUD9* fusions were expressed from high-copy plasmid. As a consequence, the amount of cells showing detectable fluorescent signals was considerably higher. Typically, the fusion protein was observed as spot at the tip of the growing daughter cell throughout cell division. Moreover, YFP-Bud9p was found to be concentrated as distinct patch at one pole in unbudded cells, and as spot between mother and daughter cell.

3.2.3.2 Localization of Bud8p and Bud9p deletion proteins

On the basis of the results described the previous section, *BUD8* deletion alleles were NH_2-terminally fused to GFP and *BUD9* deletion variants to YFP. Fusion genes were then expressed in diploid strains from high-copy plasmids to determine the localization of mutant proteins by fluorescence microscopy.

Localization analysis of different GFP-Bud8p variant in *bud8Δ* mutant strains led to three types of localization patterns (Fig. 17). The full-length protein of Bud8p and five fusion proteins (GFP-Bud8p$^{Δ7-53}$, GFP-Bud8p$^{Δ7-114}$, GFP-Bud8p$^{Δ74-114}$, GFP-Bud8p$^{Δ74-216}$ and GFP-Bud8p$^{Δ468-505}$) produced similar localization patterns and defined a first class. These proteins were localized on only one side of unbudded cells. In the case of GFP-Bud8p$^{Δ74-114}$ the localization was slightly different. Most of the unbudded cells of the corresponding strain showed a characteristic spot at one side of the cell, but in some cases had patches at both cell poles as well as weak signals along the plasma membrane were visible. This result agrees with earlier observations, where high-level expression of *GFP-BUD8* led to detectable signals at both cell poles (Harkins *et al.*, 2001). In small- and large-budded cells, Bud8p variants of this first class appeared in form of crescent-like structures at the tip of daughters and at the mother side of the bud neck (Fig. 17B, C, D, E, L). With the exception of Bud8p$^{Δ468-505}$, Bud8p variants that produce this first class of localization pattern carry truncations at the NH$_2$-terminus, indicating that the NH$_2$-terminal part of Bud8p does not carry signals for correct delivery of the protein to the distal cell pole.

GFP-Bud8p$^{Δ173-216}$, GFP-Bud8p$^{Δ173-325}$, GFP-Bud8p$^{Δ268-325}$, and GFP-Bud8p$^{Δ268-417}$ that contain truncations in the median segment of Bud8p define a second type of localization pattern. Mutant proteins belonging to this group are not delivered to the expected bud site (Fig. 17F, G, H, I). Actually, these proteins are evenly distributed at the cell periphery. Two strains of this group (carrying the *GFP-BUD8$^{Δ173-325}$* and *GFP-BUD8$^{Δ268-325}$* allele, respectively) showed an additional distinctive feature: some of the budded YF cells had detectable signals at the tip of nascent buds of various sizes (Fig. 17G, H). These observations were rather faint. To this end, it could not be clarified whether this irregular appearance of fluorescence signals at the tips of daughter cells were artefacts because of the high-level expression of the proteins or whether this pattern was actually typical for localization pattern of these mutant proteins. The results indicate that the median part of Bud8p might be required for either delivery of the proteins to polar positions or for polar maintenance after delivery.

A third type of localization pattern was defined by the *GFP-BUD8$^{Δ375-417}$*, *GFP-BUD8$^{Δ375-505}$*, and *GFP-BUD8$^{Δ513-600}$* fusion genes, which code for variants of Bud8p with truncations at the COOH-terminus (Fig. 17J, K, M). This group of proteins was characterized by their appearance as patches at the mother-daughter neck region and dot-like structures along the cell periphery of mother and daughter cells. Remarkably, rapid movement

of dot-like structures of GFP-Bud8p variants along the cell periphery could frequently be observed. In addition, a significant amount of the proteins was found to be enriched in the cytoplasm. These variants might define segments in the COOH-terminal part of the protein that are essential for the delivery of the protein to the cell surface and the distal cell pole.
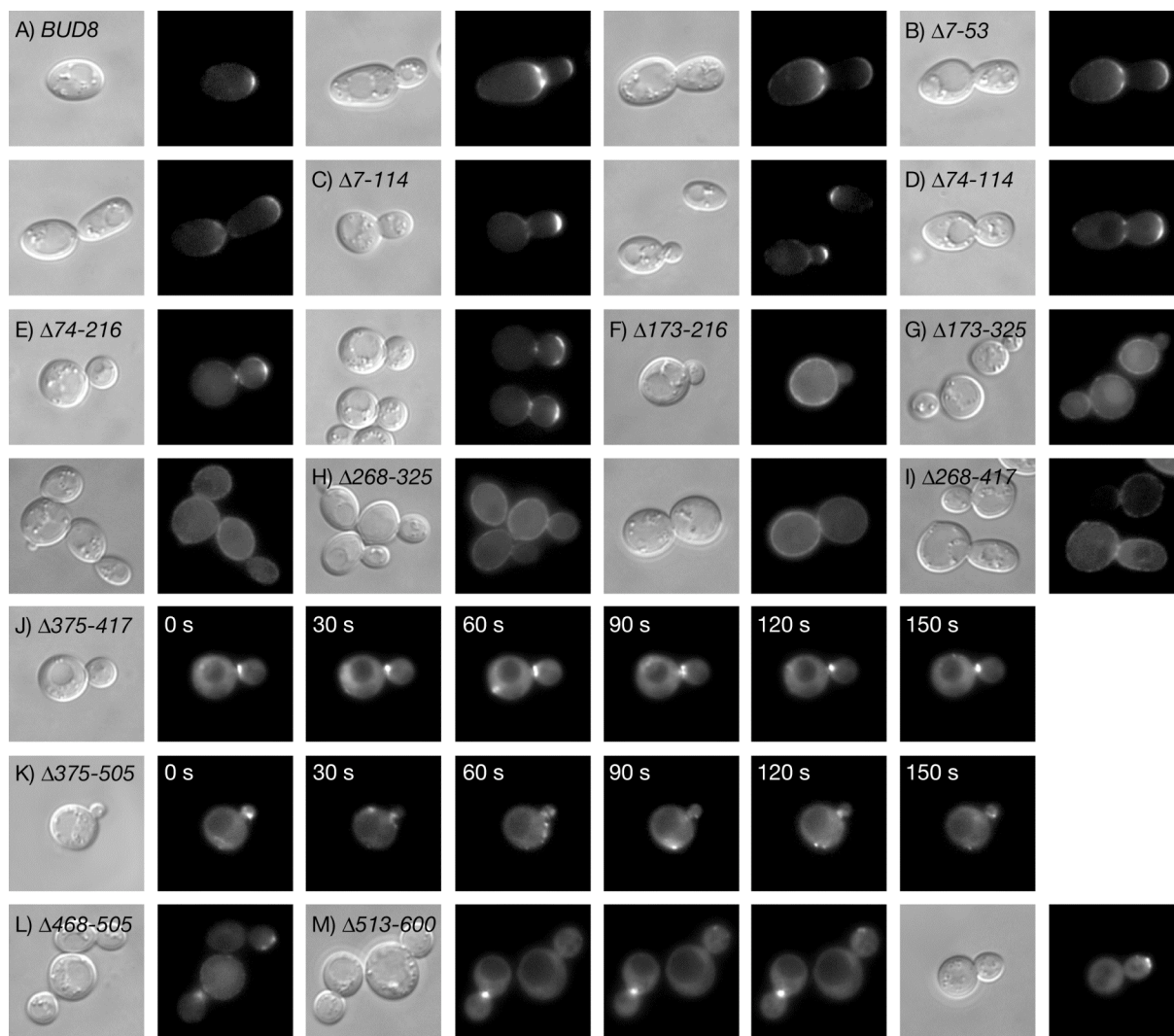

Fig. 17: Subcellular localization of GFP-Bud8p mutant proteins in living cells. Representative cells of a diploid *bud8Δ* strain RH2449 expressing either a GFP-fused wild-type version of Bud8p (A) from the plasmid BHUM824 or GFP-Bud8p variants from the plasmids BHUM825 (B, *Δ7-53*), BHUM826(C, *Δ7-114*), BHUM827 (D, *Δ74-114*), BHUM828 (E, *Δ74-216*), BHUM829 (F, *Δ173-216*), BHUM830 (G, *Δ173-325*), BHUM831 (H, *Δ268-325*), BHUM832 (I, *Δ268-417*), BHUM833 (J, *Δ375-417*), BHUM834 (K, *Δ375-505*), BHUM835 (L, *Δ468-505*), and BHUM836 (M, *Δ513-600*), respectively, were shown. Pre-cultures of corresponding *Saccharomyces cerevisiae* strains were grown overnight in YNB-medium. Main cultures were inoculated in the same medium and were grown to the exponential phase. Living cells were visualized under the microscope using Nomarski optics or fluorescence microscopy (GFP). J and K show time-lapse observations of GFP-Bud8p variants with images collected at intervals of 30 sec.

Analysis of the different YFP-Bud9p mutant proteins by fluorescence microscopy defined four different types of localization pattern (Fig. 18). The six mutant proteins YFP-Bud9p$^{\Delta 8-48}$, YFP-Bud9p$^{\Delta 8-130}$, YFP-Bud9p$^{\Delta 91-130}$, YFP-Bud9p$^{\Delta 91-218}$, YFP-Bud9p$^{\Delta 168-218}$, and the YFP-Bud9p$^{\Delta 323-369}$ produced a similar localization pattern as the full-length YFP-Bud9p control and defined a first class. In unbudded cells, these proteins appeared as single patches at one or both poles (Fig. 18B, C, D, E, F, J). The results of previous studies suggest that these cells were daughter cells that had never budded before (Harkins *et al.*, 2001). In small-budded cells, these proteins were typically found at the tip of daughters and in mother cells at the pole opposite to the neck. In large-budded cells, proteins were found at the tip of daughters and in addition with high frequency at the mother-bud neck. All proteins producing this type of localization pattern (except YFP-Bud9p$^{\Delta 323-369}$) contain truncations in the NH$_2$-terminal region, indicating that this part of protein does not carry sequences essential for normal localization of Bud9p.

A second type of localization pattern was defined by YFP-Bud9p$^{\Delta 168-263}$, YFP-Bud9p$^{\Delta 244-263}$, and YFP-Bud9p$^{\Delta 244-369}$. These proteins produced enhanced cytoplasmic staining of cells. No significant difference with regard to fluorescence intensity in budded and unbudded cells could be observed (Fig. 18G, H, I). As a common feature this group of mutant proteins contain truncations in the median segment of Bud9p, indicating that this part of the Bud9p protein might be required for correct delivery to the cell surface.

A third group of proteins included YFP-Bud9p$^{\Delta 323-450}$ and YFP-Bud9p$^{\Delta 406-450}$ that contain truncations, which are adjacent to the region coding for the transmembrane domains. Typically, fluorescent signals were detectable as patches at the tip of the daughter cells. A specific feature of this class of Bud9p proteins is that they are concentrated predominantly in small-budded YF cells (Fig. 18K, L). In general, the amount of cells producing clear signals was lower than in the wild-type strain and the patches observed at the bud tips were often diffuse. Despite these complications, the localization pattern was similar in all cells that produced a detectable signal.

A forth class of mutant proteins was defined by YFP-Bud9p$^{\Delta 406-544}$ and the YFP-Bud9p$^{\Delta 460-544}$ that are characterized by deletion of both transmembrane domains. These proteins were enriched in the cytoplasm and in addition often formed a distinct spot at the tip of the growing daughter (Fig. 18M, N). Strikingly, signals could be detected predominantly in cells with small- or medium-sized buds. In unbudded cells, YFP-Bud9p$^{\Delta 406-544}$ and

YFP-Bud9p$^{\Delta460\text{-}544}$ typically accumulated in form of a single patch at one cell pole. In exceptional cases, the proteins were delivered to the neck region (Fig. 18M).
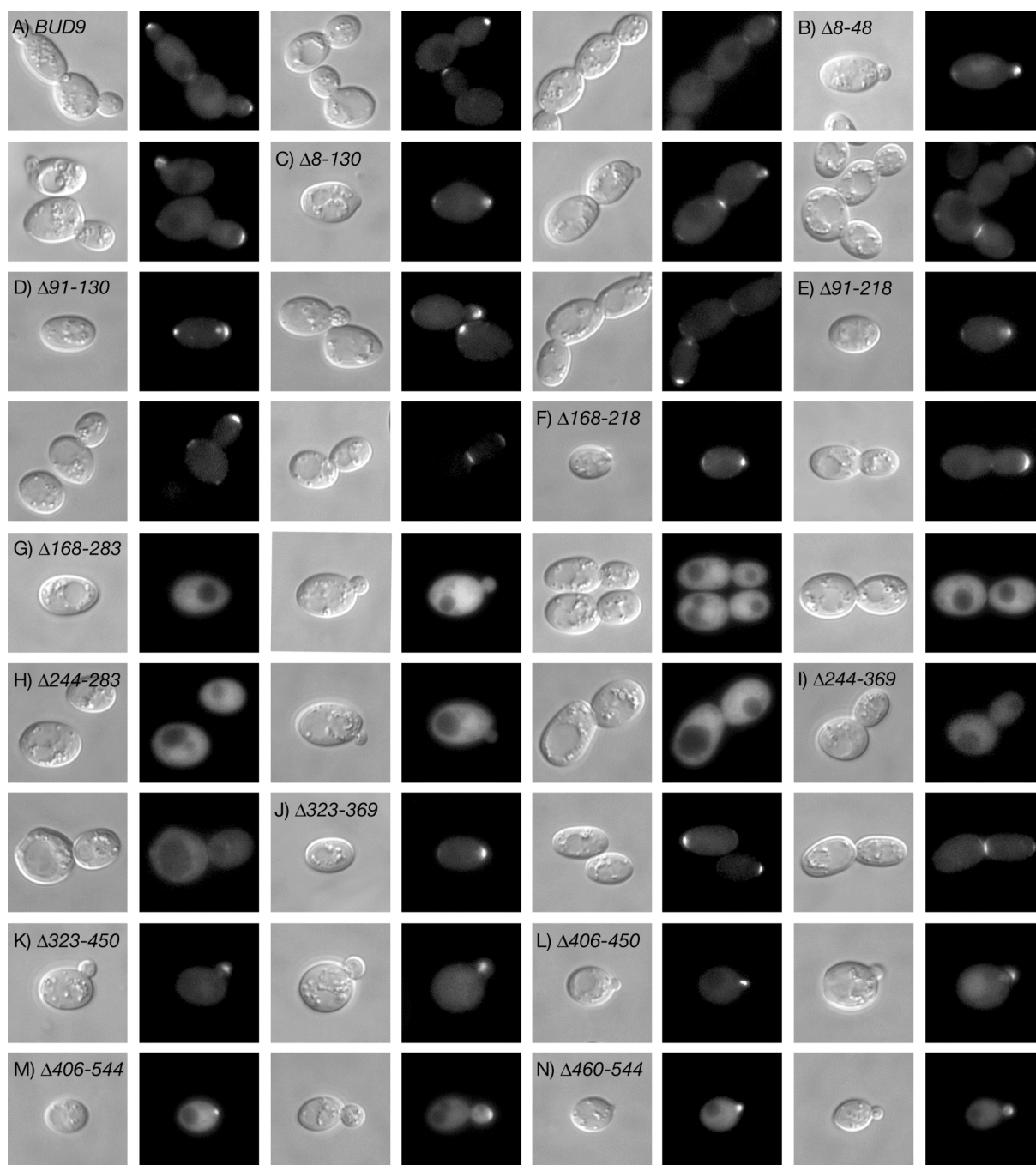

Fig. 18: Localization of Bud9p mutant proteins with the use of YFP-tagged proteins in living cells. Representative cells of a diploid *bud9Δ* strain YHUM993 expressing either an YFP-fused wild-type version of Bud9p (A) from the plasmid BHUM837 or YFP-Bud9p variants from the plasmids BHUM838 (B, *Δ8-48*), BHUM839 (C, *Δ8-130*), BHUM840 (D, *Δ91-130*), BHUM841 (E, *Δ91-218*), BHUM842 (F, *Δ168-218*), BHUM843 (G, *Δ168-283*), BHUM844 (H, *Δ244-283*), BHUM845 (I, *Δ244-369*), BHUM846 (J, *Δ323-369*), BHUM847 (K, *Δ323-450*), BHUM848 (L, *Δ406-450*), BHUM849 (M, *Δ406-544*), and BHUM850 (N, *Δ460-544*), respectively, were shown. Pre-cultures of corresponding *Saccharomyces cerevisiae* strains were grown overnight in YNB-medium. Main cultures were inoculated in the same medium and were grown to the exponential phase. Living cells of different stages of the cell cycle were chosen for photography and were viewed under the microscope using Nomarski optics or by fluorescence microscopy (YFP).

In summary, examination of the localization patterns of Bud9p deletion proteins leads to the conclusion that the NH$_2$-terminal part of Bud9p is not required for normal localization and that segments of both the median and the COOH-terminal region might confer transport of the protein to the cell surface and/or the proximal cell pole.

Thus, the segments of Bud8p and Bud9p necessary for the delivery of the proteins to the correct cell pole appear to cover similar regions of the polypeptides. In both cases the NH$_2$-terminal part is not required but delivery of the proteins to the cell periphery depends on the median part. In addition, both proteins require parts of the COOH-terminal domains for correct polar localization.

3.3 Investigation of Bud8p and Bud9p interaction partners

3.3.1 Bud9p exhibits in vivo protein-protein-association with Bud5p

Previous studies have revealed that Bud8p and Bud9p interact with the cortical tag protein Rax1p to establish the cortical landmarks (Kang *et al.*, 2004b). However, the Rax1p-interacting domains of Bud8p and Bud9p are not known. In addition, Bud8p has been shown to interact with the GDP/GTP exchange factor Bud5p, a component of the general bud site selection machinery (Kang *et al.*, 2004a). Again, the Bud5p-interacting domains of Bud8p are not known, but it has been shown that the NH$_2$-terminal part of Bud5p is required for interaction with Bud8p. Whether Bud9p also interacts with Bud5p is not known.

In a first step, the association between Bud5p and Bud8p was confirmed. For this purpose, the haploid strain YHUM1008 (*MATα, bud8Δ::HIS3, ura3-52, his3::hisG, leu2::hisG, trp1::hisG*) was transformed with BHUM1041 (*GST-BUD5$^{NΔ1-70}$*) and BHUM1042 (*GST-BUD5*), respectively. BHUM532, which carries a sequence coding for *myc^6-BUD8*, was transformed into the haploid *MATa*-strain YHUM1027 (congenic to YHUM1008). Appropriate transformants were mated to generate diploid strains expressing for co-immunoprecipitation. By crossing, two strains were obtained, one expressing myc^6-Bud8p together with GST-Bud5p, the other expressing myc^6-Bud8p in combination with the truncated version GST-Bud5p$^{NΔ1-70}$.

Further analyses revealed that GST-Bud5p was visible reproducibly as strong signal around 100 kDa. GST-Bud5p$^{NΔ1-70}$ could be detected around 90 kDa. In case of both Bud5p variants, additional signals were observed as lower molecular forms, which might be caused

by proteolytic degradation of the proteins. Myc-epitope-tagged Bud8p appeared as pattern consisting of three bands in the range from 85 to 140 kDa.

Extracts were then incubated with glutathione-sepharose to purify GST-Bud5p and associated proteins. Affinity purified extracts were again analyzed by immunoblotting for the presence of Bud5p variants and myc[6]-Bud8p (Fig. 19). As expected, these GST pulldown experiments confirmed the studies of Kang *et al.* (2004a) and demonstrate that Bud8p can be co-purified with GST-Bud5p but not with a truncated version of Bud5p lacking the N-terminal 70 amino acids (Fig. 19).

To investigate a possible interaction between Bud5p and Bud9p, transformation and crossing of corresponding yeast strains were carried out essentially as described for Bud8p: Plasmids carrying sequences encoding different Bud5p variants (see above for description of BHUM1041 and BHUM1042) were each transformed in YHUM995 (*MATα, bud9Δ::HIS3, ura3-52, his3::hisG, leu2::hisG, trp1::hisG*). Plasmid BHUM1027 carrying *myc[9]-BUD9* was transformed into the haploid *MATa*-strain YHUM994 (congenic to YHUM995). Appropriate transformants were mated to yield two strains that carry *myc[9]-BUD9/GST-BUD5[NΔ1-70]* and *myc[9]-BUD9/GST-BUD5* alleles, respectively. Immunoblot analysis of crude extracts revealed that GST-Bud5p variants and myc-tagged Bud9p were expressed properly (Fig. 19). These strains were then used for co-affinity purification analysis as described in case of Bud8p.

Analysis of affinity-purified extracts revealed Bud9p was efficiently co-purified with full-length GST-Bud5p but not with the truncated version GST-Bud5p[NΔ1-70] (Fig. 19). Thus, similar to Bud8p, Bud9p associates with Bud5p via the NH_2-terminal part of this GDP/GTP exchange factor.
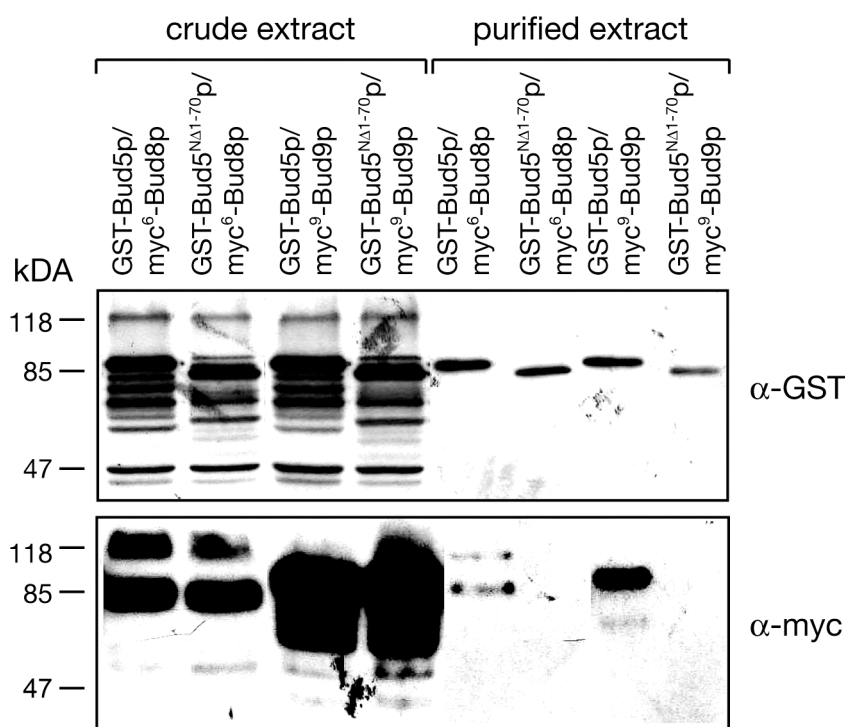
Fig. 19: Interaction of Bud8p and Bud9p proteins with Bud5p. Protein extracts were prepared from diploid yeast strains carrying the plasmid BHUM723 (*BUD8*) or BHUM1027 (*BUD9*) in combination with pHP772 (*GST-BUD5Δ1-70*; Kang *et al*., 2004a) and pHP1301 (*GST-BUD5*; Kang *et al*., 2004a), respectively. GST-Bud5p constructs were pulled down with glutathione-sepharose. Presence of Bud8p and Bud9p, respectively, was analyzed by immunoblotting with the anti-myc antibody (α-myc), and GST was detected using antibodies against GST (α-GST).

3.3.2 Distinct parts of Bud8p and Bud9p interact with Bud5p

In a next step, regions of Bud8p and Bud9p should be identified, which mediate interaction with the GDP/GTP exchange factor Bud5p. Therefore, deletion variants of Bud8p and Bud9p as described in chapter 3.2.1 were used with respect to their ability to associate with full-length Bud5p fused to GST. For this purpose, yeast strains were used that carry *GST-BUD5* on a plasmid (pHP1301) and either *myc⁶-BUD8* alleles or *myc⁹-BUD9* alleles on a second plasmid. After induction of *GST-BUD5* expression, protein extracts were prepared and analyzed by immunoblotting before and after co-affinity purification with glutathione-sepharose.
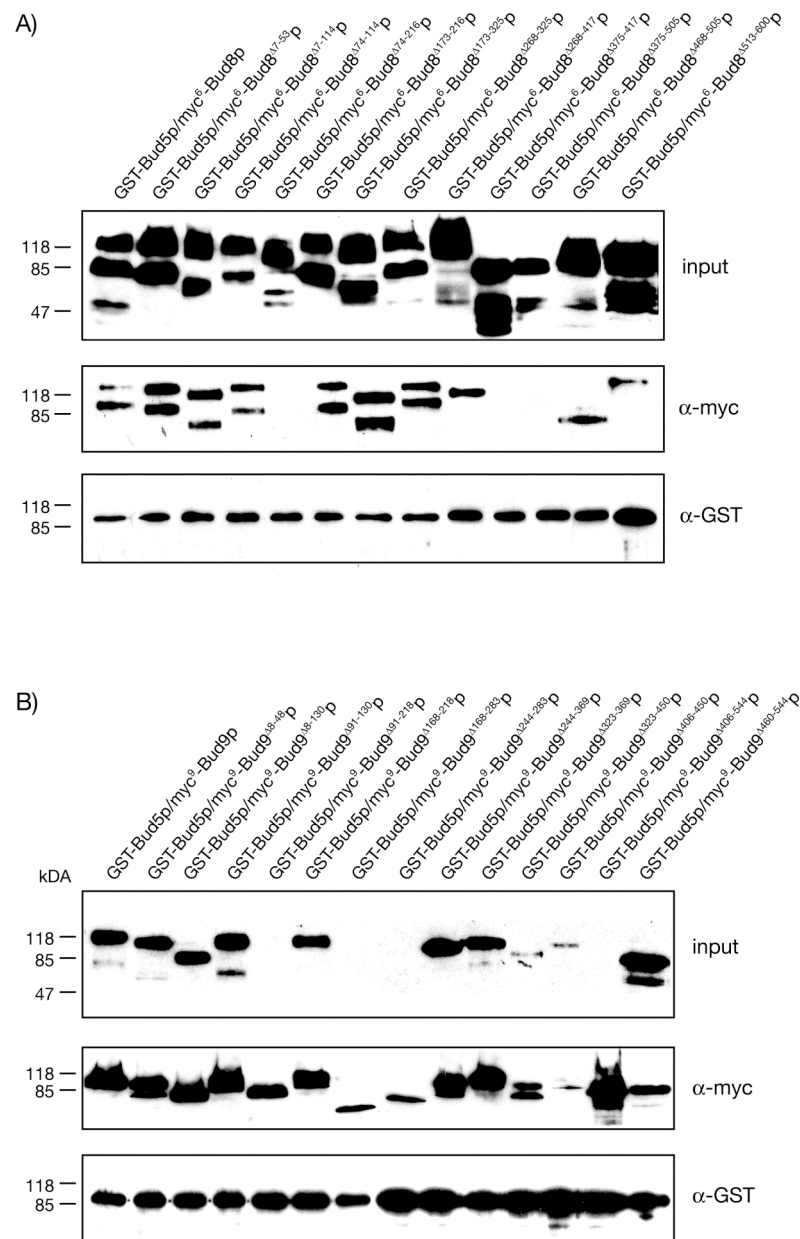
Fig. 20: Interaction of Bud8p and Bud9p deletion constructs with Bud5p. (A) Co-purification of different variants of Bud8p with GST-Bud5p. Protein extracts were prepared from diploid yeast strains carrying the plasmid pHP1301 (*GST-BUD5*; Kang *et al*., 2004a) in combination with BHUM723 (*BUD8*), BHUM1016 (Δ*7-53*), BHUM1017 (Δ*7-114*), BHUM1018 (Δ*74-114*), BHUM1019 (Δ*74-216*), BHUM1020 (Δ*173-216*), BHUM1021 (Δ*173-325*), BHUM1022 (Δ*268-325*), BHUM1023 (Δ*268-417*), BHUM1024 (Δ*375-417*), BHUM1025 (Δ*375-505*), BHUM706 (Δ*513-600*), and GST-Bud5p was pulled down with glutathione-sepharose. Presence of Bud8p proteins in extracts before (input) and after GST-Bud5p pull downs was analyzed by immunoblotting with the anti-myc antibody (α-myc), and GST was detected using antibodies against GST (α-GST). (B) Co-purification of different variants of Bud9p with GST-Bud5p was analyzed using diploid yeast strains carrying plasmid pHP1301 and the plasmid BHUM1027 (*BUD9*), BHUM1028 (Δ*8-48*), BHUM1029 (Δ*8-130*), BHUM1030 (Δ*91-130*), BHUM1031 (Δ*91-218*), BHUM1032 (Δ*168-218*), BHUM1033 (Δ*168-283*), BHUM1034 (Δ*244-283*), BHUM1035 (Δ*244-369*), BHUM1036 (Δ*323-369*), BHUM1037 (Δ*323-450*), BHUM1037 (Δ*406-450*), BHUM1038 (Δ*406-450*), BHUM1039 (Δ*460-450*), or BHUM1040 (Δ*460-544*).

In the case of Bud8p, all mutant proteins were produced at levels comparable to the wild-type protein and appeared dependent on their size between 70 and 150 kDa when analyzing crude extracts. Analysis of affinity-purified extracts showed that Bud8p$^{\Delta7-53}$, Bud8p$^{\Delta7-114}$, Bud8p$^{\Delta74-114}$, Bud8p$^{\Delta173-216}$, Bud8p$^{\Delta173-325}$, Bud8p$^{\Delta268-325}$, Bud8p$^{\Delta268-417}$, Bud8p$^{\Delta468-505}$, and Bud8p$^{\Delta513-600}$ could be co-purified with GST-Bud5p (Fig. 20A). However, Bud8p$^{\Delta74-216}$, Bud8p$^{\Delta375-417}$ and Bud8p$^{\Delta375-505}$ failed to co-purify with GST-Bud5p, indicating that the segments absent in these variants of Bud8p might confer association with Bud5p.

In the case of Bud9p, analysis of protein crude extracts showed that all fusion variants of Bud9p were detectable as multiple signals (mainly as double bands) between 70 and 115 kDa (Fig. 20B). Affinity purification revealed that Bud9p$^{\Delta8-48}$, Bud9p$^{\Delta8-130}$, Bud9p$^{\Delta91-130}$, Bud9p$^{\Delta168-218}$, Bud9p$^{\Delta244-369}$, Bud9p$^{\Delta323-369}$, and Bud9p$^{\Delta460-544}$ proteins could be co-purified with GST-Bud5p (Fig. 20B). In contrast, Bud9p$^{\Delta91-218}$, Bud9p$^{\Delta168-283}$, Bud9p$^{\Delta244-283}$, and Bud9p$^{\Delta406-544}$ did not associate with Bud5p (Fig. 20B).

In summary, the results of these interaction studies between the GDP/GTP exchange factor Bud5p and the pole marker proteins indicate that both Bud8p and Bud9p contain distinct domains that confer a direct or an indirect association with Bud5p.

3.3.3 Bud8p and Bud9p physically interact with Rax1p

3.3.3.1 Distinct parts of Bud8p and Bud9p interact with Rax1p

Based on the findings from Kang *et al.* (2004b) who identified Rax1p as interaction partner of Bud8p and Bud9p, we were interested to clarify which parts of both landmark proteins might be involved in association with Rax1p. For this purpose, the diploid strain YHUM829 was co-transformed with plasmid pHP1156 carrying *GST-RAX1* together with a second plasmid carrying either different *myc^6-BUD8* genes or *myc^9-BUD9* genes (see previous section). Protein crude extracts were then prepared and analyzed by immunoblotting before and after affinity purification with glutathione-sepharose.

These experiments revealed that mutant proteins of Bud8p lacking the regions 173-216, 268-417, 468-505, or 513-600 could be co-purified with GST-Rax1p indicating that these truncated versions of Bud8p are not required for interaction with Rax1p (Fig. 21A). In the case of Bud8p$^{\Delta74-216}$, Bud8p$^{\Delta268-325}$, and Bud8p$^{\Delta375-505}$, co-purification with Rax1p was partially reduced, suggesting that these variants lack regions that are in part essential for Rax1p-binding (Fig. 21A). In the case of Bud8p$^{\Delta7-114}$ and Bud8p$^{\Delta74-114}$, no co-purification with

GST-Rax1p was possible, indicating that the region lacking in these proteins is essential for association with Rax1p (Fig. 21A).

In the case of Bud9p, Bud9p$^{\Delta 8-48}$, Bud9p$^{\Delta 8-130}$, Bud9p$^{\Delta 91-218}$, Bud9p$^{\Delta 168-218}$, Bud9p$^{\Delta 244-369}$, and Bud9p$^{\Delta 323-450}$ could be co-purified with GST-Rax1p (Fig. 21B). In the case of Bud9p$^{\Delta 168-283}$, Bud9p$^{\Delta 406-450}$, Bud9p$^{\Delta 406-544}$, and Bud9p$^{\Delta 460-544}$, interaction with Rax1p was significantly reduced or not detectable, indicating that these variants lack domains that are essential for efficient association with Rax1p (Fig. 21B).
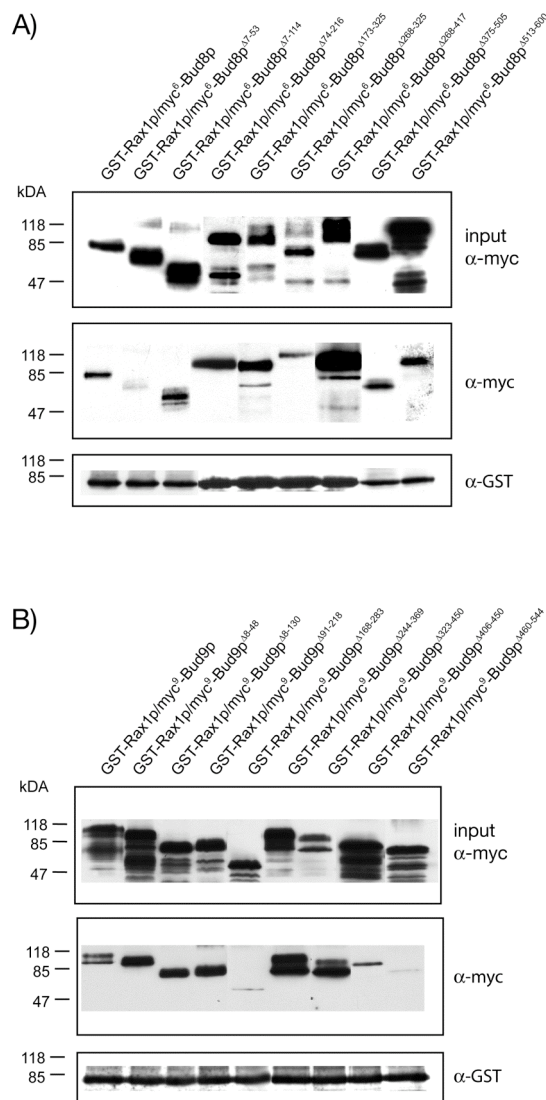
Fig. 21: Co-purification of different variants of Bud8p and Bud9p with Rax1p. Interaction of Bud8p with Rax1p was analyzed in diploid yeast strains carrying the plasmid pHP1156 (Kang *et al.*, 2004b) and either one of the plasmids expressing different variants of *BUD8* (A) or *BUD9* (B) as described in Fig. 20.

Conclusively, these results indicate that both Bud8p and Bud9p contain specific domains that confer a direct or an indirect association with Rax1p.

Table 6: Summary of properties of different *BUD8* and *BUD9* variants and encoded proteins

| | diploid budding pattern | | protein | Bud5p | Rax1p |
	homozygous	heterozygous[a]	localization	interaction	interaction
control (*BUD8*)	bipolar	bipolar	wild-type (wt)	+	+
bud8Δ	unipolar proximal	n.d.[b]			
Δ7-53	bipolar	n.d.	wt-like	+	-
Δ7-114	bipolar	n.d.	wt-like	+	+/-
Δ74-114	bipolar	n.d.	wt-like	+	n.d.
Δ74-216	unipolar proximal	n.d.	wt-like	-	+
Δ173-216	random	random	cell periphery	+	n.d.
Δ173-325	random	random	cell periphery	+	+
Δ268-325	random	random	cell periphery	+	+/-
Δ268-417	random	random	cell periphery	+	+
Δ375-417	unipolar proximal	n.d.	neck region, cytoplasm	-	n.d.
Δ375-505	unipolar proximal	n.d.	neck region, cytoplasm	-	+
Δ468-505	bipolar	n.d.	neck region, cytoplasm	+	n.d.
Δ513-600	unipolar proximal	n.d.	neck region, cytoplasm	+	+/-
control (*BUD9*)	bipolar	bipolar	wild-type (wt)	+	+
bud9Δ	unipolar distal	n.d.			
Δ8-48	bipolar	n.d.	wt-like	+	+
Δ8-130	bipolar	n.d.	wt-like	+	+
Δ91-130	bipolar	n.d.	wt-like	+	n.d.
Δ91-218	unipolar distal	n.d.	wt-like	-	+
Δ168-218	unipolar distal	n.d.	wt-like	+	n.d.
Δ168-283	unipolar distal	n.d.	cytoplasm	-	-
Δ244-283	unipolar distal	n.d.	cytoplasm	-	n.d.
Δ244-369	random/bipolar	random/bipolar	cytoplasm	+	+
Δ323-369	random/bipolar	random/bipolar	wt-like	+	n.d.
Δ323-450	unipolar distal	n.d.	small daughter cells	+/-	+
Δ406-450	unipolar distal	n.d.	small daughter cells	+/-	+/-
Δ406-544	unipolar distal	n.d.	cytoplasm, tip of daughters	-	n.d.
Δ460-544	unipolar distal	n.d.	cytoplasm, tip of daughters	+	-

[a] in combination with *BUD8* (*BUD8* variants) or *BUD9* (*BUD9* variants)

[b] not determined

3.4 Analysis of post-translational modifications of Bud8p and Bud9p

3.4.1 Bud9p is post-translationally modified within 60 minutes after synthesis

The mobility of both Bud8p and Bud9p in polyacrylamide gel electrophoresis is lower than deduced from the calculated molecular masses. Previous studies have shown that higher molecular weight forms of the proteins stem in part from *N*- and *O*-glycosylation (Harkins *et al.*, 2001). To learn more about the kinetics of post-translational modifications of Bud8p and Bud9p, the appearance of high mobility forms of the proteins should be analyzed by pulse-chase experiments. For this purpose, yeast strains expressing myc^6-*BUD8* and myc^9-*BUD9* were grown overnight at 25°C in minimal medium supplemented with nutrients as needed to maintain the corresponding plasmid. Cells were pulse-labelled with ^{35}[S]methionine/cysteine, and after 10 minutes of labeling, the chase was initiated by addition of an excess of unlabelled methionine and cysteine. Samples were then taken at different time points, with the first one directly after the pulse to define the time point '0' and the last one 30 minutes after the chase. Protein extracts were then prepared, and myc^6-Bud8p and myc^9-Bud9p proteins were analyzed by immunoprecipitation using anti-myc-antibodies and Protein A-sepharose followed by separation of the proteins in SDS-PAGE and autoradiography.

In the case of Bud8p, no specific signals could be detected preventing further analysis. However, in the case of Bud9p, the protein could be detected directly after the pulse as a well-defined signal around 85 kDa corresponding to the calculated molecular weight of myc^9-Bud9p (Fig. 22). In course of time, this signal became increasingly weaker and more indistinct. However, after 30 minutes, an additional band could be observed in the range of 95 kDa indicating the enrichment of a modified form of Bud9p.

To further characterize the kinetics of modification of Bud9p, the pulse-chase experiment was repeated, but sampling was performed in 10 minutes intervals over a time period of 60 minutes. Kinetics of Bud9p modification was similar, in that after 30 minutes approximately 50% of the protion was shifted to higher mobility. After 60 minutes, most of the signal at 85 kDa had been shifted to a signal around 95 kDa indicating that modifications of newly synthesized Bud9p takes about 60 minutes to finish.
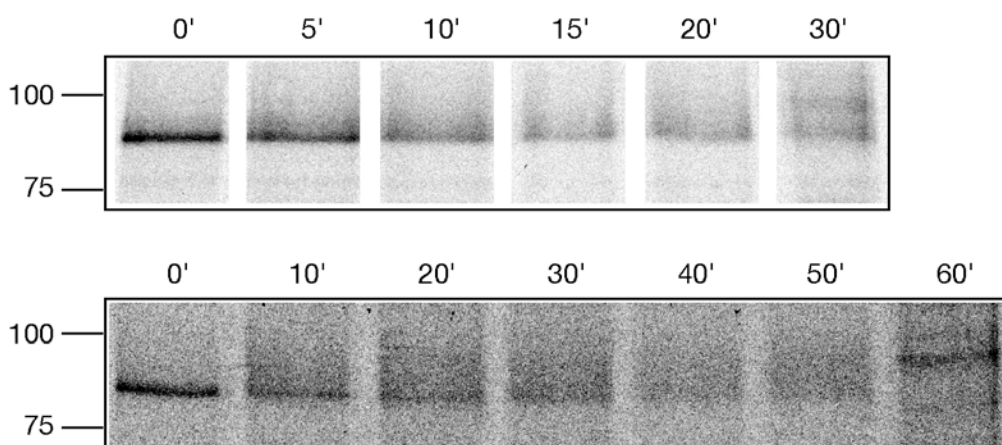
Fig. 22: Pulse-chase experiments with myc^9-Bud9p. Shown are two independent pulse chase experiments tracing myc^9-Bud9p expressed in high-copy manner in wild-type strain BY4742. After a pulse of 10 minutes with ^{35}S-methionine and ^{35}S-cysteine, samples were taken at chase time points of 0 and 5, 10, 15, 20, and 30 minutes. In the second experiment, samples were taken at time points 0 and 10, 20, 30, 40, 50, and 60 minutes. Myc^9-Bud9p was isolated from these samples by immunoprecipitation, separated by SDS-PAGE, and detected by autoradiographies after exposure to X-ray film material.

3.4.2 Post-translational modification of Bud8p and Bud9p occur independent of Sec18p

To address the question of how Bud8p and Bud9p are transported to the cytoplasmic membrane, proteins were analyzed in a temperature-sensitive *sec18* mutant. *SEC18* encodes an ATPase required for the release of Sec17p during the priming step in homotypic vacuole fusion and for ER-to-Golgi transport (Newman and Ferro-Novick, 1990). Thus, protein transport between the endoplasmic reticulum (ER) and the Golgi complex is disrupted in a *sec18^{ts}* mutant strain at restrictive temperature.

To analyze, whether transport and post-translational modification of Bud8p and Bud9p depend on Sec18p, *myc^6-BUD8* and *myc^9-BUD9* on high-copy plasmids were each transformed into the haploid wild-type strain BY4742 (Brachmann *et al.*, 1998) and the temperature-sensitive haploid *sec18-1* mutant strain S18H3 (H.-D. Schmitt, personal communication). Resulting strains were first analyzed for expression of Bud8p and Bud9p when grown at permissive temperature: Strains were grown to mid-log phase before preparation of total protein extracts and analysis of myc^6-Bud8p and myc^9-Bud9p by Western blot hybridization (Fig. 23A). In both cases the control and the *sec18^{ts}* mutant strain, myc^6-Bud8p and myc^9-Bud9p was expressed at normal levels and exhibited the post-translationally modified forms.

In a next step, Sec18p-dependent post-translational modification of Bud8p and Bud9p was analyzed by pulse-chase experiments (Fig. 23B). For this purpose, the *myc^6-BUD8*- and

myc^9-BUD9-expressing control and *sec18^{ts}* strains were grown at the permissive temperature, and pulse-chase experiments were performed both at permissive (28°C) and at restrictive (37°C) temperature. Myc^6-Bud8p and myc^9-Bud9p proteins were analyzed by immuno-precipitation followed by SDS-PAGE and autoradiography to detect ^{35}S-labelled proteins at the time points directly at the pulse and 20 minutes after the chase.

In the case of myc^6-Bud8p, the protein appeared as a distinct band at 80 kDa in the control strain grown at the permissive temperature when analyzed directly after the chase. Most likely this band represents the unmodified form, because its size corresponds to the calculated molecular weight of myc^6-Bud8p. However, a shift to a higher molecular weight of 120 kDa was observed after 20 minutes, indicating that Bud8p had become post-translationally modified. Interestingly, the higher band of 120 kDa could be observed already very slightly after the chase in control strains grown at the restrictive temperature, which might indicate, that post-translational modification is temperature-regulated. However, similar patterns were observed for myc^6-Bud8p when expressed in the *sec18^{ts}* mutant strain, although expression levels were significantly reduced. However, the time depending shift to the 120 kDa band was not suppressed at the restrictive temperature, indicating that post-translational modification observed is not dependent on Sec18p.

Similar results have been obtained for myc^9-Bud9p. A shift in the apparent molecular weight from 85 kDa to 95 kDa could be observed at the permissive temperature in both a control and a *sec18^{ts}* mutant strain. At the restrictive temperature, the higher molecular weight band at 95 kDa could be observed already after the chase (time point 0), again both in a control strain and a *sec18^{ts}* mutant strain. Thus, as in the case of Bud8p, post-translational modification of Bud9p appears to depend on the temperature but not on Sec18p.

In summary, both Bud8p and Bud9p seem to be transported to the plasma-membrane on a *SEC18*-independent mechanism, if the post-translational modifications represents *N*- and *O*-glycosylation, which is expected to occur by transport of the proteins through the secretory pathway.
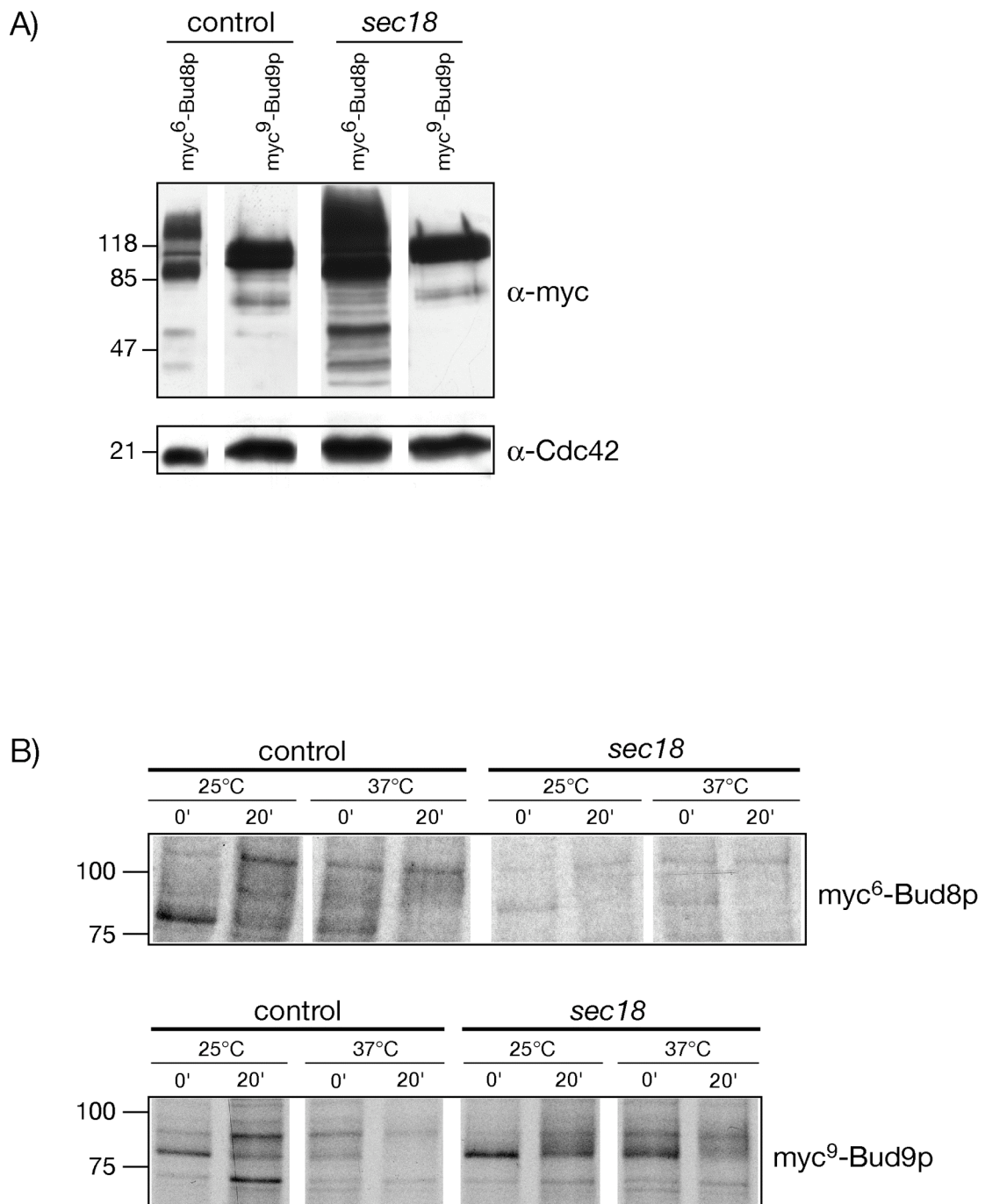
A)

B)

Fig. 23: Analysis of post-translational modifications of Bud8p and Bud9p. (A) Western analysis of myc^6-BUD8 and myc^9-BUD9 constructs. For Western hybridizations, crude extracts from yeast strains BY4742 and S18H3 were prepared, which express either six-fold myc-tagged Bud8p or nine-fold myc-tagged Bud9p, respectively, and separated under denaturing conditions by SDS-PAGE. After transfer to nitrocellulose membranes both fusion proteins were detected by cross-reaction with an anti-myc primary antibody and an anti-murine secondary antibody. For standardization of protein contents, levels of Cdc42p were detected by an anti-Cdc42p antibody. (B) Post-translational modification of Bud8p and Bud9p in a $sec18^{ts}$ mutant strain. Cultures of yeast strains BY4742 (wild-type control) and S18H3 ($sec18-1$ mutant) transformed with BHUM498 and BHUM795, respectively, were split and subjected to pulse chase experiments at 25°C or 37°C. For that purpose, cells were labeled for 10 minutes at the respective temperature by addition of ^{35}S-trans-label mix (pulse). Samples were isolated immediately after the pulse as well as after 20 minutes. Myc-tagged proteins were enriched from these samples by immunoprecipitation, separated by SDS-PAGE, and detected by autoradiography.

4. Discussion

The two membrane-bound glycoproteins Bud8p and Bud9p are thought to function as cortical tags for spatial control of cell division in *Saccharomyces cerevisiae*, which is necessary to establish the bipolar budding pattern that is observed in diploid yeast cells (Harkins *et al.*, 2001; Taheri *et al.*, 2000; Zahner *et al.*, 1996). Bud8p acts by directing bud initiation to the distal cell pole, whereas Bud9p functions to tag the proximal pole. However, the exact molecular mechanisms by which Bud8p and Bud9p act to control site-specific initiation of budding are not fully understood. It is thought that Bud8p and Bud9p are delivered to the cell surface in vesicles *via* the secretory pathway during specific stages of the cell cycle (Schenkman *et al.*, 2002). Timing of *BUD8* and *BUD9* expression appears to be important for a correct localization of both Bud8p and Bud9p, and each of the proteins must contain specific domains that are required for localization and function (Schenkman *et al.*, 2002). Two further proteins, Rax1p and Rax2p, are involved in correct localization and function of Bud8p and Bud9p (Kang *et al.*, 2004b), and the GDP/GTP exchange factor Bud5p interacts with Bud8p (Kang *et al.*, 2004a), suggesting that the Bud1p GTPase signaling module recognizes the spatial cues for bipolar budding.

In this work, the landmark proteins Bud8p and Bud9p were further characterized to better understand the polar transport and the function of these cortical tag components. The major findings of this study will be discussed below and concern (i) co-localization of Bud8p and Bud9p, (ii) post-translational modification of the proteins, and (iii) the identification of domains in Bud8p and Bud9p that are necessary for delivery and anchoring at the cell poles or interaction with the general bud site selection machinery.

4.1 Bud8p and Bud9p co-localize at the distal cell pole in growing buds

In previous studies, Bud8p could be primarily detected at the distal pole of mother and daughter cells, and Bud9p was detected at the proximal pole of the daughter cell (Harkins *et al.*, 2001; Taheri *et al.*, 2000). In addition, Bud9p was found at the distal pole, leading to the assumption that Bud9p not only fulfils the function as proximal pole marker but might also acts a negative regulator of Bud8p at the distal cell pole (Taheri *et al.*, 2000). One concern of this particular study might be the use of the genetic Σ1287b strain background to analyze the localization of Bud9p. In this previous study, carried out in this genetic background, GFP-Bud9p was predominantly detected at the tips of small- and large-budded

daughters, whereas any localization at the mother-bud neck of large-budded cells was only observed infrequently. Other studies, in which another strain background had been used, stated that GFP-Bud9p could be found predominantly at the proximal pole of unbudded cells and at the bud site of the neck in large-budded cells (Harkins *et al.*, 2001; Schenkman *et al.*, 2002). During preliminary tests, Bud9p fused to different fluorescent proteins (GFP, CFP, YFP) was investigated with respect to brightness and signal intensity; here it was found that functional YFP-Bud9p constructs produced much clearer signals in the Σ1287b strain background than the GFP-Bud9p fusion. It was possible to observe the chimeric protein with much higher frequency (up to 40% of stained cells) at the proximal pole of unbudded cells and at the mother-bud neck of large-budded cells. This localization pattern of Bud9p in the Σ1287b background is in much better agreement with the one observed in an alternative strain background and, therefore, is more consistent with the presumption of Bud9p being a landmark protein for the proximal pole. Thus, the experiments using YFP-Bud9p constructs appear to be sufficiently suited to identify putative localization signals in Bud9p, even though the reason for the additional tip localization of Bud9p that was routinely observed in the Σ1287b strain background is not known.

Previous studies had been performed with yeast strains expressing only either GFP-Bud8p or GFP-Bud9p, which do not allow observing both proteins simultaneously in individual cells. In this study, Bud8p and Bud9p proteins were for the first time co-localized at different stages of the cell cycle; these experiments confirm previous observations and refine the model on the polar localization of the two cortical tags during cell division (Fig. 24): In newborn cells, only Bud8p is localized at the distal cell pole. Bud9p appears exclusively at the proximal cell pole, excluding a negative regulation of Bud9p at the distal cell pole. Consequently, initiation of the first budding event in newborn cells occurs with a very high frequency at the distal pole because Bud8p is the more effective pole marker. During the following cell cycles, Bud9p starts to accumulate at the distal pole, leading to a partial inhibition of Bud8p at this site. As a consequence, the proximal budding frequency starts to increase until a bipolar budding pattern is established after three to four division cycles. This model presumes that Bud9p is delivered to the bud site very late during the cell cycle, which has been observed in a previous study showing that Bud9p appears at the cell surface after activation of the mitotic exit network and just before cytokinesis (Schenkman *et al.*, 2002).
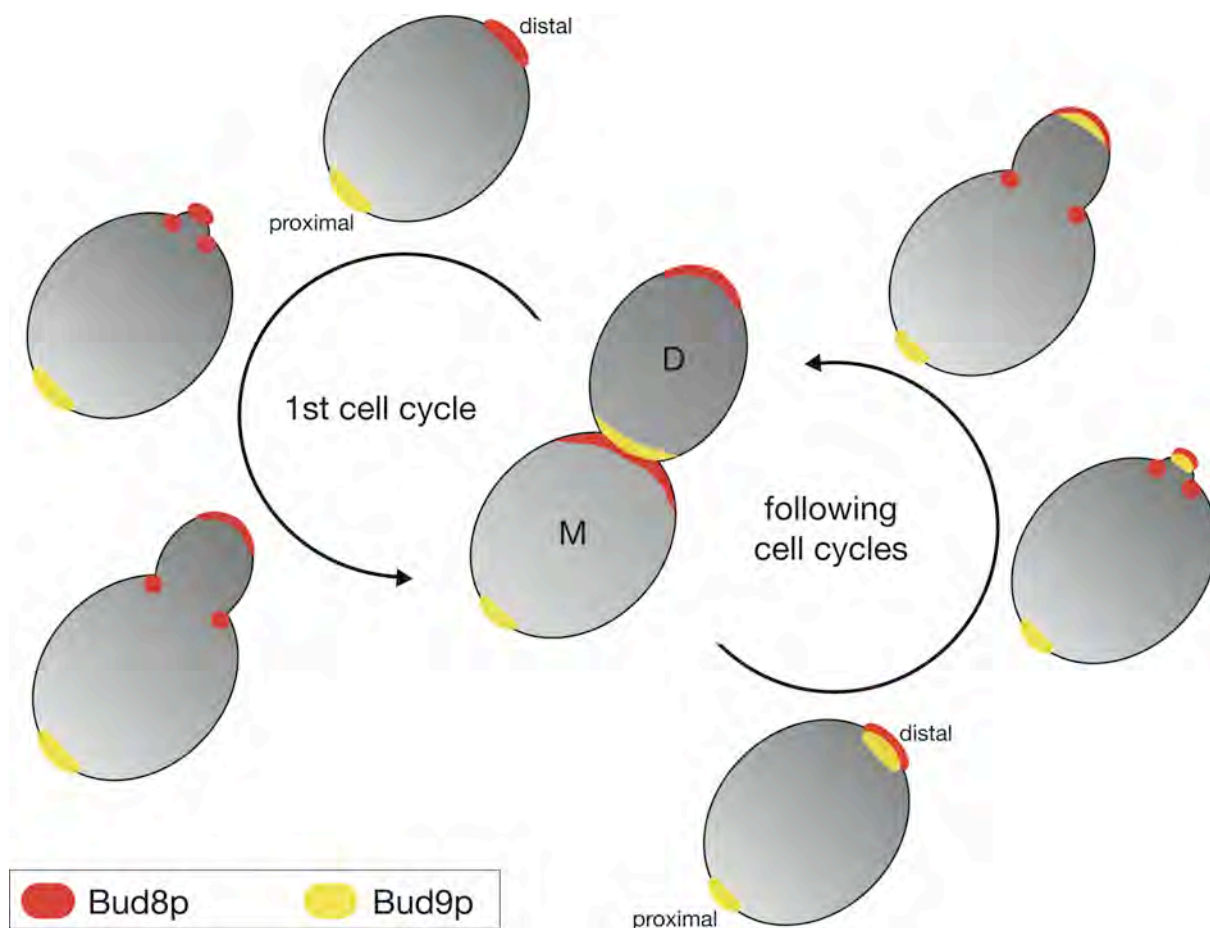
Fig. 24: Distribution of Bud8p and Bud9p during the cell cycle. The figure shows a schematic model of the distribution of Bud8p and Bud9p at the distal and the proximal cell pole during the budding process. During the first cell cycle Bud8p can be localized at the distal pole. It is assumed that inhibition of the distal pole budding does not occur because Bud9p is localized during the first cell cycle exclusively at the proximal pole. From the beginning of the second cycle Bud9p begins to accumulate also at the distal pole of the mother cell, so that a negative regulation of Bud8p by Bud9p at the distal pole allows budding at the proximal pole. 'M' signifies the mother cell, 'D' the daughter cell.

In summary, the co-localization experiments performed in this work provide an explanation for the long-known observations that the first budding events in newborn diploid daughter cells occur almost exclusively at the distal cell pole and that bipolar budding does not occur before several rounds of cell division.

4.2 Post-translational modification of Bud8p and Bud9p

Previous studies have shown that Bud8p and Bud9p appear as multiple signals in Western blot experiments, suggesting a post-translational modification of both proteins. Typically, secreted and plasma membrane proteins are characterized by different features. For instance, most of them carry NH_2-terminal sorting signals. Furthermore, the majority of these proteins

are glycoproteins. The addition of oligosaccharides occurs by *N*-linked and/or *O*-linked glycosylation, and it is necessary for proper folding of the proteins. The fact that both Bud8p and Bud9p carry multiple *N*- and *O*-glycosylation sites indicates that they might be delivered by the secretory pathway to their point of action, albeit they do not contain classical ER signal sequences (Harkins *et al.*, 2001). The results of this study's pulse-chase experiments provide further evidence for a post-translational modification of Bud8p and Bud9p. In both cases, a shift in the molecular weight can be observed within approximately one hour after protein synthesis. Interestingly, these obtained results indicate that synthesis of Bud8p and Bud9p occurs very slowly. For comparison, in an early study it was shown that the secretion of the yeast invertase Suc2p appears very rapid by demonstrating that completion of its export requires not more than 5 min (Novick *et al.*, 1981). Another protein, whose secretion has been studied in detail, is for instance the vacuolar enzyme carboxypeptidase Y (CPY). Also for this protein, processing and transport by the secretion machinery occurs with a half-time of approximately six minutes (Hasilik and Tanner, 1978; Schekman, 1985).

First hints on the transport of both proteins were gained in this study by pulse chase experiments with a *sec18-1* mutant strain that is blocked for the transport of a number of proteins through the secretory pathway (H.-D. Schmitt, personal communication). As, however, an increase in the molecular weight of both Bud8p and Bud9p was evident in such a *sec18^{ts}* mutant strain, the proteins might be transported to the cell surface through the secretory pathway by a *SEC18*-independent mechanism. Classical studies of temperature-sensitive secretory (*sec*) mutants conclude that the majority of secreted and plasma membrane proteins follow a common SEC pathway *via* the endoplasmic reticulum (ER), Golgi apparatus, and secretory vesicles to the cell periphery. Yet recently, it could be shown that the yeast integral membrane protein Ist2p travels from the ER to the plasma membrane *via* a novel route that operates independently from the formation of the coat-protein complex II (COPII)-coated vesicles (Jüschke *et al.*, 2005). The study yielded that the COOH-terminal domain of Ist2p comprises all the necessary information for the targeting of Ist2p (and other integral membrane proteins) to the plasma membrane in a *SEC18*-independent manner, defining it as a novel sorting determinant. The only requirements for sorting to the plasma membrane are the presence of upstream hydrophobic domains, which mediate the integration of the polypeptide into the ER membrane, and a topology that confers a cytosolic orientation of this domain (Jüschke *et al.*, 2005). To yield additional information on post-translational

modifications of Bud8p and Bud9p, further strains must be tested in pulse-chase experiments employing additional *sec* mutants or other mutants in, e.g., various signalling pathways to study glycosylation of these cortical tags.

4.3 Functional domains of Bud8p and Bud9p

With the exception of the predicted COOH-terminal transmembrane segments, Bud8p and Bud9p lack any known functional domains. In order to identify regions of these spatial landmark proteins, a detailed structural and functional analysis was performed here. One specific aim was to uncover regions that contain segments important for polar localization of the proteins and for mediating the interaction with the GDP/GTP exchange factor Bud5p as well as the cortical tag protein Rax1p. Systematic deletion sets of Bud8p and Bud9p were generated to achieve this aim. Previous studies had shown that in many cases this approach is promising to identify functional domains of poorly characterized proteins. Although deletion mutations bear a certain risk to create global alterations on protein conformation, many domains will fold properly if neighbouring sequences are removed or even if isolated from their natural context. In addition, deletions that affect only a subset of the properties of the full-length protein are likely to define functional domains. In this study, the construction of suitable deletion sets led to uncovering of such mutations within Bud8p and Bud9p, indicating that the omitted regions carry domains with specific functions and therefore validating the approach.

The results of this study show that deletions at the NH_2-terminus of Bud8p (residues 7-216) and Bud9p (residues 8-218) influence neither the correct localization of the proteins at the cell poles nor their function. Corresponding deletion proteins localize to the cell poles, and the mutant strains are not conspicuous with respect to their budding pattern. These results indicate that the equivalent segments do not carry any transport signals, because proteins are released to their site of action where they are able to fulfil their function as pole marker. The prediction that deletions in this part do not affect localization and/or function agrees with the fact that classical NH_2-terminal signal sequences are absent in the amino acid sequences of Bud8p and Bud9p.

As mentioned above, the results of the structure-function analyses indicate that the NH_2-terminal part does not play a role in correct localization or function of Bud8p and Bud9p. Accordingly, it is assumed that segments that are involved in the transport of Bud8p

and Bud9p can be found in the median and COOH-terminal part, respectively: Deletions in these parts of the proteins hamper correct localization, indicating that signals for transport to the cell surface and/or the cell poles are encoded in these regions. In case of Bud8p, deletions in either the median or the COOH-terminal part correlated with two distinct mislocalization patterns. Mutant proteins deleted for portions of the median part are evenly distributed at the cell surface, indicating that they are either randomly delivered to the plasma membrane or diffuse freely in the membrane after polar delivery. The data do not allow distinguishing between these two possibilities but they suggest that the median part of Bud8p does not carry sequences that are essential for cell surface delivery.

Two mutations in the COOH-terminal part (Δ375-505 and Δ513-600) cause Bud8p enrichment in the cytoplasm, indicating that the deleted segments could carry transport signals. It is noticeable that these proteins also appear frequently as patches that rapidly move within the cell. This observation might indicate that these variants get stuck during secretion to the cell surface at an unknown time point. Strikingly, the Δ375-505 mutation also blocks interaction with Bud5p and Rax1p, which led to the assumption that this deletion could cause global structure alterations that generally affect properties of Bud8p. In contrast, the Δ513-600 mutation does not influence the interaction with Bud5p and Rax1p, making it more likely that the observed localization defect is due to loss of a putative transport signal in the deleted region. Comparison of the deduced primary structure of both proteins showed that this part of Bud8p (residues 513-600) displays a high degree of similarity to the corresponding segment of Bud9p (residues 460-544). In former studies with chimeric Bud8p/Bud9p proteins it could be shown that these portions of Bud8p and Bud9p carrying two transmembrane domains that are functionally interchangeable (Schenkman *et al.*, 2002); thus, Bud8p and Bud9p might carry similar transport signals in their COOH-terminal regions. The finding that deletion of the Bud9p residues 460 to 544 also causes cytoplasmic localization strengthens this hypothesis.

A number of further deletions were found to affect localization of Bud9p. Two deletions in the median part of the protein (Δ168-283 and Δ244-369) caused Bud9p to become enriched in the cytoplasm. The Δ168-283 deletion also abolished interaction with Bud5p and Rax1p, making a definite conclusion difficult. The Δ244-369 deletion mutant was competent for binding to Bud5p and Rax1p, indicating that a specific rather than a global defect caused cytoplasmic staining, e.g., due to loss of a sequence required for transport of Bud9p to the cell

surface. However, correct transport does not appear to be completely lost in this mutant, because a bipolar budding pattern was observed for approximately 50% of mutant cells. Two mutant proteins (Δ323-450 and Δ406-450) were non-functional and appeared as patches predominantly in small-budded cells. Both variants are still competent for interaction with Bud5p and Rax1p, indicating a more specific defect and not a global alteration of protein conformation. It is assumed that the transcription of both pole marker proteins is cell cycle-regulated and that the time of transcription plays an important role for correct localization of the proteins. Former studies showed in case of *BUD9*, the abundance of mRNA peaks in late G1, whereas delivery of Bud9p appears to be delayed, because the protein arrives at the bud site of the neck very late in the cell cycle - after activation of the mitotic exit network and just before cytokinesis (Schenkman *et al.*, 2002). Thus, the Δ323-450 and Δ406-450 proteins might lack a sequence that directs Bud9p to the bud neck after peak expression. It is puzzling that these proteins accumulate as patches predominantly in small-budded cells and not in large-budded cells. A possible explanation might be altered stability of these proteins at later stages of the cell cycle. Although the exact reason(s) for the defects caused by these mutations are currently unknown, it seems likely that the deleted segments carry sequences that are involved in correct delivery of Bud9p to the proximal pole of daughter cells.

Although the NH_2-terminal part of both Bud8p and Bud9p appears to play no role for transport to the cell poles and establishment of the bipolar budding pattern, this study revealed that deletions in this part of both proteins can specifically affect the association of both Bud8p and Bud9p with Bud5p but not with Rax1p. Two variants of Bud8p (Bud8p$^{Δ74-216}$) and Bud9p (Bud9p$^{Δ91-218}$) were uncovered that are not functional *in vivo* and not able to interact with the GDP/GTP exchange factor Bud5p. Therefore, it is likely that the NH_2-terminal regions of both proteins contain a domain that mediates interaction with Bud5p to activate the general bud site selection machinery. It is noticeable that these regions of Bud8p and Bud9p carry a similar stretch of approximately 30 amino acids in length; whether these particular stretches, that share 40% identity in amino acid sequence, confer interaction with Bud5p remains to be determined.

It has been suggested that Bud8p and Bud9p might interact with downstream components through the conserved short cytoplasmic loops that are located between the two cytoplasmic domains (Harkins *et al.*, 2001). The obtained results of this study do not confirm this hypothesis, as Bud8p and Bud9p variants lacking this region are able to interact with

Bud5p. Because the portions of Bud8p and Bud9p, which are presumably necessary for the interaction with the cytoplasmic exchange factor Bud5p, are predicted to point toward the extracellular space, it is more likely that the association between the landmark proteins and Bud5p is mediated by another, yet unknown factor.

In former studies it was found that specific residues at the NH_2-terminal part of Bud5p are involved in the interaction with the spatial landmark of the distal pole Bud8p to recruit Bud5p to the proper bud site (Kang *et al.*, 2004b). The results of this study indicate that the same residues are necessary for interaction with Bud9p, suggesting that the same region of Bud5p is involved in recognition of the spatial cues. This finding is in good agreement with the fact that *bud5Δ* cells carrying deletions of the NH_2-terminal 70 residues of Bud5p show random budding in all cell types (Kang *et al.*, 2004b). Taken together, these data indicate that extracellular segments of Bud8p and Bud9p could interact with the NH_2-terminal portion of Bud5p *via* additional unknown factors; the identities of these factors remain to be clarified in future studies.

Because all mutant strains that produce proteins with deleted segments in the median part exhibited a random budding pattern, it might be assumed that the interaction between them and Bud5p is impaired. However, results of co-affinity-purifications showed that the median part does not appear to confer interaction with the general budding machinery, as deletions within this segment demonstrably do not block interaction with Bud5p. Instead, the mutations result in dominant random budding, which might be caused by the even distribution of mutant proteins on the plasma membrane. Consequently, the entire cell surface might be competent for Bud5p-binding, and subsequent budding events occur at random positions at the cell cortex.

This study uncovered several Bud8p and Bud9p mutants defective for interaction with Rax1p. In case of Bud8p mutants, the Rax1p-binding defect did not correlate with specific defects in bud site selection, Bud8p localization, or interaction with Bud5p (Table 6, p. 81). These data suggest that the Bud8p-Rax1p interaction is not essential for transport and functionality of Bud8p, a conclusion that is in agreement with the previous finding that GFP-Bud8p localization does not depend on Rax1p (Kang *et al.*, 2004a). Thus, while it is interesting to note that several regions of Bud8p might participate in Rax1p-binding, the actual role of the Bud8p-Rax1p interaction remains elusive. For Bud9p, we observed a correlation between Rax1p-binding and transport of the protein to the cell surface, because

both deletions that strongly affect Rax1p binding (Δ168-283 or Δ460-544) also caused cytoplasmic staining of Bud9p. As discussed above, the Δ168-283 mutation results in pleiotrophic defects, hampering a clear interpretation. However, in case of the Δ460-544 mutant, which is competent for interaction with Bud5p, loss of Rax1p-binding might be one of the causes for mislocalization of Bud9p. This interpretation would be in agreement with the previous finding that deletion of Rax1p causes Bud9p to become mislocalized (Kang *et al.*, 2004b).

4.4 Résumé

In conclusion, the accomplishment of structure-function analyses of Bud8p and Bud9p has defined domains for both proteins that (i) seem to be involved in delivery of the proteins to the cell surface and to polar sites, (ii) that are likely to confer interaction with components of the general budding machinery and (iii) that appear to mediate interaction with other components of the bipolar landmarks (Fig. 25). As such, the study aids in extending the still limited knowledge on structure and function of these cortical tag proteins and helps to better understand how these transmembrane glycoproteins participate in spatial control of cell division. Unfortunately, it is not possible in all cases to explain the observed phenotype or combinations of different phenotypes within one mutant in detail. This might be put back to the fact that this investigation of poorly characterized proteins using systematic deletion sets bears a risk of creating global alterations of protein conformation. In this case domains are not able to fold properly because neighbouring sequences are removed from their natural context. In addition, deletions that affect only a subset of the properties of the full-length protein are likely to define functional domains. Generation of deletion sets led to uncovering of such mutations within Bud8p and Bud9p indicating that the deleted regions carry domains with specific functions and that our approach was successful. Future studies will have to address specific partners interacting with these domains of the spatial landmarks in a stable or transient manner. Furthermore, detailed biochemical studies must resolve temporal and spatial interactions between Bud8p and Bud9p and their associated partners.
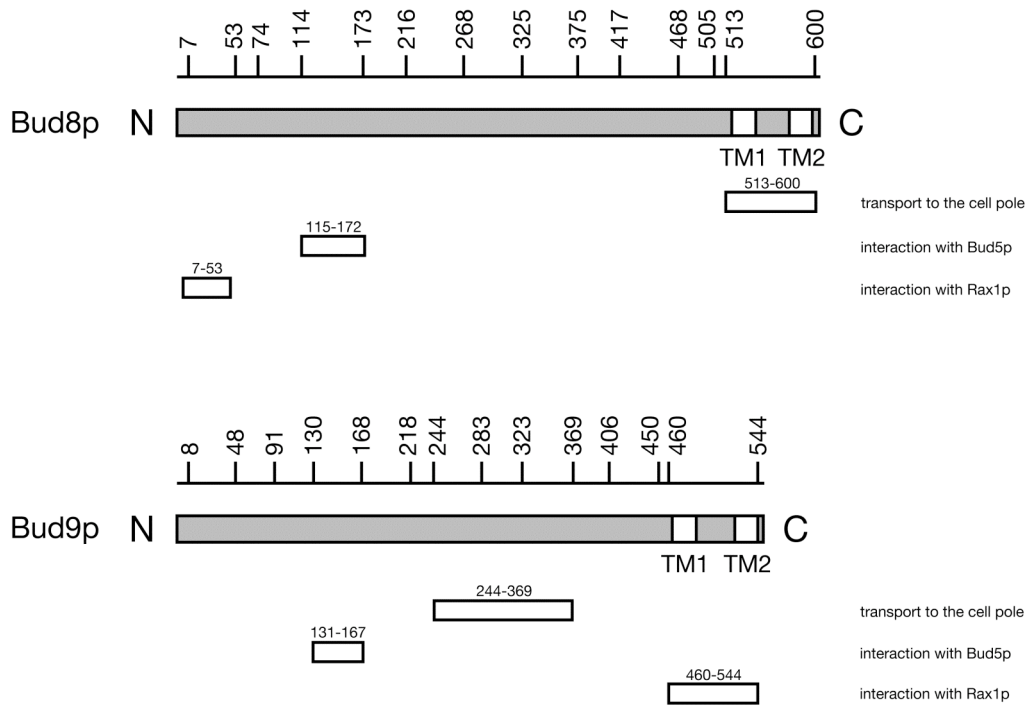
Fig. 25: Model for functional domains of Bud8p and Bud9p. Both proteins are drawn schematically as bars with NH_2-terminal (N) and COOH-terminal (C) halves shown on the left and right, respectively. TM1 and TM2 designate the two putative transmembrane domains of each protein. Regions that were identified to be necessary for proper function are drawn as rectangles with the corresponding functions of these domains noted on the right hand side.

To conclude, the aim of this study was to shed light on the molecular mechanisms that determine a fundamental feature of a simple single-celled eukaryote. Polarity, i. e. the anisotropic expression of cellular characteristics is a crucial trait especially for unicellular microorganisms in order to respond to external signals or environmental changes. The baker's yeast *Saccharomyces cerevisiae* is a well-suited model system to study such cellular qualities as it shows various but defined patterns of budding that depend on specific external conditions. Several genetic determinants necessary for this cellular program could be identified in the past, and in this study two spatial landmark proteins were characterized with respect to their cellular function. The approach chosen to do so, the generation of a comprehensive set of deletion mutants, proved to be valid as well as fruitful, as it gained novel information about the structure-function relationship of these polar markers. Moreover, by clarifying localizations and interactions of the mutant proteins with components of a polarity signalling module, further insights into this cellular process were obtained. First steps to investigate a potential role of (polarized?) secretion of both cortical tag factors top this study off, and it is desirable that future studies will that might be built up on these data will contribute to our understanding how cells in general progress in a three-dimensional context.

5. References

Adames, N., Blundell, K., Ashby, M. N., Boone, C. 1995. Role of yeast insulin-degrading enzyme homologs in propheromone processing and bud-site selection. *Science* 270:464-67.

Adams, A. E. M., Johnson D. I., Longnecker, R. M., Sloat, B. F., Pringle, J. R. 1990. *CDC42* and *CDC43*, two additional genes involved in budding and the establishment of cell polarity in the yeast *Saccharomyces cerevisiae*. *J. Cell Biol*. 111:131-42.

Adams, A. E., Botstein, D., Drubin, D. G. 1991. Requirement of yeast fimbrin for actin organization and morphogenesis in vivo. *Nature* 354:404-8.

Adams, A., Pringle, J. 1984. Relationship of actin and tubulin distribution to bud growth in wild-type and morphogenetic-mutant *Saccharomyces cerevisiae. J. Cell Biol.* 98:934-45.

Amberg, D. C., Busart, E., Botstein, D. 1995. Defining protein interactions with yeast actin in vivo. *Nat. Struct. Biol*. 2:28-35.

Amberg, D. C., Zahner, J. E., Mulholland, J. W., Pringle, J. R., Botstein, D. 1997. Aip3p/Bud6p, a yeast actin-interacting protein that is involved in morphogenesis and the selection of bipolar bud sites. *Mol. Biol. Cell* 8:729-53.

Bähler, J., Peter, M. 2000. Cell polarity in yeast. In Drubin, D. G. (ed.) *Cell polarity*. Oxford University Press, Oxford, Vol. 28, pp. 21-77.

Bauer, F., Urdaci, M., Aigle, M., Crouzet, M. 1993. Alteration of a yeast SH3 protein leads to conditional viability with defects in cytoskeletal and budding patterns. *Mol. Cell. Biol.* 13:5070-84.

Bedinger, P. A. Hardeman, K. J., Loukides, C. A. 1994. Travelling in style: the cell biology of pollen. *Trends Cell Biol*. 4:132-38.

Belmont, L. D., Drubin, D. G. 1998. The yeast V159N actin mutant reveals roles for actin dynamics *in vivo*. *J. Cell Biol*. 142:1289-99.

Bender, A., Pringle, J. R. 1989. Multicopy suppression of the *cdc24* budding defect in yeast by *CDC42* and three newly identified genes including the ras-related gene *RSR1*. *Proc. Natl. Acad. Sci. USA* 89:9976-80.

Bender, A. 1993. Genetic evidence for the roles of the bud-site-selection genes *BUD5* and *BUD2* in the control of the Rsr1p (Bud1p) GTPase in yeast. *Proc. Natl. Acad. Sci. USA* 90:9926-29.

Bi, E., Pringle, J. R. 1996. *ZDS1* and *ZDS2*, genes whose products may regulate Cdc42p in *Saccharomyces cerevisiae. Mol. Cell. Biol*. 16:5264-75.

Brachmann, C. B., Davies, A., Cost, G. J., Caputo, E., Li, J., Hieter, P., Boeke, J. D. 1998. Designer deletion strains derived from *Saccharomyces cerevisiae* S288C: a useful set of strains and plasmids for PCR-mediated gene disruption and other applications. *Yeast* 14:115-32.

Bradford, M. M. 1976. A rapid and sensitive method for the quantitation of microgram quantities of protein utilizing the principle of protein-dye binding. *Anal. Biochem*. 72:248-54.

Brown, J. L., Bussey, H. 1993. The yeast *KRE9* gene encodes an O glycoprotein involved in the cell surface β-glucan assembly. *Mol. Cell. Biol.* 13:6346-56.

Brown, J. L., Jaquenound, M., Gulli, M.-P., Chant, J., Peter, M. 1997. Novel Cdc42p-binding proteins Gic1 and Gic2 control cell polarity in yeast. *Genes Dev.* 11:2972-82.

Castrillon, D. H., Wasserman, S. A. 1994. Diaphonous is required for cytokinesis in Drosophila and shares domains of similarity with the products of the limb deformity gene. *Development* 120:3367-77.

Chang, F., Drubin, D., Nurse, P. 1997. Cdc12p, a protein required for cytokinesis in fission yeast, is a component of the cell division ring and interacts with profilin. *J. Cell Biol.* 137:169-82.

Chant, J., Corrado, K., Pringle, J. R., Herskowitz, I. 1991. The yeast *BUD5* gene, which encodes a putative GDP-GTP exchange factor, is necessary for bud-site selection and interacts with bud-formation gene *BEM1*. *Cell* 65:1213-24.

Chant, J., Herskowitz, I. 1991. Genetic control of bud-site selection in yeast by a set of gene products that comprise a morphogenetic pathway. *Cell* 65:1203-12.

Chant, J., Pringle, J. R. 1991. Budding and cell polarity in *Saccharomyces cerevisiae. Curr. Opin. Genet. Dev.* 1:342-50.

Chant, J., Mischke, M., Mitchell, E., Herskowitz, I., Pringle, J. R. 1995. Role of Bud3p in producing the axial budding pattern of yeast. *J. Cell Biol.* 129:767-78.

Chant, J., Pringle, J. R. 1995. Patterns of bud-site selection in the yeast *Saccharomyces cerevisiae. J. Cell Biol.* 129:751-65.

Chant, J. 1999. Cell polarity in yeast. *Annu. Rev. Cell Dev. Biol.* 15:365-91.

Chen, G.-C., Kim, Y.-J., Chan, C. S. M. 1997. The Cdc42p GTPase-associated proteins Gic1 and Gic2 are required for polarized cell growth in *Saccharomyces cerevisiae. Genes Dev.* 11:2958-71.

Chen, T., Hiroko, T., Chaudhuri, A., Inose, F., Lord, M., Tanaka, S., Chant, J., Fujita, A. 2000. Multigenerational cortical inheritance of the Rax2 protein in orienting polarity and division in yeast. *Science.* 290:1975-8.

Christianson, T. W., Sikorski, R. S., Dante, M., Shero, J. H., Hieter, P. 1992. Multifunctional yeast high-copy-number shuttle vectors. *Gene* 110:119-22.

Cross, F., Hartwell, L. H., Jackson, C., Konopka, J. B. 1988. Conjugation in *Saccharomyces cerevisiae. Annu. Rev. Cell Biol.* 4:429-57.

Crouzet, M., Urdaci, M., Dulau, L., Aigle, M. 1991. Yeast mutant affected for viability upon nutrient starvation: characterization and cloning of the *RVS161* gene. *Yeast* 7:727-43.

Cvrcková, F., Vergilio, C. D., Manser, E., Pringle, J. R., Nasmyth, K. 1995. Ste20-like protein kinases are required for localization of cell growth and for cytokinesis in budding yeast. *Genes Dev.* 9:1817-30.

Drees, B. L., Sundin, B., Brazeau, E., Caviston, J. P., Chen, G. C., Guo, W., Kozminski, K. G., Lau, M. W., Moskow, J. J., Tong, A., Schenkman, L. R., McKenzie, A., III, Brennwald, P., Longtine, M., Bi, E., Chan, C., Novick, P., Boone, C., Pringle, J. R., Davis, T. N., Fields, S., Drubin, D. G. 2001. A protein interaction map for cell polarity development. *J. Cell Biol.* 154:549-71.

Drubin, D. G. 1990. Actin and actin binding proteins in yeast. *Cell Motil. Cytoskelet.* 15:7-11.

Drubin, D. G., Jones, H. D., Wertman, K. F. 1993. Actin structure and function: roles in mitochondrial organization and morphogenesis in budding yeast and identification of the phalloidin-binding site. *Mol. Biol. Cell* 4:1277-94.

Drubin, D. G., Miller, K. G., Botstein, D. 1988. Yeast actin-binding proteins: evidence for a role in morphogenesis. *J. Cell Biol.* 107:2551-61.

Durrens, P., Revardel, E., Bonneu, M., Aigle, M. 1995. Evidence for a branched pathway in the polarized cell division of *Saccharomyces cerevisiae. Curr. Genet.* 27:213-16.

Emmons, S., Phan, H., Calley, J., Chen, W., James, B., Manseau, L. 1995. Cappuccino, a Drosophila maternal effect gene required for polarity of the egg and embryo, is related to the vertebrate limb deformity locus. *Genes Dev.* 9:2482-94.

Evangelista, M., Blundell, K., Longtine, M. S., Chow, C. J., Adames, N., Pringle, J. R., Peter, M., Boone, C. 1997. Bni1p, a yeast formin linking Cdc42p and the actin cytoskeleton during polarized morphogenesis. *Science* 276:118-22.

Field, C., Schekman, R. 1980. Localized secretion of acid phosphatase reflects the pattern of cell surface growth in *Saccharomyces cerevisiae. J. Cell Biol.* 86:123-28.

Flescher, E. G., Madden, K., Snyder, M. 1993. Components required for cytokinesis are important for bud site selection in yeast. *J. Cell Biol.* 122:373-86.

Freeman, G., Lundelius, J. W. 1982. The developmental genetics of dextrality and sinistrality in the gastropod *Lymnaea peregra*. *Wilhelm Roux's Arch. Dev. Biol.* 191:69-83.

Freeman, N. L., Lila, T., Mintzer, K. A., Chen, Z., Pahk, A. J., Ren, R., Drubin, D. G., Field, J. 1996. A conserved proline-rich region of the *Saccharomyces cerevisiae* cyclase-associated protein binds SH3 domains and modulates cytoskeletal localization. *Mol. Cell Biol.* 16:548-56.

Freifelder, D. 1960. Bud position in *Saccharomyces cerevisiae. J. Bacteriol.* 124:511-23.

Fujita, A., Oka, C., Arikawa, Y., Katagai, T., Tonouchi, A., Kuhara, S., Misumi, Y. 1994. A yeast gene necessary for bud-site selection encodes a protein similar to insulin-degrading enzymes. *Nature* 372:567-70.

Fujiwara, T., Tanaka, K., Mino, A., Kikyo, M., Takahashi, K., Shimizu, K., Takai, Y. 1998. Rho1p-Bni1p-Spa2p interactions: implication in localization of Bni1p at the bud site and regulation of the actin cytoskeleton in *Saccharomyces cerevisiae. Mol. Biol. Cell* 9:1221-33.

Gehrung, S., Snyder, M. 1990. The *SPA2* gene of *Saccharomyces cerevisiae* is important for pheromone-induced morphogenesis and efficient mating. *J. Cell Biol.* 111:1451-64.

Gimeno, C. J., Fink, G. R. 1992. The logic of cell division in the life cycle of yeast. *Science* 257:626.

Guthrie, C., Fink, G. R. 1991. Guide to Yeast Genetics and Molecular Biology. *Methods Enzymol.* 194.

Halme, A., Michelitch, M., Mitchell, E. L., Chant, J. 1996. Bud10p directs axial cell polarization in budding yeast and resembles a transmembrane receptor. *Curr. Biol.* 6:570-79.

Harkins, H. A., Page, N., Schenkman, L. R., De Virgilio, C., Shaw, S., Bussey, H., Pringle, J. R. 2001. Bud8p and Bud9p, proteins that may mark the sites for bipolar budding in yeast. *Mol. Biol. Cell* 12:2497-518.

Hasilik, A., Tanner, W. 1978. Biosynthesis of the vacuolar yeast glycoprotein carboxypeptidase Y. Conversion of precursor into the enzyme. *Eur. J. Biochem.* 85:599-608.

Herskowitz, I. 1988. Life cycle of the budding yeast *Saccharomyces cerevisiae. Microbiol. Rev.* 52:523-53.

Herskowitz, I., Park, H.-O., Sanders, S., Valtz, N., Peter, M. 1995. Programming of cell polarity in budding yeast by endogenous and exogenous signals. *Cold Spring Harbor Symp. Quant. Biol.* 60:717-27.

Hicks, J. B., Strathern, J. N., Herskowitz, I. 1977. Interconversion of mating types. III. Action of the homothallism (HO) gene in cells homozygous for the mating type locus. *Genetics* 85:395-405.

Hoffmann, C. S., Winston, F. 1987. A ten-minute DNA preparation from yeast efficiently releases autonomous plasmids for transformation of *Escherichia coli. Gene* 57:267-72.

Holmes, D. S., Quigley, M. 1981. A rapid boiling method for the preparation of bacterial plasmids. *Anal. Biochem.* 114:193-7.

Holtzman, D.A., Yang, S., Drubin, D. G. 1993. Synthetic-lethal interactions identify two novel genes, *SLA1* and *SLA2*, that control membrane cytoskeleton assembly in *Saccharomyces cerevisiae. J. Cell Biol.* 122:635-44.

Hyman, A. A., White, J. G. 1987. Determination of cell division axes in the early embryogenesis of *Caenorhabditis elegans. J. Cell Biol.* 105:2123-35.

Ito, H., Fukuda, Y., Murata, K., Kimura, A. 1983. Transformation of intact yeast cells treated with alkali cations. *J. Bacteriol.* 153:163-8.

Jüschke, C., Wächter, A., Schwappach, B., Seedorf, M. 2005. *SEC18*/NSF-independent, protein-sorting pathway from the yeast cortical ER to the plasma membrane. *J. Cell Biol.* 169:613-622.

Johnson, D. I., Pringle, J. R. 1990. Molecular characterization of *CDC42*, a *Saccharomyces cerevisiae* gene involved in the development of cell polarity. *J. Cell Biol*. 111:143-52.

Kabsch, W., Mannherz, H. G., Suck, D., Pai, E. F., Holmes, K. C. 1990. Atomic structure of the actin: DNase I complex. *Nature* 347:37-44.

Kang, P. J., Sanson, A., Lee, B., Park, H.-O. 2001. A GDP/GTP exchange factor involved in linking a spatial landmark to cell polarity. *Science* 292:1376-8.

Kang, P. J., Lee, B., Park, H.-O. 2004a. Specific residues of the GDP/GTP exchange factor Bud5p are involved in establishment of the cell type-specific budding pattern in yeast. *J. Biol. Chem.* 279:27980-5.

Kang, P. J., Angerman, E., Nakashima, K., Pringle, J. R., Park, H.-O. 2004b. Interactions among Rax1p, Rax2p, Bud8p, and Bud9p in marking cortical sites for bipolar bud-site selection in yeast. *Mol. Biol. Cell* 15:5145-57.

Kilmartin, J. V., Adams, A. E. 1984. Structural rearrangements of tubulin and actin during the cell cycle of the yeast *Saccharomyces. J. Cell Biol.* 98:922-33.

Kraut, R., Chia, W., Jan, L. Y., Jan, Y. N., Knoblich, J. A. 1996. Role of *inscuteable* in orienting asymmetric cell divisions in *Drosophila. Nature* 383:50-55.

Kron, S. J., Styles, C. A., Fink, G. R. 1994. Symmetric cell division in pseudohyphae of the yeast *Saccharomyces cerevisiae. Mol. Biol. Cell* 5:1003-22.

Kupfer, A., Swain, S. L., Janeway, C. A. Singer, C. S. 1986. The specific direct interaction of helper T cells and antigen-presenting B cells. *Proc. Natl. Acad. Sci. USA* 83:6080-83.

Laemmli, U. K. 1970. Cleavage of structural proteins during the assembly of the head of bacteriophage T4. *Nature* 227:680-5.

Leberer, E., Thomas, D. Y., Whiteway, M. 1997. Pheromone signalling and polarized morphogenesis in yeast.. *Curr Opin Genet Dev.* 7:59-66.

Leberer, E., Wu, C., Leeuw, T., Fourest-Lieuvin, A., Segall, J. E., Thomas, D. Y. 1997. Functional characterization of the Cdc42p binding domain of yeast Ste20p protein kinase. *EMBO J.* 16:83-97.

Leeuw, T., Fourest-Lieuvin, A., Wu, C., Chenevert, J., Clark, K., Whiteway, M., Thomas, D. Y., Leberer, E. 1995. Pheromone response in yeast: association of Bem1p with proteins of the MAP kinase cascade and actin. *Science* 270:1210-3.

Lew, D. J., Marini, N. J., Reed, S. I. 1992. Different G1 cyclins control the timing of cell cycle commitment in mother and daughter cells of the budding yeast *S. cerevisiae. Cell* 69:317-27.

Lord, M., Inose, F., Hiroko, T., Hata, T., Fujita, A., Chant, J. 2002. Subcellular localization of Axl1, the cell type-specific regulator of polarity. *Curr. Biol*. 12:1347-52.

Madden, K., Costigan, C., Snyder, M. 1992. Cell polarity and morphogenesis in *Saccharomyces cerevisiae. Trends Cell Biol*. 2:22-9.

Madden, K., Snyder, M. 1992. Specification of sites for polarized growth in *Saccharomyces cerevisiae* and the influence of external factors on site selection. *Mol. Biol. Cell* 3:1025-35.

Madden, K. and Snyder, M. 1998. Cell polarity and morphogenesis in budding yeast. *Annu. Rev. Microbiol.* 52:687-744.

Mandel, M., Higa, A. 1992. Calcium-dependent bacteriophage DNA infection. 1970. *Biotechnology* 24:198-201.

Manser, E., Leung, T., Salihuddin, H., Zhao, Z. S. 1994. A brain serine/threonine protein kinase activated by Cdc42 and Rac1. *Nature* 367:40-6.

Martin, G. A., Bollag, G., McCormick, F., Abo, A. 1995. A novel serine kinase activated by rac1/CDC42Hs-dependent autophosphorylation is related to PAK65 and STE20. *EMBO J.* 14:4385.

Martin, H., Mendoza, A., Rodriguez-Pachon, J. M., Molina, M., Nombela, C. 1997. Characterization of *SKM1*, a *Saccharomyces cerevisiae* gene encoding a novel Ste20/PAK-like protein kinase. *Mol. Microbiol*. 23:431-44.

Mass, R. L., Zeller, R., Woychik, R. P., Vogt, T. F., Leder, P. 1999. Disruption of formin-encoding transcripts in two mutant limb deformity alleles. *Nature* 346:853-5.

McCann, R. O., Craig, S. W. 1997. The I/LWEQ module: a conserved sequence that signifies F-actin binding in functionally diverse proteins from yeast to mammals. *Proc. Natl. Acad. Sci. USA* 94:5679-84.

Michelitch, M., Chant, J. 1996. A mechanism of Bud1p GTPase action suggested by mutational analysis and immunolocalization. *Curr. Biol*. 6:446-54.

Mooseker, M.S. 1985. Organization, chemistry, and assembly of the cytoskeletal apparatus of the intestinal brush border. *Annu. Rev. Cell Biol.* 1:209-41.

Mösch, H.-U. 2002 Pseudohyphal growth in yeast. In Osiewacz, H. D. (ed.) *Molecular Biology of Fungal Development*. Marcel Dekker Inc. New York: 1-27.

Mösch, H.-U., Fink, G. R. 1997. Dissection of filamentous growth by transposon mutagenesis in *Saccharomyces cerevisiae. Genetics* 145:671-84.

Newman, A. P., Ferro-Novick, S. 1990. Defining components required for transport from the ER to the Golgi complex in yeast. *Bioassays* 12:485-91.

Ni, L, Snyder, M. 2001. A genomic study of the bipolar bud site selection pattern in *Saccharomyces cerevisiae. Mol. Biol. Cell* 12:2147-70.

Novick, P., Ferro, S., Schekman, R. 1981. Order of events in the yeast secretory pathway. *Cell* 25:461-469.

Park, H.-O., Chant, J., Herskowitz, I. 1993. *BUD2* encodes a GTPase activating protein for Bud1/Rsr1 necessary for proper bud site selection in yeast. *Nature* 365:269-74.

Peter, M., Neiman, A. M., Park, H.-O., van Lohuizen, M., Herskowitz, I. 1996. Functional analysis of the interaction between the small GTP binding protein Cdc42 and the Ste20 protein kinase in yeast. *EMBO J.* 15:7046-59.

Petersen, J., Weilguny, D., Egel, R., Nielsen, O. 1995. Characterization of fus1 of *Schizosaccharomyces pombe*: a developmentally controlled function needed for conjugation. *Mol. Cell. Biol.* 15:3697-707.

Powers, S., Gonzales, E., Christensen, T., Cubert, J., Broek, D. 1991. Functional cloning of *BUD5*, a *CDC25*-related gene from S. cerevisiae that can suppress a dominant-negative *RAS2* mutant. *Cell* 65:1225-31.

Pringle, J. R., Bi, E., Harkins, H. A., Zahner, J. E., De Virgilio, C., Chant, J., Corrado, K., Fares, H. 1995. Establishment of cell polarity in yeast. *Cold Spring Harb. Symp. Quant. Biol.* 60:729-44.

Pruyne, D., Bretscher, A. 2000a. Polarization of cell growth in yeast. I. Establishment and maintenance of polarity states. *J. Cell Sci.* 113:365-375.

Pruyne, D., Bretscher, A. 2000b. Polarization of cell growth in yeast. II. The role of the cortical actin cytoskeleton. *J. Cell Sci.* 113:571-585.

Revardel, E., Bonneau, M., Durrens, P., Aigle, M. 1995. Characterization of a new gene family developing pleiotropic phenotypes upon mutation in *Saccharomyces cerevisiae. Biochim Biophys Acta.* 1263:261-5.

Roberts, R. L., Fink, G. R. 1994. Elements of a single MAP kinase cascade in *Saccharomyces cerevisiae* mediate two developmental programs in the same cell type: mating and invasive growth. *Genes Dev.* 8:2974-85.

Roemer, T., Madden, K., Chang, J., Snyder, M. 1996. Selection of axial growth sites in yeast requires Axl2p, a novel plasma membrane glycoprotein. *Genes Dev.* 10:777-93.

Roemer, T., Vallier, L. G., Snyder, M. 1996. Selection of polarized growth sites in yeast. *Trends Cell Biol.* 6:434-41.

Saiki, R. K., Scharf, S., Faloona, F., Mullis, K. B., Horn, G. T., Erlich, H. A., Arnheim, N. 1985. Enzymatic amplification of beta-globin genomic sequences and restriction site analysis for diagnosis of sickle cell anemia. *Science* 230:1350-4.

Sanders, S. L., Gentzsch, M., Tanner, W., Herskowitz, I. 1999. O-Glycosylation of Axl2/Bud10p by Pmt4p is required for its stability, localization, and function in daughter cells. *J. Cell Biol.* 145:1177-88.

Sanders, S. L., Herskowitz, I. 1996. The Bud4 protein of yeast, required for axial budding, is localized to the mother-bud neck in a cell cycle-dependent manner. *J. Cell Biol.* 134:413-27.

Schekman, R. 1985. Protein localization and membrane traffic in yeast. *Ann. Rev. Cell Biol.* 1:115-143.

Schenkman, L. R., Caruso, C., Page, N., Pringle, J. R. 2002. The role of cell cycle-regulated expression in the localization of spatial landmark proteins in yeast. *J. Cell Biol.* 156:829-41.

Shapiro, L. 1993. Protein localization and asymmetry in the bacterial cell. *Cell* 73:841-55.

Sheu, Y. J., Santos, B., Fortin, N., Costigan, C., Snyder, M. 1998. Spa2p interacts with cell polarity proteins and signaling components involved in yeast cell morphogenesis. *Mol. Cell. Biol.* 18:4053-69.

Sheu, Y. J., Barral, Y., Snyder, M. 2000. Polarized growth controls cell shape and bipolar bud site selection in *Saccharomyces cerevisiae. Mol. Cell Biol.* 20:5235-47.

Sikorski, R. S., Hieter, P. 1989. A system of shuttle vectors and yeast host strains designed for efficient manipulation of DNA in *Saccharomyces cerevisiae. Genetics* 122:19-27.

Simon, M. N., De Virgilio, C., Souza, B., Pringle, J. R., Abo, A., Reed, S. I. 1995. Role for the Rho-family GTPase Cdc42 in yeast mating-pheromone signal pathway. *Nature* 376:702-5.

Sivadon, P., Peypouquet, M. F., Doignon, F., Aigle, M., Crouzet, M. 1997. Cloning of the multicopy suppressor gene *SUR7*: evidence for a functional relationship between the yeast actin-binding protein Rvs167 and a putative membranous protein. *Yeast* 13:747.

Sloat, B., Pringle, J. R. 1978. A mutant of yeast defective in cellular morphogenesis. *Science* 200:1171-73.

Sloat, B. F., Adams, A., Pringle, J. R. 1981. Roles of the *CDC24* gene product in cellular morphogenesis during the *Saccharomyces cerevisiae* cell cycle. *J. Cell Biol.* 89:395-405.

Smith, G. R., Givan, S. A., Cullen, P., Sprague, G. F. Jr. 2002. GTPase-activating proteins for Cdc42. *Eukaryot. Cell*. 1:469-80.

Snyder, M. 1989. The *SPA2* protein of yeast localizes to sites of cell growth. *J. Cell Biol.* 108:1419-29.

Snyder, M., Gehrung, S., Page, B. D. 1991. Studies concerning the temporal and genetic control of cell polarity in *Saccharomyces cerevisiae. J. Cell Biol*. 114:515-32.

Southern, E. M. 1975. Detection of specific sequences among DNA fragments separated by gel electrophoresis. *J. Mol. Biol*. 98:503-17.

Sprague, G. F., Thorner, J. 1992. Pheromone response and signal transduction during the mating process of *Saccharomyces cerevisiae*. In Broach, J. R., Pringle, J. R., Jones, E. W. (ed.s) *The Molecular Biology of the Yeast Saccharomyces*. 2:657-744.

Stevenson, B. J., Ferguson, B., De Virgilio, C., Bi, E., Pringle, J. R., Ammerer, G., Sprague, G. F. Jr. 1995. Mutation of *RGA1*, which encodes a putative GTPase-activating protein for the polarity-establishment protein Cdc42p, activates the pheromone-response pathway in the yeast *Saccharomyces cerevisiae. Genes Dev*. 9:2949-63.

Taheri, N., Köhler, T., Braus, G. H., Mösch, H.-U. 2000. Asymmetrically localized Bud8p and Bud9p proteins control yeast cell polarity and development. *EMBO J.* 19:6686-96.

Tesfaigzi, J., Smith-Harrison, W., Carlson, D. M. 1994. A simple method for reusing Western blots on PVDF membranes. *Biotechniques* 17:268-9.

Torres, L., Martin, H., Garcia-Saez, M. I., Arroyo, J., Molina, M., Sanchez, M., Nombela, C. 1991. A protein kinase gene complements the lytic phenotype of *Saccharomyces cerevisiae lyt2* mutants. *Mol. Microbiol.* 5:2845-54.

Towbin, H., Staehelin, T., Gordon, J. 1979. Electrophoretic transfer of proteins from polyacrylamide gels to nitrocellulose sheets: procedure and some applications. *Proc. Natl. Acad. Sci. USA* 76:4350-4.

Valtz, N., Herskowitz, I. 1996. Pea2 protein of yeast is localized to sites of polarized growth and is required for efficient mating and bipolar budding. *J. Cell Biol.* 135:725-39.

Vojtek, A., Haarer, B., Field, J., Gerst, J., Pollard, T. D., Brown, S., Wigler, M. 1991. Evidence for a functional link between profilin and CAP in the yeast *S. cerevisiae. Cell* 66:497-505.

Waddle, J. A., Karpova, T. S., Waterston, R. H., Cooper, J. A. 1996. Movement of cortical actin patches in yeast. *J. Cell Biol.* 132:861-70.

Wertman, K. F., Drubin, D. G., Botstein, D. 1992. Systematic mutational analysis of the yeast *ACT1* gene. *Genetics* 132:337-50.

Yabe, T., Yamada-Okabe, T., Kasahara, S., Furuichi, Y., Nakajima, T., Ichishima, E., Arisawa, M., Yamada-Okabe, H. 1996. *HKR1* encodes a cell surface protein that regulates both cell wall beta-glucan synthesis and budding pattern in the yeast *Saccharomyces cerevisiae. J. Bacteriol.* 178:477-83.

Yang, S., Ayscough, K. R., Drubin, D. G. 1997. A role for the actin cytoskeleton of *Saccharomyces cerevisiae* in bipolar bud-site selection. *J. Cell Biol.* 136:111-23.

Zahner, J. E., Harkins, H. A., Pringle, J. R. 1996. Genetic analysis of the bipolar pattern of bud site selection in the yeast *Saccharomyces cerevisiae. Mol. Cell. Biol.* 16:1857-70.

Zhao, Z.-S., Leung, T., Manser, E., Lim, L. 1995. Pheromone signalling in *Saccharomyces cerevisiae* requires the small GTP-binding protein Cdc42p and its activator *CDC24. Mol. Cell. Biol.* 15:5246-57.

Zheng, Y., Hart, M. J., Shinjo, K., Evans, T., Bender, A., Cerione, R. A. 1993. Biochemical comparisons of the *Saccharomyces cerevisiae* Bem2 and Bem3 proteins. Delineation of a limit Cdc42 GTPase-activating protein domain. *J. Biol. Chem.* 268:24629-34.

Zheng, Y., Cerione, R., Bender, A. 1994. Control of the yeast bud-site assembly GTPase Cdc42. Catalysis of guanine nucleotide exchange by Cdc24 and stimulation of GTPase activity by Bem3. *J. Biol. Chem.* 269:2369-72.

Zheng, Y., Bender, A., Cerione, R.A. 1995. Interactions among proteins involved in bud-site selection and bud-site assembly in *Saccharomyces cerevisiae. J. Biol. Chem.* 270:626-30.

Ziman, M., Preuss, D., Mulholland, J., O'Brien, J. M., Botstein, D., Johnson, D. I. 1993. Subcellular localization of Cdc42p, a *Saccharomyces cerevisiae* GTP-binding protein involved in the control of cell polarity. *Mol. Biol. Cell.* 4:1307-16.

Danksagung

Rückblickend betrachtet gab es viele Menschen, die mir über den Zeitraum meiner Doktorarbeit zur Seite gestanden haben. An dieser Stelle möchte ich mich bei allen bedanken, die mich bei der Erstellung dieser Arbeit unterstützt haben.

Hier ist zunächst Professor Dr. Hans-Ulrich Mösch zu nennen für die Möglichkeit, meine Doktorarbeit in seiner Abteilung anzufertigen. Ein Dankeschön gebührt auch Professor Dr. Gerhard H. Braus, der sich kurzfristig bereit erklärt hat, das Korreferat dieser Arbeit zu übernehmen.

Bei meinen fleißigen Helfern David Löper und Inken Wollenweber möchte ich mich herzlich für die Ergebnisse ihrer Diplomarbeiten bedanken. Diese waren entscheidend für die Aufklärung vieler Fragen und haben damit maßgeblich zum Gelingen dieser Arbeit beigetragen.

Während meiner Zeit in Göttingen ist mir Maria Meyer eine große Hilfe gewesen. Maria hat sich nicht nur dadurch ausgezeichnet, dass sie mich in verschiedenen Phasen meiner Promotion tatkräftig unterstützt hat, sondern auch dadurch, dass sie mir den manchmal "grauen" Laboralltag mit Campingwecken und Geschichten von Berti, Pauline und Hannelore versüßt hat. Bei Dr. Hans-Dieter Schmitt möchte ich mich für seine Unterstützung bei der Durchführung der *pulse-chase*-Experimente bedanken - ohne ihn wären diese wohl nie zustande gekommen. Beeindruckt war ich von seiner spontanen Hilfe, die er mir kurz vor dem Abgabetermin dieser Arbeit gewährt hat - Danke dafür!

Ein weiteres Dankeschön geht an meine „Mitdenker", mit denen ich in vielen Stunden über die Tücken der Molekularbiologie diskutiert habe, die mich oft aber auch einfach nur auf andere, „forschungsfremde" Gedanken gebracht haben. Vor allem einigen ehemaligen Kollegen sei an dieser Stelle gedankt: Claudia, Katrin, Patrick, Britta und Malte, es war eine tolle Zeit! Ole danke ich für kritische Diskussionen, die wir während meiner Doktorarbeit mehr als einmal miteinander geführt haben. Nicht zu vergessen ist Gaby, die immer ein offenes Ohr für mich hatte: Danke dafür!

Neben den Göttingern gab es auch in Marburg einige Menschen, die zum Gelingen dieser Doktorarbeit beigetragen haben. Ein großer Dank gilt hier der Arbeitsgruppe von Professorin Dr. Regine Kahmann am MPI FÜR TERRESTRISCHE MIKROBIOLOGIE und der Arbeitsgruppe von Professor Dr. Michael Bölker am Fachbereich Biologie der PHILIPPS-UNIVERSITÄT; beide haben ein molekularbiologisches Arbeiten in Marburg überhaupt erst möglich gemacht. Ein besonderes Dankeschön möchte ich an dieser Stelle Volker Vincon und Nicole Rössel aussprechen, die mich und meine Mitstreiter auf besonders freundliche und umsichtige Art und Weise am Marburger MPI eingeführt haben. Diana Kruhl danke ich für ihre Unterstützung bei diversen praktischen Laborarbeiten. Danke auch meinen lieben Marburger Laborkollegen Reinhard Böcher und Hanne Moll: ich habe mich bei Euch sehr wohl gefühlt! Bei Steffi Lindow, Petra Mann und Lucia Forzi möchte ich mich für ihre angenehme Gesellschaft und ihre lieben (Petra, Lucia) und direkten (Steffi) Worte während mancher Kaffeepause bedanken, schön war's!

In der Riege der Kollegen, die mir während meiner Zeit in Göttingen und Marburg besonders an Herz gewachsen sind, sind Melanie und Stefan einzureihen. Ich danke Euch für die vielen anregenden Diskussionen und dafür, dass ich den Forschungsalltag gemeinsam mit Euch meistern durfte. Unvergessen werden die zahlreichen, gemütlichen Abende mit Euch beim Essen, beim Bowling oder im Kino sein. Ohne Euch wäre die Zeit nicht einmal halb so erträglich gewesen. Euch beiden Danke für alles!

Nicht vergessen möchte ich ein Dankeschön für meine treue Weggefährtin Sonja, mit der mich das vor 10 Jahren begonnene Biologiestudium in Göttingen verbindet und eine genauso lange währende Freundschaft.

Meinen Eltern und meinen Geschwistern kann ich gar nicht genug für ihre moralische Unterstützung und ihre aufmunternden Worte während meines Studiums und vor allem während des letzten Jahres danken. Es ist schön zu wissen, dass ihr mir vertraut und dass ich mich auf Euch verlassen kann!

Klein-Jonah möchte ich danken, dass er sich ganz heimlich in mein Leben geschlichen hat und damit den praktischen Arbeiten auf unkonventionelle Weise ein Ende gesetzt hat. Ein Leben ohne ihn kann und möchte ich mir nicht mehr vorstellen! Mein allergrößter Dank gebührt Sven, der mit mir alle Höhen und Tiefen dieser Arbeit durchlebt hat. Ohne ihn wäre diese Arbeit so nie zustande gekommen. Ich danke Dir dafür, dass Du mit mir diese Zeit durchgestanden hast und immer für mich da gewesen bist!

Curriculum Vitae

Name:	Anne-Brit Krappmann (geb. Obermayer)
Geburtsdatum:	19.07.1977
Geburtsort:	Cuxhaven
Nationalität:	deutsch
Familienstand:	verheiratet, 1 Sohn (1 Jahr)

Schulbildung:

1983-1987	Grundschule Grimsehlweg in Hannover-Bothfeld
1987-1989	Orientierungsstufe Gartenheimstraße in Hannover-Bothfeld
1989-1991	Leibnizschule in Hannover
1991-1996	Sophienschule in Hannover

Studium:

1996-2001	GEORG-AUGUST-UNIVERSITÄT Göttingen: Grund- und Hauptstudium im Fach Biologie
Mai 2001	mündliche Diplomprüfungen (Hauptfach: Mikrobiologie; Nebenfächer: Immunologie, Organische Chemie)
Juni 2001 - März 2002	Diplomarbeit am INSTITUT FÜR MIKROBIOLOGIE & GENETIK in der Abteilung MOLEKULARE MIKROBIOLOGIE UND GENETIK von Professor Dr. Gerhard H. Braus unter Anleitung von Dr. Hans-Ulrich Mösch Thema: "Funktionelle Analyse von Bud8p und seinen Interaktionspartnern in der Bäckerhefe *Saccharomyces cerevisiae*"
April 2002- Sept. 2004	Anfertigung der praktischen Arbeiten zur Erlangung des Doktorgrades in der Arbeitsgruppe von PD Dr. Hans-Ulrich Mösch in der Abteilung von Professor Dr. Gerhard H. Braus am INSTITUT FÜR MIKROBIOLOGIE & GENETIK der GEORG-AUGUST-UNIVERSITÄT Göttingen zum Thema "Structure-Function Analysis of the Cell Polarity Determinants Bud8p and Bud9p in *Saccharomyces cerevisiae*"
Okt. 2004 - Nov. 2005	Fortführung der praktischen Arbeiten in der Abteilung GENETIK von Professor Dr. H.-U. Mösch des FACHBEREICHS BIOLOGIE an der PHILIPPS-UNIVERSITÄT Marburg

Hiermit erkläre ich an Eides Statt, dass die vorliegende Dissertation mit dem Titel "Structure-Function Analysis of the Cell Polarity Determinants Bud8p and Bud9p in *Saccharomyces cerevisiae*" von mir selbständig und ohne unerlaubte Hilfe angefertigt wurde.

Göttingen, den 04.12.2006

....

Anne-Brit Krappmann